University of South Bohemia in České Budějovice
Faculty of Science

Protein Control over Carotenoid Spectroscopy and Functions

Ph.D. Thesis

Mgr. Václav Šlouf

Supervisor: **prof. RNDr. Tomáš Polívka, Ph.D.**
Faculty of Science, University of South Bohemia, České Budějovice

České Budějovice 2013

Dedicated to my mother

This thesis should be cited as:
Šlouf V, 2013: Protein Control over Carotenoid Spectroscopy and Functions. Ph.D. Thesis Series, No. 12. University of South Bohemia, Faculty of Science, České Budějovice, Czech Republic, 238 pp.

Annotation

The photophysics of pigments is influenced, to an extent depending on its structure, by the properties of the environment. Proteins represent a very specific environment at least in two aspects: i) they are native to most of the pigments in living systems; ii) they facilitate modifications of pigment configuration, leading to changes not only in its spectroscopic properties, but also in its functional abilities. In studies presented in this thesis, femtosecond pump-probe spectroscopy was used to study predominantly the photosynthetic antenna complexes of bacteria and algae. Based on spectroscopic evidence, the structural modifications of pigments imposed by the protein were deduced or hypothesized, together with their functional relevance.

Declaration [in Czech]

Prohlašuji, že svoji disertační práci jsem vypracoval samostatně pouze s použitím pramenů a literatury uvedených v seznamu citované literatury.

Prohlašuji, že v souladu s § 47b zákona č. 111/1998 Sb. v platném znění souhlasím se zveřejněním své disertační práce, a to v úpravě vzniklé vypuštěním vyznačených částí archivovaných Přírodovědeckou fakultou elektronickou cestou ve veřejně přístupné části databáze STAG provozované Jihočeskou univerzitou v Českých Budějovicích na jejích internetových stránkách, a to se zachováním mého autorského práva k odevzdanému textu této kvalifikační práce. Souhlasím dále s tím, aby toutéž elektronickou cestou byly v souladu s uvedeným ustanovením zákona č. 111/1998 Sb. zveřejněny posudky školitele a oponentů práce i záznam o průběhu a výsledku obhajoby kvalifikační práce. Rovněž souhlasím s porovnáním textu mé kvalifikační práce s databází kvalifikačních prací Theses.cz provozovanou Národním registrem vysokoškolských kvalifikačních prací a systémem na odhalování plagiátů.

České Budějovice, 7. listopadu 2013 .....

Václav Šlouf

Přírodovědecká
fakulta
Faculty
of Science

Financial support

The research presented in this thesis was supported by grants and projects from the Ministry of Education of the Czech Republic (MSM6007665808, AV0Z50510513, KONTAKT ME09037, Algatech CZ.1.05/2.1.00/03.0110), the Czech Science Foundation (P205/11/1164, P501/12/G055), the Grant Agency of University of South Bohemia (038/2010/P, 027/2011/P), and the Grant Agency of the Academy of Sciences of the Czech Republic (IAA608170901).

Acknowledgements

Tomáši, so many thanks belong to you. I think it would be hard to find another individual with such perfectly "tuned" professional and personal characteristics, making you an ideal guide. I intentionally do not use the word "supervisor" because it would not match the way you behaved. You never acted from a position of superiority, but as my fellow worker. Thank you so much!

My other colleagues are also greatly acknowledged for their support. *Petře*, it was great to have the opportunity to meet you. Your ability to solve any technical problem is enormous. I learned a lot from you. Your diligence and thoroughness will always be a model for me. *Marceli*, it sometimes happened that I was racking my brain with some problem or other and, having mentioned it, I realized you were also tackling the very same thing. Quite often, you knew the solution and did not hesitate to share it with me. *Milane*, owing to your general knowledge, thanks for fruitful discussions we shared on such a variety of topics. *Gürkan*, thanks to our debates on quantum mechanical modelling, I am constantly pushed forward in my knowledge of theory. More important for me is, however, that we became friends. *Valya* and *Gürkan*, I thank you for reading this thesis and giving me stimulating suggestions for improvements. *Hristina*, thank you for your help during measurements – mainly after I left for home, you often continued saving the data far into the night. *Míro*, as to my friend and former colleague, I am also very thankful to you. With your generalist's overview, but specialist's detailed knowledge, discussions with you have always been a pleasure for me. We also had a lot of fun – not only after couple of beers, but also on the trip to Baikal, during our ping-pong duels etc. *Pavle*, it was a nice stay in Lund in autumn 2011... And the icing on the cake was publishing the results in PNAS!

Many thanks belong to C. Neil Hunter, John D. Olsen, Michal Koblížek, and Laura Cranston mainly for discussions of various aspects of the samples they provided us with.

Another kind of thanks belongs to my family. I thank them for all their love. *Maminko, zůstaneš navždy v mém srdci stejně jako všechno to dobro a láska, které jsi kolem sebe rozdávala. Taťko, díky za Tvou podporu a pomoc. Lucuško a Šimonku, s Vámi a Vašimi úsměvy je každá nesnáz překonatelná a každý den krásnější...*

Last but not least, I would like to thank those not mentioned above, who stand by me.

List of papers and author's contribution

A) The thesis is based on the following papers (listed in the order of their presentation in the Research Section):

I. **Šlouf V**, Balashov SP, Lanyi JK, Pullerits T, Polívka T (2011) Carotenoid response to retinal excitation and photoisomerization dynamics in xanthorhodopsin. *Chem Phys Lett* 516: 96–101. (IF = 2.3)

VŠ conducted the time-resolved transient absorption measurements in the visible spectral region, analyzed the data, and participated in writing and revision of the manuscript.

II. Durchan M, Tichý J, Litvín R, **Šlouf V**, Gardian Z, Hříbek P, Vácha F, Polívka T (2012) Role of carotenoids in light-harvesting processes in an antenna protein from the chromophyte *Xanthonema debile*. *J Phys Chem B* 116: 8880−8889. (IF = 3.6)

VŠ participated in part of the experimental work and revision of the manuscript.

III. **Šlouf V**, Fuciman M, Johanning S, Hofmann E**,** Frank HA, Polívka T (2013) Low-temperature time-resolved spectroscopic study of the major light-harvesting complex of *Amphidinium carterae*. Accepted in *Photosynth Res*, doi: 10.1007/s11120-013-9900-8. (IF = 3.2)

VŠ participated in time-resolved transient absorption measurements, analyzed the data, and participated in writing and revision of the manuscript.

IV. **Šlouf V**, Chábera P, Olsen JD, Martin EC, Qian P, Hunter CN, Polívka T (2012) Photoprotection in a purple phototrophic bacterium mediated by oxygen-dependent alteration of carotenoid excited-state properties. *Proc Natl Acad Sci USA* 109: 8570–8575. (IF = 9.7)

VŠ participated in performing the experiments, analyzing the data, writing and revision of the manuscript.

V. **Šlouf V**, Fuciman M, Dulebo A, Kaftan D, Koblížek M, Frank HA (2012) Carotenoid charge transfer states and their role in energy transfer processes in LH1–RC complexes from aerobic anoxygenic phototrophs. *J Phys Chem B* 117: 10987−10999. (IF = 3.6)

VŠ participated in the extraction of the carotenoid bacteriorubixanthinal, conducted the time-resolved transient absorption measurements in the visible region, participated on measurements in the near-infrared region, analyzed the data, and took part in writing and revision of the manuscript.

VI. **Šlouf V**, Chábera P, Cogdell RJ, Cranston L, Dulebo A, Hunter CN, Kaftan D, Koblížek M, Martin EC, Olsen JD, Polívka T. Activation of the intramolecular charge-transfer state in LH1 complexes of various purple bacteria. *In preparation.*

VŠ conducted vast majority of the time-resolved transient absorption measurements, analyzed the data, and wrote the manuscript.

B) Papers not included in this thesis:

VII. Durchan M, Fuciman M, **Šlouf V**, Keşan G, Polívka T (2012) Excited-state dynamics of monomeric and aggregated carotenoid 8'-apo-*β*-carotenal. *J Phys Chem A* 116: 12330−12338. (IF = 2.8)

VIII. Fuciman M, Durchan M, **Šlouf V**, Keşan G, Polívka T (2013) Excited-state dynamics of astaxanthin aggregates. *Chem Phys Lett* 568–569: 21–25. (IF = 2.1)

List of abbreviations

^1X, $^3X^*$ – molecule X in the singlet (ground) state, in the triplet excited state
A. – *Amphidinium*
AAP – aerobic anoxygenic phototroph
acpPC – chlorophyll-a–chlorophyll-c_2–peridinin protein complex
BChl – bacteriochlorophyll
BR – bacteriorhodopsin
C. – *Chromatium*
Chl – chlorophyll
EADS – evolution-associated difference spectra
ESA – excited-state absorption
FCP – fucoxanthin–Chl-a–Chl-c protein
GSB – ground-state bleaching
Gya – giga (10^9) years ago
ICT – intramolecular charge-transfer (state)
IRF – instrument response function
LH1 (B875)/LH2 (B800–B850) – integral membrane antennas of purple bacteria
LHC – light-harvesting complexes (superfamily of proteins)
LHCII – integral membrane antenna of green algae and higher plants
N – number of conjugated C=C bonds
NIR – near-infrared
NPQ – non-photochemical quenching
OCP – orange carotenoid protein
OPA – optical parametric amplifier
PCP – peridinin–chlorophyll-a protein
R. – *Rhodobacter*
RC1(2) – reaction centre
S_0 – singlet ground state
S_x – x-th singlet excited state
WLC – white light continuum
XR – xanthorhodopsin

Contents

1. Introduction

1.1 General introduction

1.1.1 Personal (scientific) philosophy

Keeping in mind the full form of the degree I am applying for, *philosophiae doctor*, I hope that I am within my rights to start this thesis more generally, with a touch of philosophy. The philosophy I will try to present here is summarized in the motto:

Science can help, but the real change must occur in our brains, souls and hearts.

I think there are still more people who feel that the direction the world is going in *must* change, although they are still a minority. I am a member of this group. I simply do not believe that we should continue down the path upon which we have started, egoistically exploiting this planet and pretending that economical growth can go on forever. We should rather try hard to find new, better and sustainable ways of living. We must, however, overcome the self-delusion that all the changes will occur without any impact on our living standards. That this impact will come in the near future is inevitable. The earlier we realize that the dogmatic quest for increased consumption and economic growth is wrong, the more gradual and less painful will be the changes. The first step everybody needs to get used to is the conservation of resources. This can be achieved via the support of local food and goods suppliers, the use of public transport instead of cars, having household appliances repaired instead of buying new ones etc.

It is generally believed that science will provide humankind with a "safety net" in the form of the large-scale production of electricity in deserts, bacteria thriving on rubbish dumps producing fuel, or even more fantastic

notions such as the evacuation of humankind to a paradise planet through a wormhole. But do we want this? Do we want to continue living in the very same manner? Maybe, but I personally do not wish to participate. Although I am not against progress in general, which is demonstrated by my scientific interest in photosynthesis and a belief that accumulating knowledge in this field can *help* humankind get out of the energy crisis, I think we should not rely on science as a universal safety net. This makes people largely passive. We should take any great crisis, such as the one we face now, not as a tragedy, but as an opportunity and instruction to change ourselves.

I am aware of the (maybe legitimate) criticism which is raised by thoughts similar to those presented above. I know the concept of "the tragedy of the commons", which might serve critics as an argument against the conservation of resources (if you refrain from catching the last salmon in the river, your neighbour will do it, so it will be consumed anyway). However, I do not suffer from such scepticism and believe that humankind can do better than some bacterial colony that restricts itself to consuming resources without thinking about tomorrow. I think that all of us who think in the same or similar fashion should raise their voices, which I have tried to do with modesty in writing these introductory paragraphs. We should convince the new generations not to make the same mistakes as their parents and their grandparents before them. I hope they will have the ability to make good decisions and to be happy at even lower standards. If they succeed, they will be rewarded with more positive prospects than ours.

There is another difficulty with the public presentation of science as a universal saviour. Non-scientists can hardly recognize the basic motivation for research, which I believe is still the *curiosity* of the scientist. This is, however, a bit frustrating for a craftsman or farmer. Why should they support somebody's curiosity? They want us to invent pills against cancer or a water-fuelled car. The scientific community responds to these demands and adapts to meet public expectations. Otherwise, the budget for science would probably shrink. Consequently, we hear more and more often the mantra of *applied* research, research justified by reaching a definite and profitable final

goal. There are certainly some areas of research where one must keep such an aim in mind, but I do not think this should be confused with *science*; it should be given a proper name, *engineering*. However, this paragraph does not intend to criticize engineers, craftsmen, or farmers at all! If it is a criticism at all, then it is a criticism of scientists. We should not sell the idea of science for the pledge of a continuous supply of money. It is relevant to ask people whether they want to support science *per se*. Our task is to convince them that although science is something extra without which they can live, it should not be confused with luxury. Similarly, humankind could live without Shakespeare's work. Shakespeare did not enrich our lives in any material way. However, he did enrich us *somehow*. He enriched what could be called the *spirit of humanity*. Thus, if nothing else, Shakespeare's work and science are what makes us humans. Is it too little?

1.1.2 Biology, physics, and biophysics

I view biology as a science of diversity, while physics as a science of generality. Although biology tends to find common patterns in living organisms (e. g. DNA-based genetics, the search for common ancestors), it is still deep in its nature to be astonished by the multitude of life forms and variety on levels from molecules (usage of RNA instead of DNA to store genetic material in the case of some viruses) to ecosystems (unique marsupial-based ecosystems in Australia). Not so with physics. Any departure from established laws is considered as a stimulus for their revision. This approach proved very fruitful, as demonstrated by the failure of Newtonian mechanics at high speeds and micro scale leading to the development of special relativity and quantum mechanics. The generalizing tendency inherent to physics is well recognized in proposed theories such as The Grand Unification Theory or The Theory of Everything.

What is then the relation of biophysics to its parent disciplines? Discussing mainly experimental biophysics, it is vitally dependent on instrumentation. The pioneer application of the experimental method to a biological system usually leads to observations of general impact (confirmation of proposed double-helix DNA structure using X-ray

crystallography), while the routine usage of a method leads to revealing the diversity (for example the structures of tens of thousands of proteins known today). So it is also with pulsed lasers and their application in photosynthetic research. With every shortening of the pulse appeared a new temporal window to study. Similarly, implementation of a new method has a potential to reveal novel mechanisms, as was, for instance, the case of multiple-pulse experiments.[1–3] The femtosecond pump–probe spectroscopy method, mainly employed in studies presented in this thesis, is nowadays a well-established method. Although it may seem a less powerful tool than the recently developed state-of-the-art methods of femtosecond spectroscopy, it can still enrich science with interesting discoveries, as I hope will be demonstrated in this thesis.

1.2 Photosynthesis

Photosynthesis has influenced the Earth tremendously – its geosphere, hydrosphere, atmosphere, and biosphere. Its appearance was really a breakthrough. Life ceased to be passively dependent on energy from rather scarce complex molecules. Instead, it has since then primarily relied on an inexhaustible energy source – solar radiation.

The earliest version of photosynthesis was almost certainly anoxygenic (i.e. oxygen was not produced).[4] However, only the emergence of cyanobacterial-like oxygenic photosynthesis had a global impact. First affected was the geosphere, whose ferrous rocks underwent oxidation, serving as a buffer and preventing the massive escape of oxygen into the atmosphere. The presence of this and other buffers such as oceanic water has contributed to the restricted level of oxygen in the atmosphere. However, by around 2.4 Gya (giga years ago) the buffering capacity was no longer sufficient. As a result a massive escape of oxygen into the atmosphere occurred, so that about a tenth of the present-day oxygen concentration was reached.[4,5] Such an event must have had a disastrous effect on life because, at that time, oxygen was nothing but poison. Undoubtedly, massive extinction

must have followed. Quite symptomatically, this event is known as "The Great Oxygenation Event" or "The Oxygen Catastrophe"; it happened in the period 2.4–2.0 Gya.[5] Thus, no doubt the Earth was significantly influenced by the onset of the photosynthesis that changed its geosphere (oxidized rocks), hydrosphere (oxygenated oceans), atmosphere (oxygenated), and biosphere (extinction and many other consequences). But it was not enough. At ~1 Gya a second rise of oxygen concentration began, caused by increased photosynthetic activity mainly ascribed to photosynthetic eukaryotes.[4] Over the likely peak in the Carboniferous era,[5] the present-day oxygen concentration of ~21% was reached.

Each coin has two sides. That oxygen is poisonous is true. However, life turned a disadvantage, the presence of oxygen, into an advantage: it started utilizing oxygen as a terminal oxidant. These newly-established oxidative metabolic pathways provided organisms with far more energy than anaerobic ones. However, since then there has been a price to pay for this increased profit: a need to protect against the threat of oxidative damage (photoprotection is a central topic in Research Section B).

The only reason oxygen is produced in oxygenic photosynthesis is that it is the by-product of water oxidation which aims at electron acquisition. From the point of view of availability, water is definitely one of the best candidates as a source of electrons for photosynthesis. However, to withdraw electrons from water is not an easy task. Why? An oxygen/water redox pair has a high and positive reduction potential (0.82 V). It means that water does *not* readily donate electrons. To get electrons out of it, an even stronger oxidation agent must be applied. This is the oxidized special pair of chlorophylls ($P680^+$) in the reaction centre (RC). To compare, oxidized special pair of (non-cyano)bacterial RC is not a strong enough oxidant,[6] disabling the use of water as an electron source in bacterial photosynthesis. They, thus, depend on other electron donors such as H_2S, H_2 etc.

Despite the large diversity of photosynthetic organisms, there are only two general modes of photosynthesis: RC-based and rhodopsin-based.[4,7] There are two main types of RC, which are distinguished according to the terminal acceptors of the electrons, a Fe-S cluster for type-1 RC (RC1) and a

quinone for type-2 RC (RC2). Some organisms use only one type of RC (RC1: green sulphur bacteria, heliobacteria, and acidobacteria; RC2: filamentous anoxygenic bacteria and purple bacteria), while some use both types (cyanobacteria and all photosynthetic eukaryotes, which are the endosymbiotic descendants of cyanobacteria).[4,7] Compared to the substantial complexity of RC-based energy conversion, photosynthesis employing rhodopsins is much simpler. The absorption of a photon by the terpenoid retinal results in its isomerization and through changes in the protein it eventually leads to the translocation of protons[a] across the membrane. So established electrochemical gradient can then be used to drive cellular processes. These "photosynthetic rhodopsins" (as opposed to rhodopsins with sensory or other function) are exclusively found in prokaryotes.

Also the pigment composition of RCs is rather conservative and is restricted to Chl-a, Chl-d, BChl-a, BChl-b, (bacterio)pheophytins and a handful of carotenoids; rhodopsin-based photosynthesis with a single pigment retinal does not enrich the list much. A far higher diversity in both structure and pigment composition is observed in light-harvesting complexes (Section 1.3.5). However, before diving into this diversity, the next chapter will address the question of its evolution.

1.2.1 Underwater photosynthesis

Although competition for light also operates in terrestrial ecosystems, underwater conditions are much more complex. The following factors influence the intensity of light at a particular wavelength and depth below the water's surface: absorption and/or scattering by water, (coloured) dissolved organic carbon (usually <0.2 µm particles), particulate organic matter (>0.2 µm particles), and organisms, mainly phytoplankton.[9,10] The absorption of longer wavelengths (>600 nm) dominates in pure water, which is best demonstrated in >100 m depths by the prevailing blue light.[10,11] It implies

[a] Chloride ions instead of protons are translocated by halorhodopsin. However, it is used to maintain osmotic balance. Thus the definition of photosynthesis according to Blankenship[8] is not met for this pump.

that light scattering by water molecules, acting predominantly on shorter wavelengths, is relatively less significant than water absorption. Dissolved organic matter influences the light conditions both by the enhancement of Rayleigh scattering ("standard" and coloured dissolved organic matter) and absorption below 500 nm (coloured dissolved organic matter), thus leading to the gradual attenuation of short wavelengths with increasing depth. Combined with the absorption of water at longer wavelengths, in coastal waters rich in (coloured) dissolved organic matter green light penetrates the deepest.[10] Particulate organic matter does not influence a specific spectral region because Mie scattering acting on particles with sizes roughly matching the wavelength of light is independent of wavelength. When the absorption of organisms higher in the water column is taken into account together with all other effects, a multitude of photic niches can be identified based on varying relative contributions of these effects.[10]

The presence of such niches undoubtedly led to the evolution of pigments and light-harvesting complexes. The variety of light harvesting strategies among underwater organisms contrasts with the uniformity in terrestrial photosynthetic life, underscoring the importance of the aquatic environment in the development of the diversity of photosynthesis.[12]

1.2.2 Photosynthetic pigments

From the structural point of view, there are two main classes of photosynthetic pigments, tetrapyrroles and terpenoids. The former group can be further divided into two subgroups, comprising linear (phycobilins) and cyclic tetrapyrroles (Chls, BChls, (bacterio)pheophytins). The distinction between Chls and BChls, however, does not follow a chemical, but "phylogenetic" logic: *bacteria* contain *bacterio*chlorophylls (excluding cyanobacteria); chlorophylls are employed by cyanobacteria and photosynthetic eukaryotes. Chemically, tetrapyrroles are classified according to the degree of reduction of the macrocycle into the following categories: porphyrins (Chl-c_1, Chl-c_2; least reduced), chlorins (Chls a, b, d, f; BChls c, d, e, f), and bacteriochlorins (BChls a, b, g; most reduced).

The latter group, terpenoids (alternatively called isoprenoids), is further divided into many subgroups according to the number of isoprene units forming the molecule. However, only two of these subgroups contain photosynthetic pigments: diterpenoids (retinal) and tetraterpenoids (carotenoids). Among carotenoids purely hydrocarbon (carotenes) and oxygen-containing molecules (xanthophylls) are further recognized. The information given in this and the foregoing paragraph is lucidly summarized in Table 1-1.

Pigments used in photosynthesis serve several functions:[8,13–18]

- light harvesting of photons ((B)Chls a,b,c,d, BChl-e, BChl-f, BChl-g, phycobilins, carotenoids)
- photochemical energy transduction in RCs (Chl a, Chl d, Bchl a, Bchl b, BChl-g)
- photoprotection (carotenoids)
- structural function ((B)Chls, carotenoids).

The roles of carotenoids will be dealt with in more detail in Section 1.3.

Photosynthetic pigments	Tetrapyrroles	Linear	Phycobilins		Phycocyanobilin, phycoerythrobilin...
		Cyclic	Porphyrins		Chl-c_1, Chl-c_2
			Chlorins		Chls a, b, d, f; BChls c, d, e, f
			Bacteriochlorins		BChls a, b, g
	Terpenoids	Diterpenoids	Retinal		
		Tetraterpenoids	Carotenoids	Carotenes	neurosporene, lycopene, *β*-carotene…
				Xanthophylls	spheroidene, spheroidenone, zeaxanthin, peridinin

Table 1-1: Categories of pigments.

What gives pigments their colour? It is the absorption of photons of a specific energy in the visible part of the electromagnetic spectrum. The colour perceived by humans then corresponds to the transmitted/reflected

photons. The part of the molecule responsible for its colour is the *chromophore*. It consists of alternating single and double bonds, forming a *conjugated system* (*N* stands for the number of conjugated C=C bonds). It is created by connecting multiple atomic p-orbitals into a molecular π-orbital, whose delocalized electrons can be promoted into a higher electronic excited state upon photon absorption. The longer the conjugation length, the more are the electronic transitions shifted to lower energies. This can be in a simplified way rationalized using the analogy with the particle-in-a-box case:[b] the π-orbital can be seen as a box for the electron. The energy of the particle is proportional to $1/x^2$, x standing for the size of the box. This simplified picture is, however, directly applicable only to linear symmetric polyenes. Cyclization and the presence of central atoms and functional groups may represent a stronger effect, effectively overwhelming the trend of decreasing energy with conjugation length.

1.3 Carotenoids

Compared to other natural pigments, carotenoids are very diverse, with more than 1000 different structures identified so far.[19] Belonging to the class of tetraterpenoids, most carotenoids contain 40 carbon atoms. Their actual structures may differ in several aspects: the conjugation length; the presence of atoms other than carbon and hydrogen (oxygenated xanthophylls are the most common, but also sulphur-containing carotenoids exist[20]); the presence of various functional groups; symmetry. These features affect the properties of carotenoids, resulting in their purpose-specific utilization.

Carotenoids serve multiple functions in photosynthesis. As light harvesters, their absorption maxima are usually in the blue-green spectral region, thus effectively covering the window not accessible to (B)Chls. They also act as photoprotective agents, posing a multiple-stage defence system against oxidative damage. Additionally, they serve as crucial structural

[b] I thank Tjaart Krüger for drawing my attention to this analogy.

elements; their absence may even result in improper folding or failure in the higher-order structure formation of some photosynthetic pigment-protein complexes.[21,22]

Carotenoids are, however, employed not only by photosynthetic organisms. They appear in almost all organisms, highlighting their importance. In non-photosynthetic organisms, their role is mostly a paraphrase of their photoprotective function in photosynthesis, which is apparent from the name they are usually given in this context: *antioxidants*.

As evident from the information given so far, carotenoids are required by almost all organisms. Yet until recently, they have been believed to be synthesized only by microorganisms, plants and fungi. However, in 2010 genes for carotenoid synthesis were found and proven to be expressed also in pea aphids, making these animals exceptional in being independent of dietary carotenoids.[23]

1.3.1 Excited states of carotenoids

The photophysics of carotenoids is rather distinctive compared to other pigments. The uniqueness consists mainly in the following features: the final state of the strongly one-photon-allowed transition, which gives the carotenoids their characteristic colour, is not the lowest excited state; the fluorescence quantum yield is very low and for carotenoids with $N \geq 8(9)$[24] fluorescence does not take place from the lowest excited state, violating Kasha's rule.

The background of carotenoid photophysics is based on studies of symmetric polyenes. These compounds belong to the C_{2h} point symmetry group, which is basically a set of symmetry operations relevant to the particular object such as the whole molecule, its orbital or molecular electronic state. The symmetry operations of the C_{2h} group are the identity, the two-fold rotational axis, the plane of symmetry, and the centre of inversion (Figure 1-1). The orbitals and states express different behaviour

under the action of symmetry operations. Based on this behaviour, they are given specific symbols such as B_u or A_g.[c]

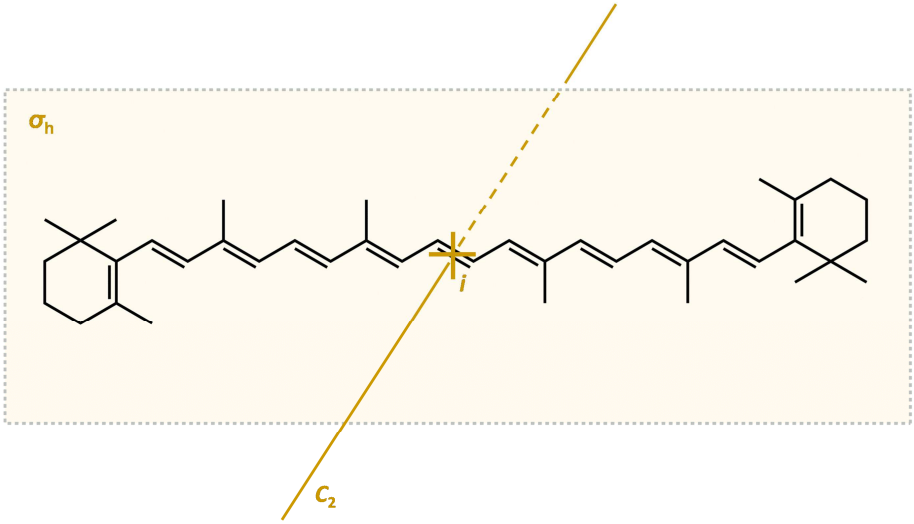

Figure 1-1: Symmetry operations of the C_{2h} point symmetry group: identity, two-fold rotational axis (C_2), plane of symmetry (σ_h), and centre of inversion (i).

The quantity crucial for governing the electronic transition is the transition dipole moment. It is defined as

$$\boldsymbol{\mu_{nm}} = \int \psi_n \hat{\boldsymbol{\mu}} \psi_m dV \qquad (1.1)$$

where ψ_m and ψ_n are wavefunctions of the initial and final states, respectively, and $\hat{\boldsymbol{\mu}}$ is the electric dipole moment operator. For the transition to be allowed, the integral must have a nonzero value. The essential condition for this is that the overall function to be integrated must be totally symmetric, i.e. symmetric with respect to all symmetry operations of the point symmetry group.[25,d] In terms of the C_{2h} group, the function must possess the A_g symmetry.

[c] Uppercase letters (e.g. B_u) are used for states, lowercase (e.g. b_u) for orbitals.[25]

[d] The integral may, however, turn out to be zero for reasons different than symmetry.

Thus, we are able to derive the selection rules based on symmetry. The ground state of polyenes is of A_g, while the strongly absorbing excited state is of B_u symmetry. For polyenes with $N \leq 3$ the latter is also the lowest excited state. However, for longer polyenes ($N > 3$) a state of A_g symmetry has a lower energy than the B_u state. Thus the lowest singlet excited state, S_1, is the state with A_g symmetry, while the S_2 state is that with B_u symmetry. This order of energy states is also relevant to all naturally occurring carotenoids, because for most of them the conjugation length is between 7 and 13 (Figure 1-2).[24] The basic selection rule, which follows from symmetry considerations and application of Eq. (1.1), determines the A_g–B_u transition as allowed, but A_g–A_g as forbidden. The other selection rule emerges when the electronic correlation (interaction between electrons in the molecule) is taken into account. Additional pseudoparity signs will appear in the designations of symmetries of the states,[26] so the carotenoid ground state will be of A_g^- symmetry and the first two excited singlet states of A_g^- and B_u^+ symmetry, respectively. The additional selection rule requires a change in pseudoparity symbols of the states involved in the allowed transition. As stated in the beginning of this section, the strongly one-photon-allowed transition of carotenoids is not the S_0–S_1 (A_g^-–A_g^-), but S_0–S_2 (A_g^-–B_u^+). This statement now becomes supported by theory because only

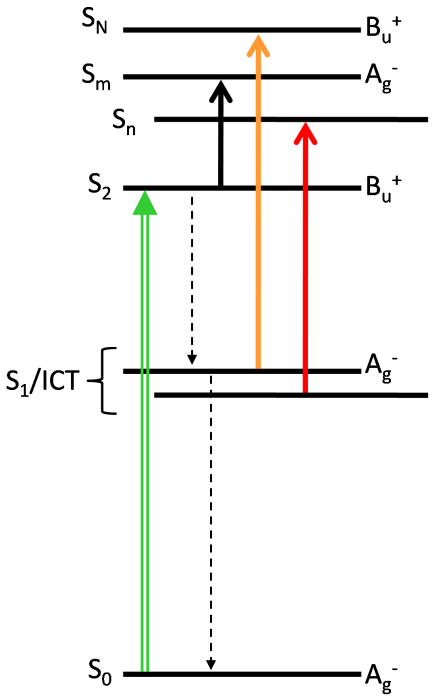

Figure 1-2: Energy level diagram of a carbonyl carotenoid. The double arrow corresponds to excitation, while the other solid arrows symbolize typical transitions recorded during a time-resolved measurement (orange arrow: S_1–S_N, red arrow: ICT–S_n, black arrow: S_2–S_m transition). The dashed arrows represent internal conversion processes.

the latter transition fulfils both selection rules. However, one must keep in mind that the analysis given here is completely valid only for totally symmetric molecules with respect to the C_{2h} point symmetry group. Any departure from this total symmetry results in weakening of the selection rules. A typical example is that the S_1-S_0 transition may become slightly allowed, as it is for the highly-substituted carotenoid peridinin.

The low fluorescence yield is the result of the extremely fast internal conversion processes. The lifetime of the S_2 state is thus on the order of several hundreds of femtoseconds.[24] The mechanistic explanation of this ultrashort lifetime is still a matter of debate, mainly because of its unexpected dependence on conjugation length. From calculations it follows that another electronic state, which possesses the B_u^- symmetry, is present in the S_2-S_1 gap,[27] which would cause rapid depopulation of the S_2 state. However, convincing experimental evidence is still missing.[28] The lifetime of the S_1 state is typically one to two orders of magnitude longer than that of the S_2 state, but it is still short enough to efficiently compete with radiative transition. The origin of the short S_1 lifetime is better understood than that of the S_2 state. Because the decrease of frequency of the C=C stretching mode in ^{13}C labelled β-carotene led to S_1 lifetime prolongation,[29] the strong vibronic coupling between S_0 and S_1 states through this vibrational mode is the key factor determining the fast S_1 deexcitation.

1.3.2 Carbonyl carotenoids

I have devoted a special section to these carotenoids because they are of much interest in most of the studies presented in the Research Section (only the study presented in Section 4 does not refer to them).

Carbonyl carotenoids contain a carbonyl group in conjugation. Figure 1-3 shows two important representatives: peridinin, the most extensively studied carbonyl carotenoid, and spheroidenone, which is central to Research Section B of this thesis. The conjugated carbonyl group imparts to these pigments a unique property not observed in other carotenoids. Carbonyl carotenoids exhibit polarity-dependent behaviour, which is facilitated by the presence of an additional electronic state in the excited-state manifold, the

intramolecular charge-transfer (ICT) state. Spectroscopic features associated with this state become more pronounced with any increase of polarity of the environment. Such behaviour is the consequence of the large dipole moment of the ICT state, which is stabilized in the polar environment.[30–32] The spectroscopic "markers" of the ICT state are manifested in the transient absorption spectra as i) a positive band red-shifted from the S_1-S_N transition (Ref. 33, for definitions of the transitions see Figure 1-2) and ii) a negative feature associated with the stimulated emission, which can be observed in the NIR region.[31] Moreover, the appearance of the ICT-related spectroscopic features is associated with S_1 state lifetime shortening.[31,33] The ICT state thus probably induces stronger coupling to the ground state.[32]

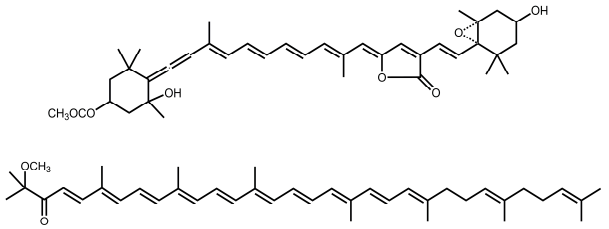

Figure 1-3: Structures of two important carbonyl carotenoids, peridinin (above) and spheroidenone (below).

Despite extensive theoretical and experimental efforts, the structural nature of this state and its relation to the S_1 state are still a matter of debate. Basically four models have been proposed:

1) The ICT state is a separate electronic state distinct from the S_1 state (S_1 + ICT).[33–35]
2) The ICT state is strongly coupled to the S_1 state (S_1/ICT; see Figure 1-2).[30,36–38]
3) The ICT state is indeed the S_1 state with a significant charge-transfer character (S_1 = ICT).[39,40]
4) The ICT state is formed via the mixing of S_1 and S_2 states ((S_1 + S_2)/ICT).[32]

It is beyond the scope of this thesis to analyse all aspects of the respective models. However, some comments may be made here. First, none of the models is robust enough to account for all experimental observations,

mainly the lifetime shortening with an increasing polarity of the environment. The early model 1) has been mainly challenged by the fact that both S_1-like and ICT-like bands decay with identical time constants. Moreover, because of the problematic description of charge-transfer states by the time-dependent density functional theory,[41] model 1) has also lost theoretical support.[34] The uniform dynamics of the broad peridinin transient absorption signal has led to the proposal of model 2), in which the S_1/ICT potential energy surface has two energy minima.[30,36] Model 3) of Shima et al.[39] has not been rejected in its entirety, although the particular findings related to this model were challenged, mainly due to the fact that the most dramatic polarity-induced changes take place in the ground state.[42] However, we have recently revived this model by matching the S_1-S_3 transition of 8′-apo-β-carotenal in hexane with the ICT-S_n transition (see Figure 1-2), hypothesizing that the ICT state is indeed the S_1 state. The more polar the environment, the more is the molecule distorted from the idealized C_{2h} symmetry. Therefore the S_1-S_3 transition, forbidden in the C_{2h} symmetry group, becomes allowed. The opposite is true of the S_1-S_N transition. Thus, the more polar the environment, the stronger is the S_1-S_3 transition and the weaker the S_1-S_N transition, matching experimental results. Model 4) resulted from the logical, but so far not considered, assumption that the ICT state cannot be formed from the ground-state conformation. Instead, it requires a conformation following relaxation from the higher (S_2) state.[32] This assumption has a realistic basis in the fact that weak fluorescence from the lowest-lying state of peridinin has been observed,[43] but corresponding absorption has never been observed. This model can thus be simplified as "from below is not the same as from above".

Throughout the Research Sections only the "traditional" S_1/ICT model is considered, which is mainly given by the restricted amount of established competing models at the date of origin of the contributions. I personally believe that the model closest to reality is #3 with some features of model #4, although it is still necessary to test these models on a wider range of carbonyl carotenoids to allow a more generalised conclusion. The crucial properties of model #4 are i) the mixing of the S_1 (A_g^-) state with the S_2 (B_u^+) state

resulting in the observed dipolar characteristics of the ICT state, and ii) the fact that "from below is not the same as from above". Interestingly, the predicted doubly-excited character of the ICT state added to its B_u^+-related ionicity[32] is achieved very elegantly in that the ICT state *is* the S_1 (A_g^-) state, which is known to possess this doubly excited character[e].

The polarity-dependent behaviour described above is not expressed by all carbonyl carotenoids. For example for spheroidenone in solution the polarity-induced effects are rather insignificant, both in the spectral (almost no ICT-like band) and temporal (insignificant lifetime shortening) domain.[42] One could ascribe this feature to the long conjugation length of spheroidenone ($N = 10$ compared to $N = 7$ for peridinin, neglecting the carbonyl), leading to the relative weakness of ICT–S_n compared to S_1–S_N transition. However, one of the findings appearing in this thesis is that even spheroidenone can produce a strong ICT-related signal – not in solution, but in the protein (see Section 6/Ref. 44). The key difference between spheroidenone in solution with inactive ICT state and other carbonyl carotenoids (peridinin, fucoxanthin, siphonaxanthin), whose ICT state may be activated in polar solvents, is the configuration of the carbonyl group. While it is s-*cis* in the case of spheroidenone,[45] it is s-*trans* in peridinin,[46] fucoxanthin,[47] and siphonaxanthin.[48] The s-*cis* position of the carbonyl group thus leads to its effective isolation from the conjugation. Therefore, we have proposed that the configuration of the spheroidenone carbonyl group in the LH1 complex, where the ICT state is activated, is s-*trans* (see Section 6/Ref. 44). Thus the conditions for ICT state activation should be extended, both the high polarity of the environment *and* the s-*trans* configuration of the carbonyl with respect to the conjugated chain being seen as critical.

[e] I am aware of an apparent disagreement with the earlier statement regarding departure from the C_{2h} symmetry in polar environment and thus weakening the doubly-excited character of the ICT state. However, this departure is probably only partial, similarly as is the ionic character. Overall, these tendencies may match the predicted pattern of the S_1 = ICT state possessing both the ionic and doubly excited character.

1.3.3 Light harvesting function of carotenoids

Naturally occurring carotenoids have *N* ranging from 7 to 13. They absorb light mainly from the blue-green region. This spectral window is almost inaccessible to (B)Chls[24] which, being capable of photochemical energy conversion, are the final acceptors of excitation energy. Thus, carotenoids transfer the excitation energy to (B)Chls, both S_2 and S_1 states serving as energy donors (Figure 1-4).

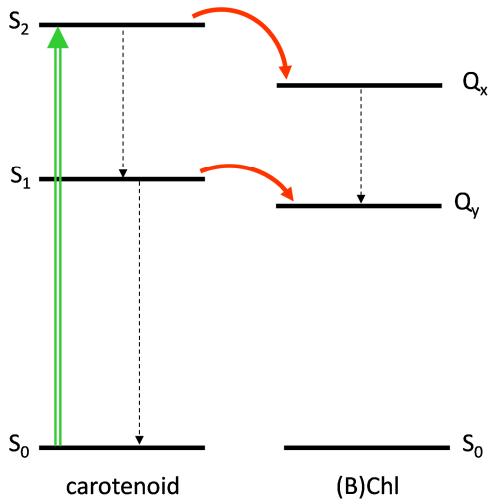

Figure 1-4: Illustration of carotenoid–to–(B)Chl energy transfer process.

What governs the choice of carotenoids with specific conjugation lengths in light harvesting? Carotenoids with $N < 7$ absorb mainly UV radiation, so the reason they are not employed may be that the photon flux becomes restricted for shorter wavelengths. On the other hand, accessing of longer-wavelength light by carotenoids with $N > 13$ may be advantageous. However, there are limitations regarding the position of the S_1 state, which is one of the donor states from which energy is transferred to (B)Chls. For the $N > 13$ carotenoids the S_1 state is too low to transfer energy not only to Q_y of Chl-a, but also to BChl-a.[19]

The energy transfer processes are strongly dependent on mutual orientation and the distance of the donor and acceptor pigments, which are fixed at proper positions thanks to the protein scaffold (see Section 1.3.5).

One would not consider carotenoids as ideal partners for energy transfer. The lifetimes of S_1 (order of units to tenths of picoseconds) and S_2 (less than 300 fs) states, which are energy donors for (B)Chls, are much shorter compared to other photosynthetic pigments such as (B)Chls (for Q_y on the order of nanoseconds). Energy transfer thus must effectively compete with these short intrinsic lifetimes (i.e. lifetime for the case when no process with origin "outside" the molecule takes place). Widespread appearance of carotenoids as light harvestors in photosynthetic systems demonstrates that energy transfer is indeed successful in this competition.

How can one determine the energy transfer times (τ_{ET}) or the related rate constant k_{ET}, for which the following relation

$$k_{ET} = \frac{1}{\tau_{ET}} \qquad (1.2)$$

is valid? This question is often asked because it is a prerequisite for determination of energy transfer efficiencies Φ_{ET}:

$$\Phi_{ET} = \frac{k_{ET}}{k_{ET} + k_N} = 1 - \frac{\tau_t}{\tau_N}, N = 1,2 \qquad (1.3)$$

where τ_N is the intrinsic lifetime of the particular carotenoid excited state with the following relation to the associated rate constant k_N:

$$\tau_N = \frac{1}{k_N} \qquad (1.4)$$

One could think that the main difficulty in determining k_{ET} is a sufficient time resolution of the measuring device. Even when this problem is solved, from such measurements one obtains only the total rate constant k_t,[f] which is the inversed value to the total lifetime given in Eq. (1.3):

$$k_t = k_N + k_{ET} \qquad (1.5)$$

To obtain k_{ET}, one must obviously know k_N or τ_N. This is, however, not a trivial task. The most usual means is to measure the intrinsic lifetimes of the carotenoid in solution. Yet, two difficulties come with this approach. The

[f] Alternatively, the total rate constant is denoted as *k* without any index, as in Section 7.

first is the choice of the solvent and the other arises from the fact that the actual configuration of the pigment in solution may differ from that in protein. The former problem may be rationalized by the fact that the lifetimes of carotenoid excited states do not significantly depend on solvent properties. There is, however, an exception to this rule, i.e. the case of carbonyl carotenoids. Peridinin, the most extreme example from this group, has a S_1 lifetime of ~160 ps in hexane, while it is ~10 ps in methanol.[31,33] One could, in principle, estimate the τ_N in protein from the relative magnitude of the ICT state signal with respect to that of the S_1 state because it is considered as a measure of the charge-transfer character of the S_1/ICT state, which is in turn related to the S_1/ICT lifetime.[30,33,44] The strategy would be to find a solvent which produces an ICT state signal of similar relative magnitude to that in the protein, and to use the τ_N from measurements in solution. The trouble with this approach is the potential presence of other signals in the protein, interfering with the desired ICT state signal.

Even "normal" (non-carbonyl) carotenoids are, however, not trouble-free, which brings us to the other problem of the actual carotenoid configuration in protein. Carotenoids with the conjugation extended to the terminal rings may be stabilized in the protein in a configuration, which results in a different effective conjugation length than in solution. Having been theoretically confirmed,[49] these and similar modifications were hypothesized to be expressed in case of zeaxanthin in LH1 (see Section 7/Ref. 50) and diadinoxanthin/diatoxanthin in XLH (see Section 4/Ref. 51). Examples combining the problem of polarity with that of extended conjugation length in protein are the cases of carbonyl carotenoids hydroxyechinenone in the orange carotenoid protein (OCP)[52] and spheroidenone in LH1 (see Research Section B/Refs. 44 and 50).

There is another approach which could lead to τ_N determination. It is a modification of the so called pump-dump-probe experiment,[35,53] in which one of the pulses pre-excites the acceptors, (B)Chls, while the other two pulses are used to carry out a standard pump-probe experiment, but with acceptors already excited, thus incapable of receiving energy from carotenoids. To my best knowledge, no study using this approach has been

published. One of the obstacles may be that all the traps in the particular pigment-protein complex must be pre-excited. Taking into account the size of the pigment protein complexes and the amount of (B)Chls (more than 20 in LH2), extremely high-intensity pulses would need to be applied, leading to interference with higher-order nonlinear effects. Thus apart from the rare exceptions where it is possible to simply uncouple the energy transfer pathway,[54] determination of the τ_N and, consequently, efficiency of the particular energy transfer pathway, remains only approximate.

Let us assume we are able to approximately determine τ_1 and τ_2. What is then the appropriate procedure for determining the efficiencies of particular energy transfer routes? To show the procedure, I will use hypothetical "measured" values (Table 1-2), which, however, are realistic. Using the last part of Eq. (1.3), the efficiencies of both channels are calculated. Moreover, there is another approach for dealing with efficiencies, used e.g. in Ref. 55. In this case, the actual efficiencies are weighted by the branching ratio. To specify, the efficiency of the S_1-Q_y channel (0.75) is multiplied by the percentage of population arriving at the S_1 level (0.5). I call this efficiency a *weighted efficiency*, which amounts to 37,5% for the S_1-Q_y channel. To add to the complexity, the sum of the weighted efficiencies amounts to the *total efficiency*. It can be alternatively calculated as a ratio of areas below the fluorescence excitation spectrum and the absorption spectrum. The independent determination of total efficiency from the fluorescence excitation spectra is useful because when combined with the known efficiency of the S_2-mediated energy transfer, one can calculate k_1, as has been done for peridinin–chlorophyll-a protein, PCP.[56] Figure 1-5 illustrates the issues mentioned above.

Carotenoid in solution (measured values)		Carotenoid in protein (measured values)		Channel efficiency	Weighted efficiency
τ_2	200 fs	τ_{t2}	100 fs	50%	50.0%
τ_1	20 ps	τ_{t1}	5 ps	75%	37.5%
				total efficiency	**87.5%**

Table 1-2: Illustration of different concepts of efficiencies of energy transfer processes.

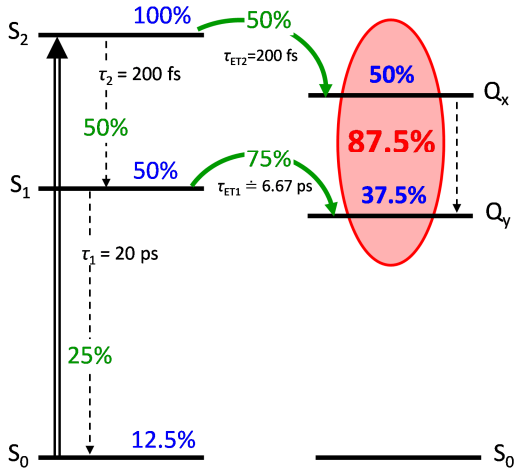

Figure 1-5: Graphical illustration of different concepts of efficiencies of energy transfer processes.

The discussion held so far has not dealt with the *mechanisms* of energy transfer. The theoretical approach may provide the investigator with additional information and physical insights into energy transfer processes. The energy transfer rate can be generally expressed as

$$k_{ET} = \frac{1}{\hbar^2 c} V^2 J \qquad (1.6)$$

where V is the coupling between the donor and acceptor states and J is the spectral overlap between donor emission and acceptor absorption ensuring energy conservation. Thus the only term which is specific to the particular energy transfer mechanism is V. Depending on its form, either a short-range Dexter (electron exchange) or long-range Förster (Coulombic) energy transfer occurs. The former mechanism involves an exchange of electrons and therefore proceeds over shorter distances (<10 Å), while the latter can be thought of as enabled by virtual photon exchange and thus proceeding at distances of up to ~100 Å with electrons remaining within the same molecule during the process (Figure 1-6).[25,57]

The coupling term in the original **Förster theory** is described only in terms of dipole-dipole interaction:

$$V = \frac{1}{4\pi\varepsilon_0}\frac{\mu_D \mu_A \kappa}{{r_{AD}}^3} \qquad (1.7)$$

μ_A and μ_D being the transition dipole moments of donor and acceptor, respectively, κ is the orientation factor taking into account the vector nature of μ_A and μ_D, and r_{AD} is the distance between donor and acceptor molecules. From the combination of Eq. (1.6) and Eq. (1.7) it becomes clear that the energy transfer rate for the Förster mechanism scales as $1/{r_{AD}}^6$.

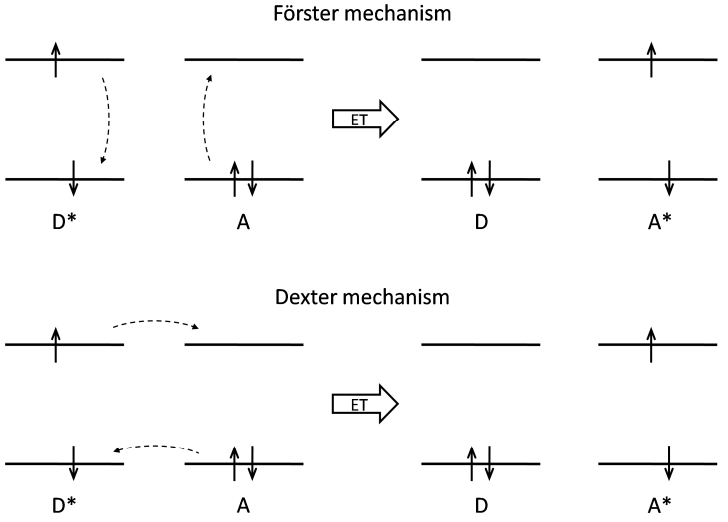

Figure 1-6: Förster and Dexter mechanisms of energy transfer. D – donor, A – acceptor, ET – energy transfer.

There are, however, limitations for the use of the coupling defined in this way. The dipole-dipole approximation is only applicable for interchromophoric distances much larger than the sizes of the chromophores. Otherwise this approximation breaks down and no longer reproduces the experimentally obtained values. In phycobiliproteins, the dipole-dipole approximation was found to give reasonable results for interchromophore distances >40 Å and reproduce some aspects of energy transfer even for distances in the range of 25–40 Å.[58] The problem is that in most light

harvesting systems the donor–acceptor distance is well below 20 Å.[19] Moreover, carotenoids as donors are rather elongated molecules (>20 Å), so the calculations using the dipole-dipole approximation produce only rough estimations in most carotenoid-containing systems.

Another problem to tackle is the high carotenoid S_1-mediated energy transfer efficiency. The S_0-S_1 transition possesses a virtually zero transition dipole moment (carotenoid S_0-S_1 absorption is not observed), which precludes the traditional dipole-dipole-based Förster mechanism from operating (see Eq. (1.7)). The Dexter mechanism would be a logical candidate for the energy transfer mechanism because it i) operates at short distances and ii) does not depend on transition dipole moments.[59–61] However, calculations have proved that the Dexter contribution to the carotenoid–BChl energy transfer is negligible.[62,63] To cope with these challenges, the Coulombic interaction was expanded to higher orders including dipole-quadrupole, dipole-octupole, and quadrupole-quadrupole couplings. However, such multipole approximation improved the results only slightly compared to the dipole-dipole approximation.[57,64] The reason for this is, in my opinion, the same in most cases of point-form di- or multipolar approach breakdown: this approach is not applicable to closely-packed molecules. Consequently, in order to properly describe the couplings and energy transfer processes between closely packed molecules, the shape of the molecules must be taken into account.[57]

This is accomplished by the method called the *transition density cube* (TDC).[65] Here, the transition densities of both donor and acceptor are represented by an array of discrete charges, and the Coulombic interaction between each pair is determined. These contributions are then summed to receive the overall interchromophore coupling. This method reached a reasonable match between experimentally and theoretically obtained values of k_{ET}. The full 3D information of transition densities is also accounted for in the method called *transition charge from electrostatic potential*, which was presented as numerically more efficient and not suffering from finite grid errors compared to TDC.[66] These methods thus kill two birds with one stone – they i) do not break down at short interchromophore distances and,

consequently, ii) are able to reproduce carotenoid S_1-mediated energy transfer times and efficiencies, inaccessible within the framework of dipole-dipole approximation.

An additional piece of information must be mentioned here. Because in the Förster mechanism the electrons remain attached to original molecules, only processes in which no change in spin multiplicity of either the donor or the acceptor occurs are allowed. This rule is a consequence of the forbidden nature of transitions between singlet and triplet states.[25] From this point of view, the mechanism described in the text above is the singlet–singlet energy transfer process:[25]

$$^1D^* + {}^1A \rightarrow {}^1D + {}^1A^*.$$

The coupling term of the **Dexter energy transfer** mechanism scales exponentially with interchromophore distance r_{AD}:

$$V^2 \propto e^{-\frac{2r_{AD}}{l}} \qquad (1.8)$$

where l is the van der Waals radius of the donor-acceptor pair, which is the sum of the van der Waals radii of the donor and the acceptor. Compared to the Förster mechanism with $1/r_{AD}^6$ dependence, k_{ET} of Dexter scales exponentially with r_{AD}. This explains the fact that the Dexter mechanism operates at rather shorter distances to the Förster mechanism.

As mentioned above, although the Dexter mechanism was invoked to account for short-range singlet–singlet energy transfer in LH2,[59–61] its participation has later been recognized as minor.[62,63] To my best knowledge, singlet–singlet Dexter mechanism does not dominate in any known light-harvesting complex, although its participation in energy transfer at distances shorter than 10 Å cannot be ruled out.

The situation is, however, the reverse for energy transfer processes involving a change in spin multiplicity. These are forbidden for the Förster mechanism (see above) and are thus realm of the Dexter mechanism. Some of these processes relevant to photosynthesis should be mentioned:

$^3D^* + {}^3A \rightarrow {}^1D + {}^1A^*$

(D = Chl, A = O_2; generation of harmful singlet oxygen)

$^3D^* + {}^1A \rightarrow {}^1D + {}^3A^*$

(D = Chl, A = carotenoid: quenching of Chl triplets by carotenoids)

$^1D^* + {}^1A \rightarrow {}^3D + {}^3A^*$

(D = O_2, A = carotenoid: singlet oxygen quenching by carotenoids).

The first process is harmful and the next two are employed by photosynthetic organisms to prevent it and the consequent harmful processes from occurring. This topic will be dealt with in more detail in the next section.

1.3.4 Photoprotective function of carotenoids

There is no doubt that photosynthetic organisms are vitally dependent on light. However, having too much of a good thing is no longer beneficial. This applies also to light. In fact, the problem is not in the light itself, but in the almost ubiquitous oxygen.

The process of Chl excitation can be schematically described as follows:

$$^1Chl \xrightarrow{h\nu} {}^1Chl^*$$

There are a number of scenarios for the fate of $^1Chl^*$, say, in the photosynthetic antenna (Figure 1-7):

1) it will return back to ground state while emitting a photon, i.e. fluorescence
2) the excitation energy will be dissipated as heat by means of internal conversion
3) the excitation energy will be finally used to drive the photochemical reactions of photosynthesis

4) Chl molecule will undergo an intersystem crossing, resulting in Chl triplet excited state formation:

$^1Chl^* \rightarrow {}^3Chl^*$.

$^3Chl^*$ can react with oxygen, whose ground state is of triplet nature, to produce excited singlet oxygen (see also Section 1.3.3):

$^3Chl^* + {}^3O_2 \rightarrow {}^1Chl + {}^1O_2{}^*$.

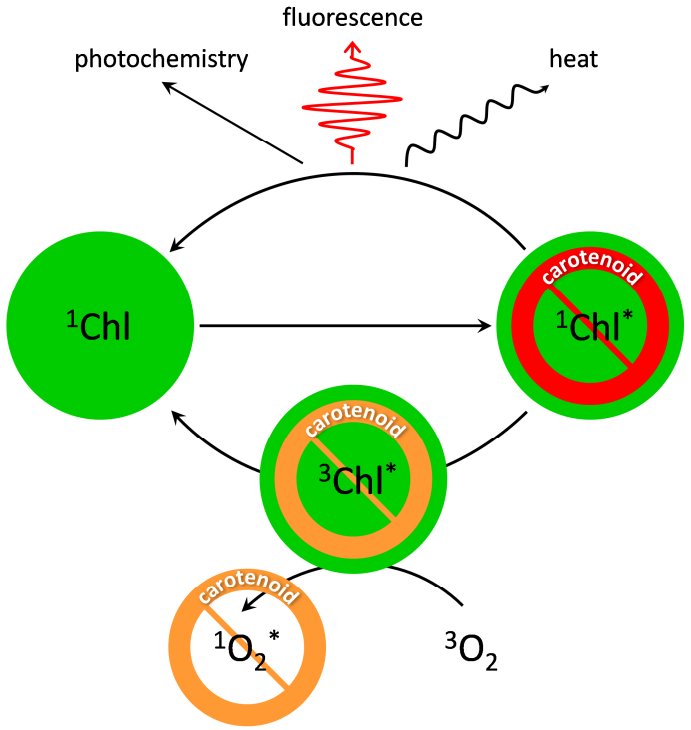

Figure 1-7: Multiple ways of chlorophyll deexcitation. Carotenoid photoprotective action is also illustrated by red circular symbols: for the responsive mechanism of NPQ, i.e. the one able to reflect actual needs for photoprotection, the symbol is red; the non-responsive mechanisms are given an orange mark.

Thus, in the processes described in point #4 there is a danger of overexcitation by the strong light because singlet oxygen is an extremely reactive agent, causing damage to biomolecules including DNA and proteins.

The higher the light intensity, the larger the amount of singlet oxygen created, and the greater the damage. Of course, photosynthetic organisms have developed mechanisms to prevent such photooxidative damage, the central role in these processes being played by carotenoids. Essentially all (photosynthetic) organisms employ carotenoids, so the list given above should be enriched by another item:

5) photoprotective mechanisms, mediated by carotenoids, promote deexcitation of Chl molecules.

The last point is intentionally put vaguely because carotenoid photoprotection operates on multiple levels, capable of lowering the concentration of all potentially dangerous species, i.e. $^1Chl^*$, $^3Chl^*$, and $^1O_2{}^*$ (see Figure 1-7). The processes of $^3Chl^*$ and $^1O_2{}^*$ quenching are rather straightforward and can be simplified as follows:[18]

$$^3Chl^* + {}^1Car \rightarrow {}^1Chl + {}^3Car^*$$

$$^1O_2{}^* + {}^1Car \rightarrow {}^3O_2 + {}^3Car^*.$$

Neither process, both requiring a change of spin multiplicity, can be mediated by Coulomb coupling (Förster mechanism).[25,57,67,68] Instead, these processes proceed via the Dexter electron exchange mechanism (see Section 1.3.3 and Refs. 16,25,68). The common feature is the formation of a carotenoid triplet excited state, $^3Car^*$, which must be low enough to become an acceptor of excitation energy from $^3Chl^*$ and/or $^1O_2{}^*$. The energy of this triplet state is, consequently, harmlessly dissipated as heat. The mechanism of $^1Chl^*$ quenching, known as non-photochemical quenching (NPQ) and most intensively studied in higher plants, is still a vividly debated topic. At present, it seems that multiple mechanisms are responsible for NPQ.[69–72] Less frequent studies on NPQ in other organisms mainly rely on the observation of correlations.[73] An important feature of NPQ is that its efficiency can be regulated according to environmental conditions, making it a “responsive” photoprotective mechanism, as opposed to “non-responsive”

ones such as $^{3}Chl^{*}$ and $^{1}O_{2}^{*}$ quenching (see Figure 1-7). This topic is discussed in greater detail in the Introduction of Section 8.

To add to the largely physical quenching mechanisms discussed so far, carotenoids are also capable of the chemical quenching of singlet oxygen,[74] which must participate only to limited extent in total quenching capacity due to its low quenching rate.[75]

1.3.5 Carotenoid–protein complexes

1.3.5.1 Antenna complexes

Antennas are pigment-protein complexes whose function is to capture photons and to transfer energy of the light quantum into the RC. They are utilized by all chlorophyll-based photosynthetic organisms.[76] The reason for employing antennas is that the photon flux is insufficient to maintain the costly biochemical machinery, which converts light energy into chemical energy, at continuous operation. Instead, the strategy is to harvest more photons by relatively "cheap" antennas and to supply the rare RCs with a sufficient energy flux.[8]

Integral membrane antennas			Peripheral membrane antennas
Fused	Core	Accessory	
PSI RC	**LH1**	LH2	**PCP**
RC of GSB	CP 43 & CP 47	LHC superfamily	phycobilisomes
RC of heliobacteria		**acpPC**	chlorosomes
		FCP	FMO complex
		XLH	
		LHCI	
		LHCII etc.	

Table 1-3: Classification of antennas. Antennas relevant to this thesis are given in bold.

The classification of antennas is given in Table 1-3. The first criterion expresses the affinity of the antenna to the membrane: it can either be embedded in the membrane and thus insoluble in water (*integral membrane antenna*), or simply anchored to the membrane, but otherwise exposed to the water-based cellular environment (*peripheral membrane antenna*). The former group is further divided into three subgroups. The *fused antenna* is an inseparable part of the RC. The *core antenna* is in an intimate contact with the RC, but is usually biochemically separable from it. The connection of the *accessory antenna* with the RC is usually only temporary. Such antennas are present in variable amounts depending on growth conditions.[8]

A single antenna contains a number of pigment types and a photosynthetic organism usually contains a number of kinds of antenna. The direction of energy flow is given by the funnel effect (Figure 1-8). It is virtually a paraphrase of the law of conservation of energy. The energy is transferred from shorter-wavelength (higher energy) absorbing pigments to longer-wavelength (lower energy) absorbing pigments. The trap for this "energy in motion" is the RC. An excellent illustration of the funnel effect is provided by the purple bacterial photosynthetic unit (Figure 1-9). It consists of LH2 and LH1 complexes together with the RC. The shortest-wavelength absorbing BChls appear in the LH2 complex and are called B800. In the same complex are also found B850 BChls, to which is energy transferred from B800. Next, energy flows to LH1 (B875) and from there to the RC. Moreover, in each complex are also found carotenoids, which transfer energy to BChls, also in agreement with the funnel concept. It must be noted that there are exceptions that do not follow the funnel concept

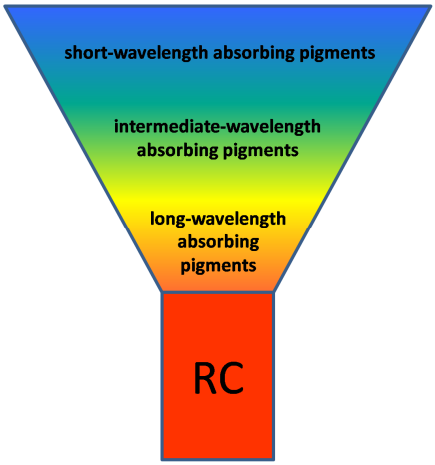

Figure 1-8: The funnel effect depicting the energy flow within antennas and between them.

because in some cases the energy of the acceptor may be slightly lower than that of the donor. However, at physiological temperatures the energy related to thermal motion of molecules also adds to the donor-side energy, resulting in an apparent “uphill” energy transfer.

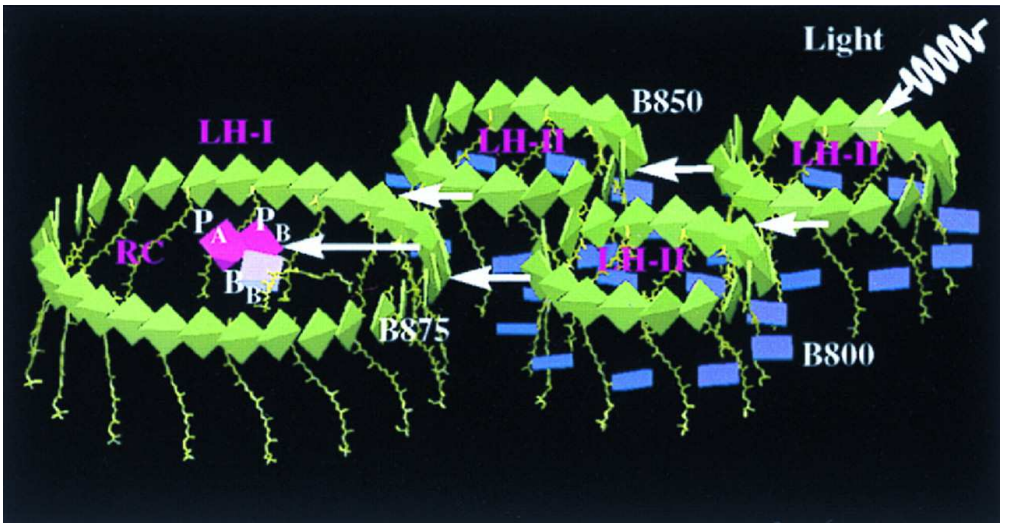

Figure 1-9: The purple bacterial photosynthetic unit consisting of LH2 and LH1 antennas, and the RC. The figure is reprinted from Ref. 16.

The pigment-protein complexes relevant to this thesis will be described below.

1.3.5.1.1 Chlorophyll-a–chlorophyll-c_2–peridinin protein complex (acpPC)

Chlorophyll-a–chlorophyll-c_2–peridinin protein complex (acpPC) is a membrane-bound light-harvesting complex of peridinin-containing dinoflagellates (*Dinoflagellata*).[77] Because this pigment-protein complex belongs to the LHC (light-harvesting complexes) superfamily, it shares homology with the LHCII complex of green plants. As LHCII, acpPC also consists of three transmembrane helices,[78] but does not contain the short α-helix found on the lumenal side of LHCII of higher plants.[79] However, the most prominent difference between the plant LHCs and acpPC is the pigment composition. While plant LHCs generally bind Chl-a and Chl-b (thus, belonging to the Cab group of LHC superfamily), the acpPC of

dinoflagellates employs Chl-a and Chl-c,[77] and thus belongs to the Cac group.[80] The carotenoids in acpPC are peridinin and diadinoxanthin. The stoichiometric ratio (Chl-a:Chl-c:peridinin:diadinoxanthin) is 7:4:12(10):2.[81] Because the total of pigment molecules is even higher than for LHCII (Chl-a:Chl-b:lutein:violaxanthin:neoxanthin is 7:5:2:1:1), it is argued in Ref. 38 that the numbers from the stoichiometric ratio may be higher than the actual amount of pigments per monomer. The reason for this is that the expected tight packing of molecules would lead to excitonic interactions as in LHCII, where the maximum of the Q_y band is consequently shifted to ~680 nm.[82] No such shift is observed in acpPC, suggesting that the number of pigments per monomer is likely lower. The role of peridinin in acpPC is mainly light harvesting, which is almost certainly not the role of diadinoxanthin in this complex (see Section 5/ Ref. 38 and Ref. 83). One is tempted to conclude that diadinoxanthin is important for photoprotection because the diadinoxanthin-diatoxanthin pair constitutes the xanthophyll cycle in diatoms.[84] There are, however, no studies so far correlating diadinoxanthin/diatoxanthin accumulation with ^{1}Chl-a* fluorescence quenching. Regarding ^{3}Chl-a* quenching by diadinoxanthin, recent studies of Ref. 85 and Ref. 86 do not support this idea. It can consequently be hypothesized that diadinoxanthin/diatoxanthin in acpPC directly quenches singlet oxygen. This idea is tempting mainly in the case of diatoxanthin because its effective conjugation length is close to that of lycopene (N = 11), the most efficient singlet oxygen quencher.[87] However, experimental evidence on diatoxanthin accumulation in acpPC in significant amounts is, to my best knowledge, missing.

1.3.5.1.2 Xanthophytes light harvesting (XLH) complex

Xanthophytes (*Xanthophyceae*) are counted among the heterokont algae (*Heterokontophyta*, *Chromophyta*) and their antenna thus belongs to the Cac group. However, xanthophytes and their antenna, XLH, are unique. First, they do not contain the carbonyl carotenoid fucoxanthin, which is the dominant carotenoid in other heterokonts; additionally, xanthophytes usually contain negligible amounts of Chl-c.[88] Thus, although the XLH apoprotein

probably does not differ much from the fucoxanthin–Chl-a–Chl-c protein (FCP) of other groups,[80,89] a distinct name and abbreviation was chosen for it. XLH contains Chl-a, diadinoxanthin, diatoxanthin, heteroxanthin, and vaucheriaxanthinester in the molar ratio of 28:11:5:4:1. Although diadinoxanthin-diatoxanthin are pigments considered as responsible for photoprotection in algae,[90,91] in XLH diadinoxanthin serves as a light-harvesting pigment, capable of energy transfer to Chl-a (see Section 4/Ref. 51).

1.3.5.1.3 Light-harvesting 1 (LH1) complex

The LH1 complex is the core light harvesting complex of purple photosynthetic bacteria. It is part of the photosynthetic unit, which also contains the LH2 complex and the RC. The RC is encircled by the LH1 complex, so the two components form a 1:1 RC-LH1 stoichiometric couple.[92] The basic structural organization of both LH1 and LH2 complexes is the same. The minimal structural unit is a pair of α-helical polypeptides with low molecular weight (5 – 7 kDa), called α- and β-subunit.[92] The LH2 is a circular oligomer of $\alpha\beta$ pairs, while LH1 can assume a number of configurations: it can be seen as an ellipse with 15 $\alpha\beta$ pairs as in *Rhodopseudomonas palustris*,[92] or with 16 $\alpha\beta$ pairs as in *Rhodospirillum rubrum*;[93] alternatively, it can form an S-shaped supercomplex[94] consisting of two 14-mers of $\alpha\beta$ pairs interconnected by the PufX protein.[95] In LH2 there are two spectroscopic sets of BChl-a molecules, with absorption maxima of around 800 nm (B800, one BChl-a molecule per $\alpha\beta$ monomer) and 850 nm (B850, two BChl-a molecules per $\alpha\beta$ monomer).[96,97] The red-shift of B850 BChls is achieved by an excitonic interaction established between closely packed molecules[64] and by the interaction of BChls with the protein.[98] In case of LH1 only one spectroscopic set of BChl-a molecules is accommodated. The absorption maximum of these molecules, also partially reached thanks to excitonic interactions, is usually around 875 nm, so their designation is B875.[99] Two BChl-a molecules per $\alpha\beta$ pair are accommodated. While only one carotenoid per $\alpha\beta$ monomer was identified in LH2 crystal

structures,[96,97] in LH1, using biochemical methods, either one,[100] or two carotenoids were found.[101]

1.3.5.2 Carotenoid as an antenna in xanthorhodopsin

As the name indicates, xanthorhodopsin (XR) belongs to the family of opsins[g]. There are two classes of opsins. Type I opsins are employed by prokaryotes, algae and fungi.[102] They function mainly as light-responsive ion pumps or photoreceptors and contain a retinal as a chromophore (opsins with retinal are called rhodopsins). Crucial for the action of these opsins is the light-induced photoisomerization of retinal from its all-*trans* to 13-*cis* configuration (Figure 1-10). Type II opsins are utilized by higher eukaryotes, where they are mainly responsible for vision.[102,103] Here, the photoisomerization reaction is different: 11-*cis* retinal or its analogue[104,105] is converted into the all-*trans* configuration. The two types of opsins do not seem to be related and have rather appeared independently in evolution.[106] This finding is surprising taken into account the similarity of their structure: opsins of both groups contain seven transmembrane helices;[107] at least in rhodopsins, the retinal is covalently bound to the conserved lysine in the seventh helix, forming the protonated Schiff base.[102,103] Such protonation is crucial for a red-shift of the absorption of the bound retinal. Deprotonation, which is of crucial importance to the function of most opsins, leads to a blue-shift of the absorption spectrum with a maximum on the UV/VIS region threshold.[108] It has been demonstrated that changing the local environment close to the Schiff base leads to dramatic changes of retinal absorption maximum, which can be tuned in a more than 200-nm range.[109] Such amino

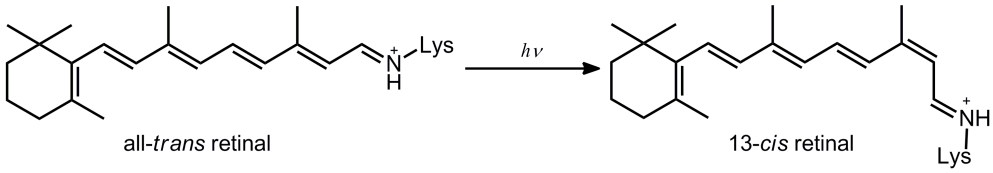

Figure 1-10: Photoisomerization reaction of retinal in Type I opsins.

[g] The nomenclature is not uniform. As opsin is sometimes considered the whole pigment-protein complex, sometimes only the apoprotein.[105]

acid alterations thus must be responsible for the wide range of spectral types of rhodopsins.[109]

An important functional subgroup of Type I rhodopsins are those capable of proton translocation across the membrane. Generally, the absorption of light by retinal causes not only its isomerization, but also initiates a sequence of structural changes and proton-transfer processes, which lead to the overall movement of the proton across the membrane against the electrochemical potential. The states of the so-called photocycle can also be characterized spectrally.[102] The established proton gradient can then be used for ATP synthesis, active transport across the membrane, or cell motility.

The most thoroughly studied proton translocating rhodopsin is the archaeal bacteriorhodopsin.[110] Another proton pump of *Archaea* is archaerhodopsin.[111] Large-scale gene surveys have revealed that protoerhodopsin[112] and related proteins are frequently used by marine bacteria.[113,114] One must point out that not all proteorhodopsins are proton pumps.[115] XR, on which this section is focused, seems to be a rather unique and interesting member of the Type I rhodopsin group.[116] A eukaryotic representative of this functional group is the leptosphaeria rhodopsin.

XR is a proton pump from an extremely halophilic bacterium *Salinibacter ruber*.[116] However, it has not become famous for its ability to transport protons across the membrane against the electrochemical gradient. Its fame arose from the fact that it employs the simplest known antenna, a single carotenoid molecule called salinixanthin. The carbonyl carotenoid salinixanthin is locked into the protein so that its ring containing the conjugated carbonyl group is effectively isolated from the rest of the conjugation. That is the reason why no ICT state is detected in the transient absorption spectra of XR. Ultrafast spectroscopic investigation has also revealed that energy is transferred to retinal from the S_2 state of salinixanthin with an efficiency of ~40%.[54,116] The mutual orientation of retinal and salinixanthin axes is 46°, which seems to be a compromise between an orientation best suited for maximum light capture (90°) and most efficient energy transfer (0°).[117]

There are indications that the concept of carotenoid antenna is not unique to XR. Based on sequence similarity, it could be rather common in the "Xanthorhodopsin clade".[118] However, direct evidence of carotenoid involvement in energy transfer to retinal in another system than in XR is still missing, the most promising being the case of gloeobacter rhodopsin.[118]

References

1. Brixner T, Stenger J, Vaswani HM, Cho M, Blankenship RE, Fleming GR (2005) Two-dimensional spectroscopy of electronic couplings in photosynthesis. *Nature* 434: 625–628.
2. Collini E, Wong CY, Wilk KE, Curmi PMG, Brumer P, Scholes GD (2010) Coherently wired light-harvesting in photosynthetic marine algae at ambient temperature. *Nature* 463: 644–647.
3. Butkus V, Zigmantas D, Valkunas L, Abramavicius D (2012) Vibrational vs. electronic coherences in 2D spectrum of molecular systems. *Chem Phys Lett* 454: 40–43.
4. Hohmann-Marriott MF, Blankensip RE (2011) Evolution of photosynthesis. *Annu Rev Plant Biol* 62: 515–548.
5. Holland HD (2006) The oxygenation of the atmosphere and oceans. *Philos Trans R Soc Lond B* 361: 903–15.
6. Visschers RW, Vulto SIE, Jones MR, van Grondelle R, Kraayenhof R (1999) Functional LH1 antenna complexes influence electron transfer in bacterial photosynthetic reaction centers. *Photosynth Res* 59: 95–104.
7. Bryant DA, Frigaard NU (2006) Prokaryotic photosynthesis and phototrophy illuminated. *Trends Microbiol* 14: 488–96.
8. Blankenship RE (2002) Molecular mechanisms of photosynthesis. *Blackwell Science*, Oxford, UK.
9. Tiwari SP, Shanmugam P (2011) An optical model for the remote sensing of coloured dissolved organic matter in coastal/ocean waters. *Estuar Coast Shelf S* 93: 396–402.
10. Stomp M, Huisman J, Stal LJ, Matthijs HCP (2007) Colorful niches of phototrophic microorganisms shaped by vibrations of the water molecule. *ISME J* 1:271–282.
11. Johnsen S, Sosik H (2004) Shedding light on light in the ocean. *Oceanus* 43: 1–5.
12. Stomp M, Huisman J, de Jongh F, Veraart AJ, Gerla D, Rijkeboer M, Ibelings BW, Wollenzien UIA, Stal LJ (2004) Adaptive divergence in pigment composition promotes phytoplankton biodiversity. *Nature* 432: 104–107.
13. Scholes GD, Fleming GR, Olaya-Castro A, van Grondelle R (2011) Lessons from nature about solar light harvesting. *Nat Chem* 3: 764–774.
14. Chen M, Schliep M, Willows RD, Cai ZL, Neilan BA, Scheer H (2010) A red-shifted chlorophyll. *Science* 329: 1318–1319.
15. Heinnickel M, Golbeck JH (2007) Heliobacterial photosynthesis. *Photosynth Res* 92: 35–53.

16. Hu XC, Damjanovic A, Ritz T, Schulten K (1998) Architecture and mechanism of the light-harvesting apparatus of purple bacteria. *Proc Natl Acad Sci USA* 95: 5935–5941.
17. Tomo T, Okubo T, Akimoto S, Yokono M, Miyashita H, Tsuchiya T, Noguchi T, Mimuro M (2007) Identification of the special pair of photosystem II in a chlorophyll d-dominated cyanobacterium. *Proc Natl Acad Sci USA* 104: 7283–7288.
18. Cogdell RJ (1985) Carotenoids in photosynthesis. *Pure Appl Chem* 57: 723–728.
19. Polívka T, Frank HA (2010) Molecular factors controlling photosynthetic light harvesting by carotenoids. *Acc Chem Res* 43: 1125–1134.
20. Yurkov VV, Beatty JT (1998) Aerobic anoxygenic phototrophic bacteria. *Microbiol Mol Biol R* 62: 695–724.
21. Ng IW, Adams PG, Mothersole DJ, Vasilev C, Martin EC, Lang HP, Tucker JD, Hunter CN (2011) Carotenoids are essential for normal levels of dimerisation of the RC–LH1–PufX core complex of *Rhodobacter sphaeroides*: Characterisation of R-26 as a crtB (phytoene synthase) mutant. *Biochim Biophys Acta* 1807: 1056–1063.
22. Plumley FG, Schmidt GW (1987) Reconstitution of chlorophyll a/b light-harvesting complexes–xanthophyll-dependent assembly and energy transfer. *Proc Natl Acad Sci USA* 84: 146–150.
23. Moran NA, Jarvik T (2010) Lateral transfer of genes from fungi underlies carotenoid production in aphids. *Science* 328: 624–627.
24. Polívka T, Sundström V (2004) Ultrafast dynamics of carotenoid excited states: From solution to natural and artificial systems. *Chem Rev* 104: 2021–2071.
25. Gilbert A, Baggott J (1991) Essentials of Molecular Photochemistry. *CRC Press*, London, UK.
26. Pariser R (1956) Theory of the electronic spectra and structure of the polyacenes and of alternant hydrocarbons. *J Chem Phys* 24: 250–268.
27. Koyama Y, Rondonuwu FS, Fujii R, Watanabe Y (2004) Light-harvesting function of carotenoids in photosynthesis: The roles of the newly found $1^1B_u^-$ state. *Biopolymers* 74: 2–18.
28. Polívka T, Sundström V (2009) Dark excited states of carotenoids: Consensus and controversy. *Chem Phys Lett* 477: 1–11.
29. Nagae H, Kuki M, Zhang JP, Sashima T, Mukai Y, Koyama Y (2000) Vibronic coupling through the in-phase, C=C stretching mode plays a major role in the $2A_g^-$ to $1A_g^-$ internal conversion of *all-trans-β*-carotene. *J Phys Chem A* 104: 4155–4166.
30. Frank HA, Bautista JA, Josue J, Pendon Z, Hiller RG, Sharples FP, Gosztola D, Wasielewski MR (2000) Effect of the solvent environment on the spectroscopic

properties and dynamics of the lowest excited states of carotenoids. *J Phys Chem B* 104: 4569–4577.

31. Zigmantas D, Polívka T, Hiller RG, Yartsev A, Sundström V (2001) Spectroscopic and dynamic properties of the peridinin lowest singlet excited states. *J Phys Chem A* 105: 10296–10306.
32. Wagner NL, Greco JA, Enriquez MM, Frank HA, Birge RR (2013) The nature of the intramolecular charge transfer state in peridinin. *Biophys J* 104: 1314–1325.
33. Bautista JA, Connors RE, Raju BB, Hiller RG, Sharples FP, Gosztola D, Wasielewski MR, Frank HA (1999) Excited state properties of peridinin: observation of a solvent dependence of the lowest excited singlet state lifetime and spectral behavior unique among carotenoids. *J Phys Chem B* 103: 8751–8758.
34. Vaswani HM, Hsu CP, Head-Gordon M, Fleming GR (2003) Quantum chemical evidence for an intramolecular charge-transfer state in the carotenoid peridinin of peridinin–chlorophyll–protein. *J Phys Chem B* 107: 7940–7946.
35. Papagiannakis E, Larsen DS, van Stokkum IHM, Vengris M, Hiller RG, van Grondelle R (2004) Resolving the excited state equilibrium of peridinin in solution. *Biochemistry* 43: 15303–15309.
36. Zigmantas D, Hiller RG, Yartsev A, Sundström V, Polívka T (2003) Dynamics of excited states of the carotenoid peridinin in polar solvents: dependence on excitation wavelength, viscosity, and temperature. *J Phys Chem B* 107: 5339–5348.
37. Linden PA, Zimmermann J, Brixner T, Holt NE, Vaswani HM, Hiller RG, Fleming GR (2004) Transient absorption study of peridinin and peridinin–chlorophyll a–protein after two-photon excitation. *J Phys Chem B* 108: 10340–10345.
38. Polívka T, van Stokkum IHM, Zigmantas D, van Grondelle R, Sundström V, Hiller RG (2006) Energy transfer in the major intrinsic light-harvesting complex from *Amphidinium carterae*. *Biochemistry* 45: 8516–8526.
39. Shima S, Ilagan RP, Gillespie N, Sommer BJ, Hiller RG, Sharples FP, Frank HA, Birge RR (2003) Two-photon and fluorescence spectroscopy and the effect of environment on the photochemical properties of peridinin in solution and in the peridinin–chlorophyll protein from *Amphidinium carterae*. *J Phys Chem A* 107: 8052–8066.
40. Durchan M, Fuciman M, Šlouf V, Keşan G, Polívka T (2012) Excited-state dynamics of monomeric and aggregated carotenoid 8'-apo-*β*-carotenal. *J Phys Chem A* 116: 12330–12338

41. Dreuw A, Head-Gordon M (2004) Failure of time-dependent density functional theory for long-range charge-transfer excited states: the zincbacteriochlorin-bacteriochlorin and bacteriochlorophyll-spheroidene complexes. *J Am Chem Soc* 126: 4007–4016.
42. Zigmantas D, Hiller RG, Sharples FP, Frank HA, Sundström V, Polívka T (2004) Effect of a conjugated carbonyl group on the photophysical properties of carotenoids. *Phys Chem Chem Phys* 6: 3009–3016.
43. Zimmermann J, Linden PA, Vaswani HM, Hiller RG, Fleming GR (2002) Two-photon excitation study of peridinin in benzene and in the peridinin chlorophyll a-protein (PCP). *J Phys Chem B* 106: 9418–9423.
44. Šlouf V, Chábera P, Olsen JD, Martin EC, Qian P, Hunter CN, Polívka T (2012) Photoprotection in a purple phototrophic bacterium mediated by oxygen-dependent alteration of carotenoid excited-state properties. *Proc Natl Acad Sci USA* 109: 8570–8575.
45. Takaichi S, Furihata K, Harashima K (1991) Light-induced changes of carotenoid pigments in anaerobic cells of the aerobic photosynthetic bacterium, *Roseobacter denitrificans* (*Erythrobacter* species OCh 114): reduction of spheroidenone to 3,4-dihydrospheroidenone. *Arch Microbiol* 155: 473–476.
46. Haugan JA, Englert G, Glinz E, Liaaen-Jensen S (1992) Algal carotenoids. 48. Structural assignments of geometrical isomers of fucoxanthin. *Acta Chem Scand* 46: 389–395.
47. Ricketts TR (1971) The structures of siphonein and siphonaxanthin from *Codium fragile. Photochemistry* 10: 155.
48. Mimuro M, Nishimura Y, Takaichi S, Yamano Y, Ito M, Nagaoka S, Yamazaki I, Katoh T, Nagashima U (1993) The effect of molecular structure on the relaxation processes in carotenoids containing carbonyl group. *Chem Phys Lett* 213: 576–580.
49. Cerezo J, Zúñiga J, Bastida A, Requena A, Cerón-Carrasco JP, Eriksson LA (2012) Antioxidant properties of *β*-carotene isomers and their role in photosystems: Insights from ab initio simulations. *J Phys Chem A* 116: 3498–3506.
50. Šlouf V, Fuciman M, Dulebo A, Kaftan D, Koblížek M, Frank HA (2012) Carotenoid charge transfer states and their role in energy transfer processes in LH1–RC complexes from aerobic anoxygenic phototrophs. *J Phys Chem B* 117: 10987−10999.
51. Durchan M, Tichý J, Litvín R, Šlouf V, Gardian Z, Hříbek P, Vácha F, Polívka T (2012) Role of carotenoids in light-harvesting processes in an antenna protein from the chromophyte *Xanthonema debile*. *J Phys Chem B* 116: 8880−8889.

52. Polívka T, Kerfeld CA, Pascher T, Sundström V (2005) Spectroscopic properties of the carotenoid 3′-hydroxyechinenone in the orange carotenoid protein from the cyanobacterium *Arthrospira maxima*. *Biochemistry* 44: 3994–4003.

53. Papagiannakis E, Vengris M, Larsen DS, van Stokkum IHM, Hiller RG, van Grondelle R (2006) Use of ultrafast dispersed pump–dump–probe and pump–repump–probe spectroscopies to explore the light-induced dynamics of peridinin in solution. *J Phys Chem B* 110: 512–521.

54. Polívka T, Balashov SP, Chábera P, Imasheva ES, Yartsev A, Sundström V, Lanyi JK (2009) Femtosecond carotenoid to retinal energy transfer in xanthorhodopsin. *Biophys J* 96: 2268–2277.

55. Papagiannakis E, Kennis JTM, van Stokkum IHM, Cogdell RJ, van Grondelle R (2002) An alternative carotenoid-to-bacteriochlorophyll energy transfer pathway in photosynthetic light harvesting. *Proc Natl Acad Sci USA* 99: 6017–6022.

56. Zigmantas D, Hiller RG, Sundström V, Polívka T (2002) Carotenoid to chlorophyll energy transfer in the peridinin–chlorophyll-a protein complex involves an intramolecular charge transfer state. *Proc Natl Acad Sci USA* 99: 16760–16765.

57. Scholes GD (2003) Long-range resonance energy transfer in molecular systems. *Annu Rev Phys Chem* 54: 57–87.

58. Doust AB, Wilk KE, Curmi PMG, Scholes GD (2006) The photophysics of cryptophyte light-harvesting. *J Photochem Photobiol A* 184: 1–17.

59. Naqvi KR (1980) The mechanism of singlet–singlet excitation energy transfer from carotenoids to chlorophyll. *Photochem Photobiol* 31: 523–524.

60. van Grondelle R (1985) Excitation energy transfer, trapping and annihilation in photosynthetic systems. *Biochim Biophys Acta* 811: 147–195.

61. Cogdell RJ, Frank HA (1987) How carotenoids function in photosynthetic bacteria. *Biochim Biophys Acta* 895: 63–79.

62. Damjanović A, Ritz T, Schulten K (1999) Energy transfer between carotenoids and bacteriochlorophylls in light-harvesting complex II of purple bacteria. *Phys Rev E* 59: 3293–3311.

63. Nagae H, Kakitani T, Katoh T, Mimuro M (1993) Calculation of the excitation transfer-matrix elements between the S_2 or S_1 state of carotenoid and the S_2 or S_1 state of bacteriochlorophyll. *J Chem Phys* 98: 8012–8023.

64. Hsu CP, Walla PJ, Head-Gordon M, Fleming GR (2001) The role of the S_1 state of carotenoids in photosynthetic energy transfer: The light-harvesting complex II of purple bacteria. *J Phys Chem B* 105: 11016–11025.

65. Krueger BP, Scholes GD, Fleming GR (1998) Calculation of couplings and energy transfer pathways between the pigments of LH2 by the ab initio transition density cube method. *J Phys Chem B* 102: 5378–5386.

66. Madjet ME, Abdurahman A, Renger T (2006) Intermolecular coulomb couplings from ab initio electrostatic potentials: Application to optical transitions of strongly coupled pigments in photosynthetic antennae and reaction centers. *J Phys Chem B* 110: 17268–17281.

67. Naqvi KR, Steel C (1970) Exchange-induced resonance energy transfer. *Chem Phys Lett* 6: 29–32.

68. Dexter DL (1953) A theory of sensitized luminiscence in solids. *J Chem Phys* 21: 836–50.

69. Holt N, Zigmantas D, Valkunas L, Li XP, Niyogi KK, Fleming GR (2005) Carotenoid cation formation and the regulation of photosynthetic light harvesting. *Science* 307: 433–436.

70. Ruban AV, Berera R, Ilioaia C, van Stokkum IHM, Kennis JTM, Pascal AA, van Amerongen H, Robert B, Horton P, van Grondelle R (2007) Identification of a mechanism of photoprotective energy dissipation in higher plants. *Nature* 450: 575–578.

71. Bode S, Quentmeier CC, Liao PN, Hafi N, Barros T, Wilk L, Bittner F, Walla PJ (2009) On the regulation of photosynthesis by excitonic interactions between carotenoids and chlorophylls. *Proc Natl Acad Sci USA* 106: 12311–12316.

72. Müller MG, Lambrev P, Reus M, Wientjes E, Croce R, Holzwarth AR (2011) Singlet energy dissipation in the photosystem II light-harvesting complex does not involve energy transfer to carotenoids. *ChemPhysChem* 11: 1289–1296.

73. Kaňa R, Kotabová E, Sobotka R, Prášil O (2012) Non-photochemical quenching in cryptophyte alga *Rhodomona ssalina* is located in chlorophyll a/c antennae. PLoS One 7: e29700.

74. Liebler DC (1993) Antioxidant reactions of carotenoids. *Ann N Y Acad Sci* 691: 20–31.

75. Wilkinson F, Helman WP, Ross AB (1993) Quantum yields for the photosensitized formation of the lowest electronically excited singlet state of molecular oxygen in solution. *J Phys Chem Ref Data* 22: 113–262.

76. Green BR, Parson WW, Eds (2003) Light-harvesting antennas in photosynthesis. *Kluwer Academic Press*, Dordrecht, The Netherlands.

77. Falkowski PG, Katz ME, Knoll AH, Quigg A, Raven JA, Schofield O, Taylor, FJR (2004) The evolution of modern eukaryotic phytoplankton. *Science* 305: 354–360.

78. Green BR, Pichersky E (1994) Hypothesis for the evolution of three-helix Chl a/b and Chl a/c light-harvesting antenna proteins from two-helix and four-helix ancestors. *Photosynthesis Research* 39: 149–162.

79. Kühlbrandt W, Wang DN, Fujiyoshi Y (1994) Atomic model of plant light-harvesting complex by electron crystallography. *Nature* 367: 614–621.

80. Boldt L, Yellowlees D, Leggat W (2012) Hyperdiversity of genes encoding integral light-harvesting proteins in the dinoflagellate *Symbiodinium* sp. *PLoS One* 7: e47456.

81. Hiller RG, Wrench PM, Gooley AP, Shoebridge G, Breton J (1993) The major intrinsic light-harvesting protein of *Amphidinium*–characterization and relation to other light-harvesting proteins. *Photochem Photobiol* 57: 125–131.

82. van Amerongen H, van Grondelle R (2001) Understanding the energy transfer function of LHCII, the major light-harvesting complex of green plants. *J Phys Chem B* 105: 604–617.

83. Šlouf V, Fuciman M, Johanning S, Hofmann E**,** Frank HA, Polívka T (2013) Low-temperature time-resolved spectroscopic study of the major light-harvesting complex of *Amphidinium carterae*. *Photosynth Res.* doi: 10.1007/s11120-013-9900-8

84. Yamamoto HY (1985) Xanthophyll cycles. *Methods Enzymol* 110: 303–312.

85. Di Valentin M, Salvadori E, Agostini G, Biasibetti F, Ceola S, Hiller R, Giacometti GM, Carbonera D (2010) Triplet–triplet energy transfer in the major intrinsic light-harvesting complex of *Amphidinium carterae* as revealed by ODMR and EPR spectroscopies. *Biochim Biophys Acta* 1797: 1759–1767.

86. Niedzwiedzki DM, Jiang J, Lo CS, Blankenship RE (2013) Spectroscopic properties of the chlorophyll-*a*–chlorophyll-c_2–peridinin protein complex (acpPC) from the coral symbiotic dinoflagellate *Symbiodinium*. *Photosynth Res*. doi: 10.1007/s11120-013-9794-5

87. Di Mascio P, Kaiser S, Sies H (1989) Lycopene as the most efficient biological carotenoid singlet oxygen quencher. *Arch Biochem Biophys* 274: 532–538.

88. Baldisserotto C, Ferroni L, Moro I, Fasulo MP, Pancaldi S (2005) Modulations of the thylakoid system in snow xanthophycean alga cultured in the dark for two months: comparison between microspectrofluorimetric responses and morphological aspects. *Protoplasma* 226: 125–135.

89. Gardian Z, Tichý J, Vácha F (2011) Structure of PSI, PSII and antenna complexes from yellow-green alga *Xanthonema debile*. *Photosynth Res* 108: 25–32.

90. Frank HA, Cua A, Chynwat V, Young A, Gosztola D, Wasielewski MR (1996) The lifetimes and energies of the first excited singlet states of diadinoxanthin and

diatoxanthin: The role of these molecules in excess energy dissipation in algae. *Biochim Biophys Acta* 1277: 243−252.

91. Gundermann K, Büchel C (2008) The fluorescence yield of the trimeric fucoxanthin–chlorophyll–protein FCPa in the diatom *Cyclotella meneghiniana* is dependent on the amount of bound diatoxanthin. *Photosynth Res* 95: 229−235.
92. Roszak AW, Howard TD, Southall J, Gardiner AT, Law CJ, Isaacs NW, Cogdell RJ (2003) Crystal structure of the RC-LH1 core complex from *Rhodopseudomonas palustris*. *Science* 302: 1969–1972.
93. Karrasch S, Bullough PA, Ghosh R (1995) The 8.5 Å projection map of the light-harvesting complex I from *Rhodospirillum rubrum* reveals a ring composed of 16 subunits. *EMBO J* 14: 631–638.
94. Jungas C, Ranck J, Rigaud J, Joliot P, Vermeglio A (1999) Supramolecular organization of the photosynthetic apparatus of *Rhodobacter sphaeroides*. *EMBO J* 18: 534–542.
95. Qian P, Hunter CN, Bullough PA (2005) The 8.5 Å projection structure of the core RC–LH1–PufX dimer of *Rhodobacter sphaeroides. J Mol Biol* 349: 948–960.
96. McDermott G, Prince SM, Freer AA, Hawthornwaite-Lawless AM, Papiz MZ, Cogdell RJ, Isaacs NW (1995) Crystal structure of an integral membrane light-harvesting complex from photosynthetic bacteria. *Nature* 374: 517–521.
97. Koepke J, Hu XC, Muenke C, Schulten K, Michel H (1996) The crystal structure of the light-harvesting complex II (B800-850) from *Rhodospirillum molischianum*. *Structure* 4: 581–597.
98. McLuskey K, Prince SM, Cogdell RJ, Isaacs NW (2001) The crystallographic structure of the B800-820 LH3 light-harvesting complex from the purple bacteria *Rhodopseudomonas acidophila* strain 7050. *Biochemistry* 40: 8783–8789.
99. Wacker T, Gadon N, Becker A, Mantele W, Kreutz W, Drews G, Welte W (1986) Crystallization and spectroscopic investigation with polarized light of the reaction center–B875 light-harvesting complex of *Rhodopseudomonas palustris*. *FEBS Lett* 197: 267–273.
100. Picorel R, Bélanger G, Gingras G (1983) Antenna holochrome B880 of *Rhodospirillum rubrum* S1. Pigment, phospholipid, and polypeptide composition. *Biochemistry* 22: 2491–2497.
101. Broglie RM, Hunter CN, Delepelaire P, Niederman RA, Chua NH, Clayton RK (1980) Isolation and characterization of the pigment–protein complexes of *Rhodopseudomonas sphaeroides* by lithium dodecyl sulfate/polyacrylamide gel electrophoresis. *Proc Natl Acad Sci USA* 77: 87–91.

102. Zhang F, Vierock J, Yizhar O, Fenno LE, Tsunoda S, Kianianmomeni A, Prigge M, Berndt A, Cushman J, Polle J, Magnuson J, Hegemann P, Deisseroth K (2011) The microbial opsin family of optogenetic tools. *Cell* 147: 1446–1457.
103. Sakmar TP (2002) Structure of rhodopsin and the superfamily of seven-helical receptors: the same and not the same. *Curr Opin Cell Biol* 14: 189–195.
104. Seki T, Vogt K (1998) Evolutionary aspects of the diversity of visual pigment chromophores in the class Insecta. *Comp Biochem Physiol* 119B: 53–64.
105. Shichida Y, Matsuyama T (2009) Evolution of opsins and phototransduction. *Phil Trans R Soc B* 364: 2881–2895.
106. Fernald RD (2006) Casting a genetic light on the evolution of eyes. *Science* 313: 1914–1918.
107. Fryxell KJ, Meyerowitz EM (1991) The evolution of rhodopsins and neurotransmitter receptors. *J Mol Evol* 33: 367–378.
108. Sakmar TP, Franke RR, Khorana HG (1989) Glutamic acid-113 serves as the retinylidene Schiff base counterion in bovine rhodopsin. *Proc Natl Acad Sci USA* 86: 8309–13.
109. Wang W, Nossoni Z, Berbasova T, Watson CT, Yapici I, Lee KSS, Vasileiou C, Geiger JH, Borhan B (2012) Tuning the electronic absorption of protein-embedded all-*trans*-retinal. *Science* 338: 1340–1343.
110. Oesterhelt D, Stoeckenius W (1974) Isolation of the cell mambrane of *Halobacterium halobium* and its fractionation into red and purple membrane. *Methods Enzymol* 31: 667–678.
111. Mukohata Y, Sugiyama Y, Ihara K, Yoshida M (1988) An Australian halobacterium contains a novel proton pump retinal protein: archaerhodopsin. *Biochem Biophys Res Commun* 151: 1339–1345.
112. Béjà O, Aravind L, Koonin EV, Suzuki MT, Hadd A, Nguyen LP, Jovanovich SB, Gates CM, Feldman RA, Spudich JL, Spudich EN, DeLong EF (2000) Bacterial rhodopsin: evidence for a new type of phototrophy in the sea. *Science* 289: 1902–1906.
113. Venter JC, Remington K, Heidelberg JF, Halpern AL, Rusch D, Eisen JA, Wu DY, Paulsen I, Nelson KE, Nelson W et al. (2004) Environmental genome shotgun sequencing of the Sargasso Sea. *Science* 304: 66–74.
114. Sabehi G, Loy A, Jung KH, Partha R, Spudich JL, Isaacson T, Hirschberg J, Wagner M, Béjà O (2005) New insights into metabolic properties of marine bacteria encoding proteorhodopsins. *PLoS Biol*. 3: e273.

115. Spudich JL (2006) The multitalented microbial sensory rhodopsins. *Trends Microbiol* 14: 480–487.

116. Balashov SP, Imasheva ES, Boichenko VA, Antón J, Wang JM, Lanyi JK (2005) Xanthorhodopsin: A proton pump with a light-harvesting carotenoid antenna. *Science* 309: 2061–2064.

117. Luecke H, Schobert B, Stagno J, Imasheva ES, Wang JM, Balashov SP, Lanyi JK (2008) Crystallographic structure of xanthorhodopsin, the light-driven proton pump with a dual chromophore. *Proc Natl Acad Sci USA* 105: 16561–16565.

118. Imasheva ES, Balashov SP, Choi AR, Jung KH, Lanyi JK (2009) Reconstitution of *Gloeobacter violaceus* rhodopsin with a light-harvesting carotenoid antenna. *Biochemistry* 48: 10948–10955.

2. Experimental Methods and Data Analysis

In this section the experimental methods used by the author of this thesis, relevant to studies presented in both Research Sections, will be presented.

2.1 Steady-state absorption spectroscopy

A spectrophotometer, a device capable of taking absorption spectra, is indispensable in any lab, where light-absorbing molecules are studied. It measures light intensity at a specific wavelength with ($I(\lambda)$) and without ($I_0(\lambda)$) the test sample (alternatively $I_0(\lambda)$ is measured on a reference sample such as solvent). According to the means by which the two intensity values are obtained, the device architecture is either single-beam ($I_0(\lambda)$ is measured before the test sample is inserted and $I(\lambda)$ after that), or double-beam ($I_0(\lambda)$ and $I(\lambda)$ are measured simultaneously in parallel light paths). The other distinction is whether the whole absorption spectrum is taken in a "single-shot" manner using a diode array or a CCD as a detector, or in successive $\Delta\lambda$ steps using (a) photodiode(s). The spectrophotometer used in our lab is of the double-beam type with photodiode detectors. Its scheme is presented in Figure 2-1.

There are multiple ways to present the measured data. The simplest is in terms of transmittance T:

$$T = \frac{I(\lambda)}{I_0(\lambda)} \qquad (2.1)$$

Because the light intensities may vary within a wide range, the logarithmic scale is more appropriate. We thus define absorbance, A, as follows:

$$A = \log\frac{I_0}{I} = c\varepsilon(\lambda)l \qquad (2.2)$$

where $\varepsilon(\lambda)$ is the molar extinction coefficient specifying the strength of light absorption at a given wavelength and l is the pathlength. Moreover, another advantage of using the logarithmic scale to define the measured quantity is linear dependence on the chromophore's concentration c.

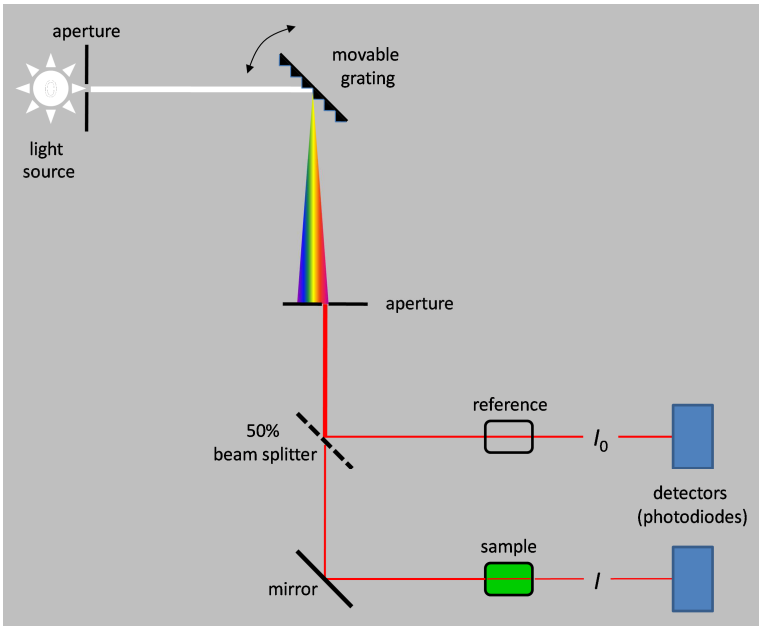

Figure 2-1: A scheme of a double-beam spectrophotometer with photodiode detectors.

The usefulness of the absorption spectra goes beyond the determination of chromophore concentration. It provides a link to quantum mechanics in the sense that it enables the calculation of a transition dipole moment, μ_{mn}, which is a measure of transition intensity (see Section 1.3.1). For a narrow absorption band, the following expression can be written:[1]

$$\mu_{mn} = \frac{1}{\pi}\sqrt{\frac{3hc\varepsilon_0}{2N_A}\frac{\int \varepsilon(\nu)\mathrm{d}\nu}{\nu_{max}}} = \frac{1}{\pi}\sqrt{\frac{3hc\varepsilon_0}{2N_A}\frac{\mathcal{E}_{int}}{\nu_{max}}} \qquad (2.3)$$

In this expression[h] ν_{max} is the frequency at absorption maximum and ε_{int} is the integrated extinction coefficient. Transition dipole moments determined in this way can then be used as input values for the calculation of rates of Förster energy transfer (see Section 1.3.3).

2.2 Femtosecond transient absorption spectroscopy

When one wants to obtain information about the dynamics of processes, then some form of time-resolved technique must be employed. Apart from this, the use of time-resolved spectroscopy enables us, for instance, to obtain information about one-photon-forbidden states, such as the S_1 state of carotenoids (see Section 1.3.1).

There are basically two ways to reach time resolution in an experiment.[i] In the first approach, a trigger perturbing the system is used with consequent probing by a continuous-wave beam. The detector must then be fast enough to "spot" the intensity changes during the process itself (Figure 2-2). One kind of such detector is the streak camera, which can reach a <200 fs time resolution.[2] The other approach is to use a pulsed probe, each pulse "seeing" the process at a different instance. Upon repeating the experiment with differing timing for the probe with respect to the trigger, the dynamics of the process can be recorded. In this case a "slow" detector is sufficient because it must only operate at a frequency given by the period between the discrete experiments (Figure 2-2). The temporal resolution is on the order of the length of the trigger (pump) pulse. The femtosecond transient absorption spectroscopy (alternatively called femtosecond pump-probe

[h] To use Eq. (2.3) to calculate the transition dipole moment, one must know the concentration c and pathlength l to obtain the extinction coefficient ε because from the absorption spectrum one obtains a λ-dependence of absorbance A (see Eq. (2.2)). One must also transpose the x-scale from wavelength λ into frequency ν.

[i] This paragraph was inspired by Jens Bredenbeck, who gave a nice course "Dynamics of biomolecules" during the summer school in Jyväskylä, 2010.

spectroscopy) working in the pulsed regime, which was used in majority of experiments presented in Research Sections, will be described here.

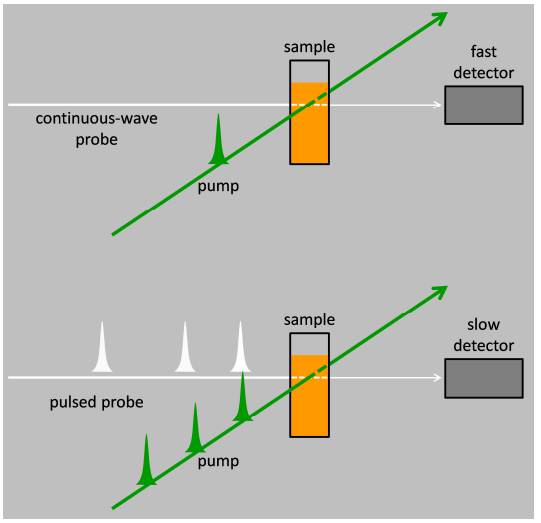

Figure 2-2: Differences between time-resolved experiments accomplished by continuous (above) and pulsed probing (below).

2.2.1 General considerations

A possible setup for a typical pump-probe experiment is shown in Figure 2-3. The laser system provides femtosecond pulses with a central wavelength typically around 800 nm. The main output beam is then divided into two, one called *pump* (excitation beam or "trigger" as in the previous section), and the other *probe*. To reach selectivity in excitation and for versatile use, the pump pulse should be spectrally narrow and tuneable. This is usually achieved in the *optical parametric amplifier* (OPA). On the other hand, the probe should be spectrally broad enough to cover all possible regions of interest. Thus an ideal candidate for the probe light is a white light continuum (WLC) that is generated via a nonlinear process achievable in media such as sapphire, calcium fluoride, water etc. Both beams then coincide in the sample: the pump perturbs the sample by exciting the molecules and the other beam probes it. The probe beam then continues into the detector. To achieve the required time resolution during the

measurement, a *delay line* is placed into pathway of the pump or probe, which enables to vary the mutual delay between both pulses. The delay line consists of a corner reflector mounted on a base, which is moved by a stepper motor.

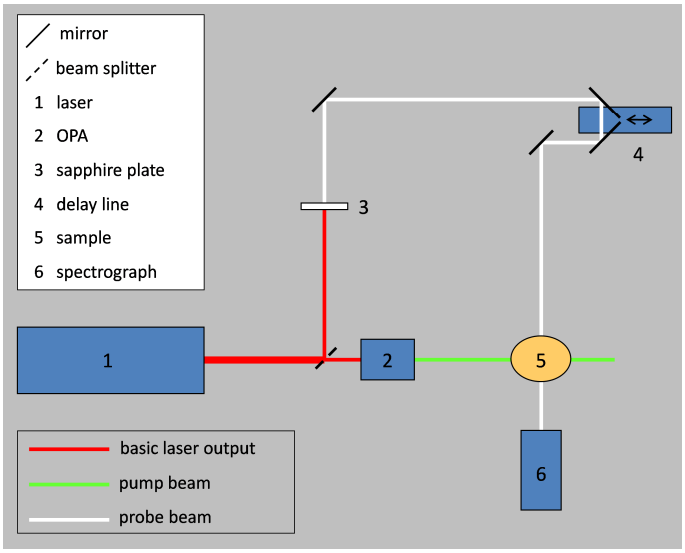

Figure 2-3: A simplified scheme of the pump-probe experiment.

2.2.2 Experimental details

The detailed scheme of the setup from our laboratory is depicted in Figure 2-4. The source of pulses is a one-box multiple-component laser system Integra-*i*. It is based on an Erbium-doped fibre oscillator, which provides <110-fs pulses at a high repetition rate (50 MHz), but low pulse energy (<1 nJ). These pulses are amplified in Ti-sapphire amplifiers (regenerative and multipass), which are pumped by a Nd-YLF nanosecond laser operating at 1 kHz. However, the amplification cannot be achieved with short pulses because high power reached in amplified pulses would lead to material damage. Thus the <110 fs pulses are first stretched to ~400 ps and after amplification compressed again to final pulse width of ~120 fs. The output pulses thus have the following parameters: central wavelength ~785 nm, power 1.6 W, duration ~120 fs.

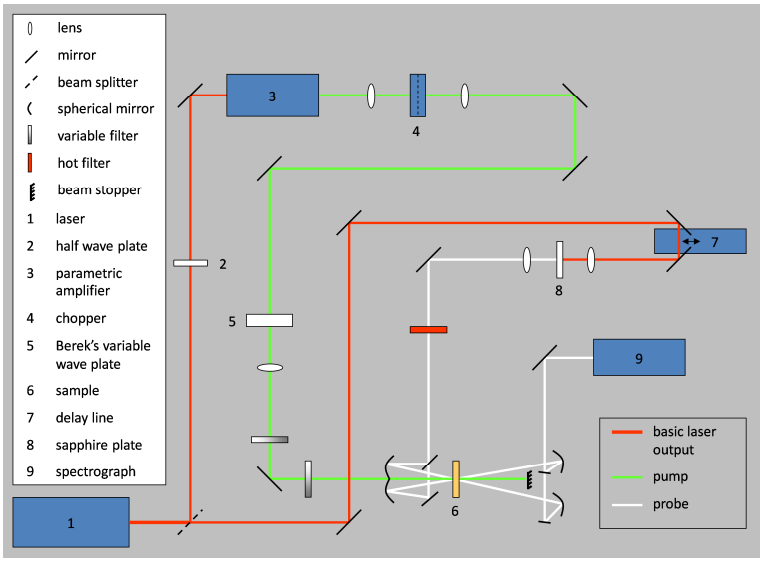

Figure 2-4: A scheme of the pump-probe setup from our lab.

Next the pathway of the pump beam is traced. To reach the desired wavelength for specific excitation, the beam passes through the OPA. This device serves not only to generate the wavelength of interest from the 790-nm input in the broad 240 – 2500 nm range, but also to amplify the desired wavelength. The former is achieved by means of frequency doubling or sum/difference frequency generation, while the latter by the process of parametric amplification. These are second-order nonlinear processes, which occur in non-centrosymmetric crystals. The next important device is a chopper, which blocks every second pump pulse and thus enables us to increase the signal/noise ratio of the measurement by introducing the correction to laser power fluctuations (see below). All measurements relevant to this thesis were conducted with mutual pump-probe polarization set to 54.7°, which prevents the occurrence of polarization and photoselection effects (for details see Section 2.2.4).[3] The desired polarization is achieved by means of *Berek's variable wave plate* by the appropriate tilting and rotation of the birefringent crystal. After the pump beam interacts with the sample, it is blocked.

The probe beam first passes through the delay line, which sets the required delay between pump and probe. It is then led through the sapphire

crystal where WLC is generated via third-order nonlinear processes. The main contributor to this effect is self-phase modulation,[4] whose physical basis consists in the variation of the nonlinear refractive index with intensity, the Kerr effect. Before the probe beam hits the sample, it is split into two: probe and reference. To focus the beam into the sample, spherical mirrors are used instead of conventional lenses. This arrangement prevents the introduction of additional *chirp* (time-dependent frequency distribution within the pulse caused by dispersion: blue light travels slower than red light through optical elements with normal dispersion), which is inherent to the probe beam owing to the process of WLC generation. Both probe and reference beams then continue into the spectrograph, where they are dispersed onto two separate diode arrays with 1024 elements by means of a grating. The transient absorption (ΔA) signal is then calculated using the expression

$$\Delta A(\Delta t, \lambda) = \log\frac{I_{ref}}{I_{pp}} - \log\frac{I_{ref}}{I_{np}} \qquad (2.4)$$

where I_{ref} is the intensity of the reference beam, I_{pp} the intensity of the pre-pumped probe and I_{np} the intensity of the unpumped probe. The second term on the right-hand side of Eq. (2.4) is the correction for laser intensity fluctuations; it should ideally amount to zero. Since each data point depends on two variables (Δt – delay between pump and probe, λ – probe wavelength), the whole dataset forms a matrix, which can be depicted as a 3D graph (Figure 2-5A). The data are typically presented as sections through this 3D graph either in the spectral or temporal domain (Figure 2-5B,C).

One can identify three main contributions to the ΔA signal: ground-state bleaching (GSB), stimulated emission, and excited-state absorption (ESA).

Ground-state bleaching. Because a fraction of the molecules is promoted into the excited state by the pump pulse, the probe "sees" fewer molecules in the ground state than the reference. Fewer photons are thus absorbed from the probe than from the reference beam at GSB-specific spectral region ($I_{pp} > I_{ref}$), resulting in the negative signal (Figure 2-5C) according to Eq. (2.4).

Stimulated emission. It is a mirror process to absorption. This fact is reflected in the Einstein coefficients for absorption and stimulated emission being equal in a two-level system ($A_{12} = A_{21}$). Both processes will also occur to a significant extent only for allowed transitions. When the molecule is promoted into the excited state, an incident probe photon can induce the stimulated emission, resulting in a return of the molecule into the ground state and the production of a photon identical (including the direction) to that which triggered the process. I_{pp} will thus be larger than I_{ref}, leading again to a negative signal according to Eq. (2.4). Because of vibrational relaxation in the excited state, most of the stimulated emission events occur from the relaxed higher state. Consequently, the stimulated emission signal is usually red-shifted with respect to GSB.[5]

Excited-state absorption. Molecules in the excited state generally absorb photons of different energy than those in the ground state. In some spectral regions the excited molecules will thus absorb *extra* photons compared to reference, resulting in a positive signal (Figure 2-5C), as follows from Eq. (2.4) for $I_{pp} < I_{ref}$.

It is worth mentioning here that there are still other possible sources of transient signals, i.e. those from the energy acceptors or photoproducts. The energy acceptor can modulate the transient absorption spectra via all of the above-mentioned contributions, i.e. GSB, stimulated emission, and ESA. One example is (B)Chl bleaching, which appears after carotenoid excitation in light-harvesting complexes (see Sections 4, 5, and Figure 2-5). The photoproduct can influence the final signal also by its steady state absorption because it generally differs from that of the reactant. This absorption will decrease the intensity I_{pp} with respect to I_{ref} promoting a positive ΔA signal. An example of this contribution is the signal of 13-*cis* retinal as a photoproduct of the retinal isomerization reaction (see Section 3 and Ref. 44).

To prevent photoinduced degradation, samples are placed in a rotational cuvette and spun at a rate ensuring that each pump pulse hits a fresh sample.

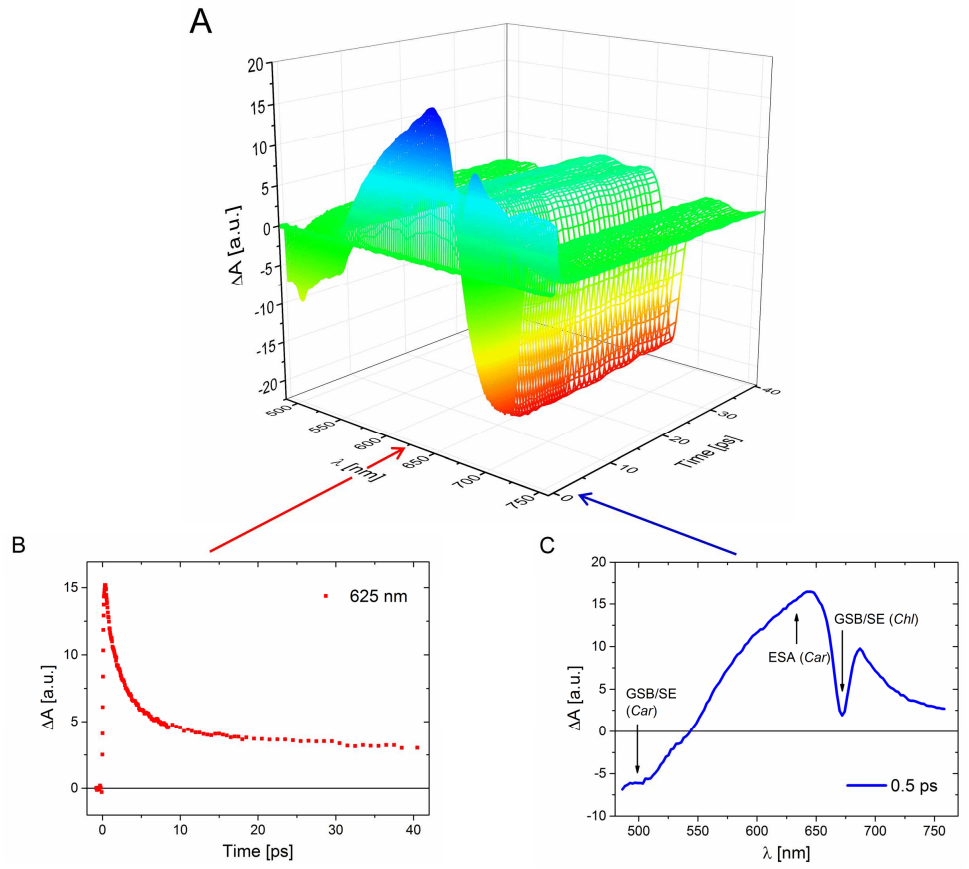

Figure 2-5: A) 3D graph depicting the result of a time-resolved measurement performed on an antenna complex containing carotenoids and chlorophylls. Sections through this graph: B) the kinetics, C) the transient absorption spectrum. The coloured arrows indicate the position of the section in the 3D graph. In panel C are also shown the contributions to the transient signal specific to the carotenoid (*car*) and chlorophyll (*Chl*). This dataset was recorded after carotenoid excitation, so Chl bleaching is the result of an energy transfer process. SE – stimulated emission.

2.2.3 Time resolution and spectral selectivity

The instrument response function (IRF) gives the time resolution of the pump-probe experiment. The IRF is in turn given by the cross-correlation between the pump and probe pulses, which can be monitored as a sum-

frequency signal generated in an anisotropic crystal. Even if the probe pulse is chirped, the time resolution is not affected. This is so because one could think of the pump-probe experiment as composed of many single-wavelength partial experiments, each of them having its own instrument response function. From that follows, broadly speaking, that the duration of the pump pulse, which mainly governs the time resolution, is crucial here. A logical path towards higher resolution is thus further compression of the pump pulse. Although 5-fs pulses are available even for spectroscopy,[6] they are not employed in pump-probe experiments because spectral selectivity is lost. The uncertainty relation

$$\Delta E \Delta t \geq \frac{\hbar}{2} \qquad (2.5)$$

applies also to laser pulses, so short pulses become spectrally broad. More precisely, the uncertainty relation takes the form of the *time-bandwidth product*. For a Gaussian shape of pulse, the following relation is valid

$$\tau_p \Delta\nu \geq 0.441 \qquad (2.6)$$

where τ_p is the pulse duration and $\Delta\nu$ the consequent bandwidth. At the same time, the relationship between energy, frequency and wavelength is

$$E = h\nu = h\frac{c}{\lambda} \qquad (2.7)$$

which gives after differentiation and dividing by h,

$$\Delta\nu = \frac{c}{\lambda^2}\Delta\lambda \qquad (2.8)$$

Upon insertion of Eq. (2.8) into Eq. (2.6), we will obtain

$$\frac{\tau_p c \Delta\lambda}{\lambda^2} \geq 0.441 \qquad (2.9)$$

For a 5-fs pulse with a central wavelength of 800 nm, the spectral bandwidth is at least 180 nm. For a 100-fs pulse, the minimum bandwidth is 8 nm. One thus must keep in mind when planning the experiment that high spectral selectivity and high time resolution cannot be achieved simultaneously.

It should be mentioned, however, that the disadvantage of the broad spectrum from the point of view of limited selectivity can become an advantage and even a requirement for modern spectroscopic techniques such as electronic 2D spectroscopy.[7]

2.2.4 FAQ

This section contains some of the questions I frequently asked in the course of the time spent in our lab, accompanied by the respective answers. Some of the findings may seem trivial, but might still serve as a quick reference for those starting in the field of time-resolved spectroscopy.

How can the lifetime be approximately determined from the kinetic trace?

Let us assume a single-exponential decay as in Figure 2-6. The signal $S(t)$ can be mathematically described as

$$S(t) = Ae^{-kt} = Ae^{-\frac{t}{\tau}} \qquad (2.10)$$

where A is the amplitude, k the rate constant, and τ is the reciprocal value of the rate constant, the lifetime. At the time when signal is e-times lower than the amplitude, Eq. (2.10) becomes

$$\frac{A}{e} = Ae^{-\frac{t}{\tau}} \qquad (2.11)$$

Applying simple math (dividing by A, taking a natural logarithm of both sides of the equation) will give the result

$$t = \tau \qquad (2.12)$$

It, thus, means that when taking an e-times lower value than the maximum on y-axis, the corresponding value on the x-axis gives the lifetime. This method of lifetime determination is of course precisely valid only for single-exponential decays. However, it can also be applicable for multiexponential decays when one of the exponentials dominates, which is,

for instance, usually the case of decay of the S_1-S_N ESA signal in carotenoids.

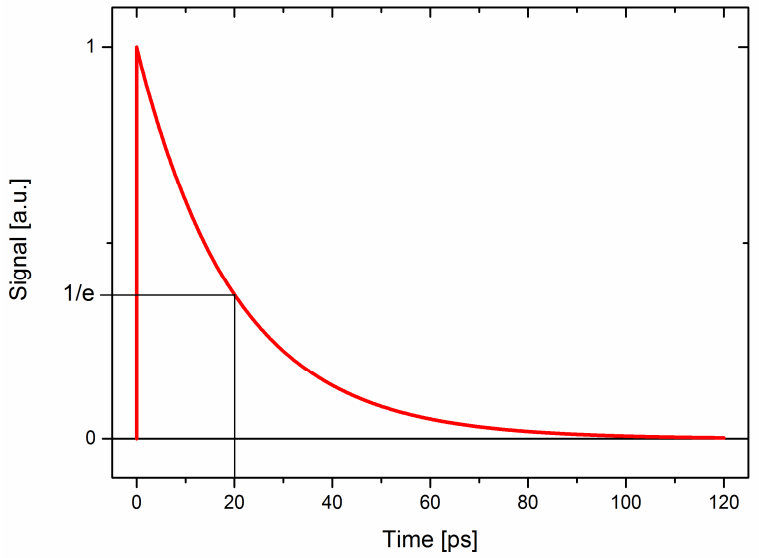

Figure 2-6: Visualization of the approximate determination of the time constant from the exponential decay. The lifetime is 20 ps in this case.

Normal dispersion causes a delay of the blue part of the probe spectrum with respect to the red part. Why then does the signal in the blue region precede the signal in the other regions?[j]

In the right part of Figure 2-7 is shown the sequence of signal evolution in the data acquisition window of the program, which enables real-time signal observation. It is obvious that the signal moves "from blue to red". This seemed counterintuitive to me taking into account the fact that "blue" is delayed with respect to "red" in the probe pulse. Figure 2-7 illustrates the explanation. Each measurement starts with negative delay times, i.e. the probe precedes the pump. As the delay line moves (regardless of whether it is placed in the pathway of probe, or pump), both pulses get closer both in time and space. Notice that the first interaction takes place between the "blue part" of the probe and pump! Therefore, the spectrograph will first record the

[j] I am thankful to Marcel Fuciman, who answered this question.

signal in blue, and the lower-energy spectral contributions follow. Only after the pump interacts with the reddest part of the probe, is the first *complete* spectrum recorded (Figure 2-7D).

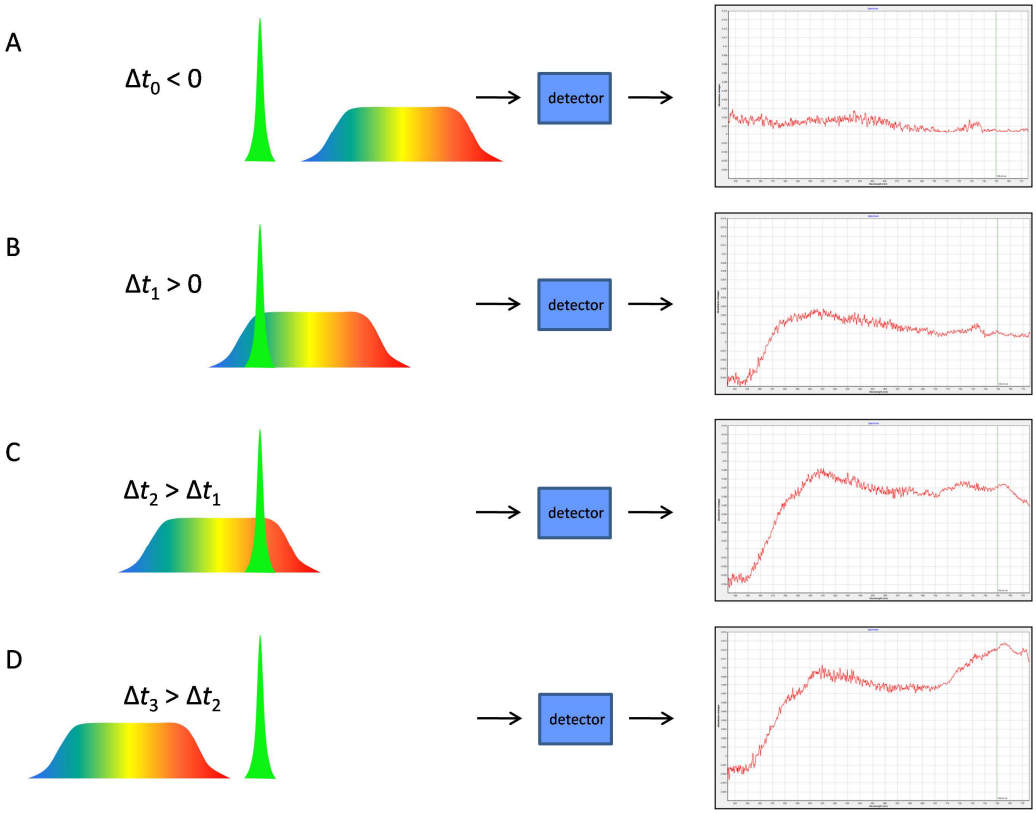

Figure 2-7: Illustration of the dependence of signal appearance on the delay time between pump (green) and probe (multicoloured).

Why is the bleaching always (at least in case of Chl) red-shifted with respect to the corresponding steady-state absorption band?

The formulation of this question is not precise because, as mentioned in section 2.2.2, stimulated emission also contributes to the negative signal. Because the stimulated emission signal is usually red shifted due to the Stokes shift (similarly to the fluorescence spectrum),[5] convolution of the GSB with the stimulated emission leads to an overall red-shift of the negative signal with respect to the steady-state absorption band.

What is the precise reason for measuring the anisotropy-effects-free data at the magic angle (54.7°) between pump and probe?

The answer to this question is usually restricted to the explanation that "magic-angle detection was performed in order to avoid anisotropy effects". However, this statement does not really explain much, so a more rigorous answer is presented here.

The pump pulses are linearly polarized. The probability of absorption is then also affected by the orientation of the transition dipole moment of the chromophores in the sample in respect to the polarization of the pump beam – the closer the orientation to that of the pump polarization, the higher the probability.[8] The fact that not all chromophores are affected equally is called *photoselection*. The absorption probability of the probe pulse, which can be considered as an analyser in the polarizer-analyser setup, then does not only depend on the similarity between orientations of the (excited-state) transition dipole moment versus the probe polarization, but also on the time delay between pump and probe due to the rotational motion of the chromophores (the longer the delay, the more the transition dipole moments move off the original position until an equilibrium value is reached). The aim is thus to avoid another delay-dependent photoselection by the probe beam, which can be achieved by recording the *total*, and not the *polarized*, probe intensity. How to achieve this will be explained next.

The vector of the chromophore's transition dipole moment has three spatial components. Owing to this, arbitrarily chosen polarizations of the probe beam generally result in varying transient absorption intensities, ΔA. One way to prevent this is to conduct two measurements, one with a parallel ($\Delta A_{\parallel}$) and one with a perpendicular ($\Delta A_{\perp}$) polarization with respect to the pump. The total ΔA is then free of polarization effects:

$$\Delta A = \Delta A_{\parallel} + 2\Delta A_{\perp} \qquad (2.13)$$

To realize why the perpendicular term is taken twice follows from the fact that without such a treatment only transient absorption contributions along two axes, say, z- ($\Delta A_{\parallel}$) and x- ($\Delta A_{\perp}$) axis, but not the y-axis, would be taken

into account. Because the absorption probability along the y-axis is the same as that of along the x-axis, $\Delta A_{\perp}$ is taken twice in Eq. (2.13).[8]

There is, however, a simpler way to get ΔA. For that purpose, one must know that for a measurement with an angle φ between pump and probe, the following relations apply:[8]

$$\Delta A_{\parallel} \propto \cos^2 \varphi \qquad (2.14)$$

$$\Delta A_{\perp} \propto \frac{1}{2} \sin^2 \varphi \qquad (2.15)$$

To follow the logic of Eq. (2.13), one must conduct the measurement under such an angle for which $\Delta A_{\perp}$ is weighted twice with respect to $\Delta A_{\parallel}$. We will thus get the conditions

$$2\cos^2 \varphi = \sin^2 \varphi \qquad (2.16)$$

or, alternatively put

$$\tan^2 \varphi = 2 \qquad (2.17)$$

which will return

$$\varphi \doteq 54.74° \qquad (2.18)$$

This value is denoted as the *magic angle*. If the angle between pump and probe polarizations is set to the magic angle, one obtains the total transient absorption intensity, which is free of polarization effects due to the rotational motion of chromophores.

2.3 Global fitting analysis

The term *global fitting*, as opposed to *single-decay analysis*, refers to the simultaneous fitting of the whole spectro–temporal dataset, which arises,

for instance, from the pump-probe experiment. The main advantage of the global fitting approach is that it requires a smaller amount of parameters.[9]

The most straightforward method of global fitting is a simple extension of the single-decay analysis approach. Here, the data are fitted to a sum of exponentials, each of which is weighted by the amplitude A_j:

$$S(t,\lambda_i) = \sum_{j=1}^{n} A_j(\lambda_i) e^{-\frac{t}{\tau_j}} \qquad (2.19)$$

This formula alone, however, basically describes the multi-exponential decay at each detection wavelength λ_i. The global fitting is accomplished so that such single-decay fitting is *simultaneously* conducted at all detection wavelengths λ_i. The amplitudes A_j plotted as a function of λ_i constitute the so called *decay-associated difference spectra* (DADS). They are interpreted as a loss or gain of absorption with a certain lifetime.[10] This kind of global fitting is sometimes called *mathematical*[9] or *parallel-model-fitting*.[10]

Although we can obtain a perfect fit using such a purely mathematical approach, the outcomes of this procedure match the behaviour of the physical system only rarely. Let us take into account a simple example of the carotenoid in solution. Here the population flows in cascade from the initially excited S_2 state via the S_1 state down to the ground state (Figure 1-2). When using the mathematical fitting, one inherently assumes the parallel, but not the realistic sequential scheme of system evolution, inevitably leading to skewed results.[10] To reflect the properties of the studied system, a physical model[k] is constructed. It consists of multiple compartments (the electronic state can for instance be considered as a compartment), which mutually communicate due to population flows characterized by rate constants/lifetimes. Very frequently, the sequential model is applied, in which the compartments irreversibly decay into each other:

$$A \overset{\tau_1}{\rightarrow} B \overset{\tau_2}{\rightarrow} C \overset{\tau_3}{\rightarrow} D \ldots$$

[k] Because the simultaneous fitting to a sum of exponentials inherently assumes the parallel model, this kind of fitting is sometimes described as *parallel-model-fitting*.

The resulting *evolution-associated difference spectra* (EADS) represent the spectral evolution, i.e. the second EADS appears with the first lifetime (τ_1) and decays with the second lifetime (τ_2), and so on.

To return to our example, the presented sequential scheme now perfectly matches the physical properties of the carotenoid molecule: the compartments (states) follow one after another and the time constants represent the reciprocal values of the internal conversion rates. When the condition for proper physical representation of the system by the model is met, as it would be in the carotenoid in solution example, the EADS correspond to the pure spectra of the intermediate states, *species-associated difference spectra* (SADS), the acquisition of which is the ultimate aim of the researcher. The first EADS thus matches the SADS of the carotenoid S_2 state, which decays with τ_1 into the second EADS, which is the SADS of the carotenoid S_1 state, returning to ground state with τ_2. The sequential scheme is even applicable in more complicated situations, e.g. when branching due to energy transfer occurs. Although the EADS then do not represent the SADS, one can still use the total time constants τ_t obtained from the global fit to calculate other parameters of interest, such as the energy transfer time τ_{ET} (see Section 1.3.3). This operation is analogous to splitting of the population route, which was artificially considered as coupled due to the application of the sequential model. Generally, one should test multiple models and then consider the physical relevance of the results. From such *target analysis* should arise a model, which best characterizes the system under study.[1]

The global fitting analysis was used in most of the studies presented in the Research Sections. It was implemented using the program DAFit

[1] The author is aware that the terminology used here may be different than elsewhere in literature. *Global fitting* is sometimes considered as an equivalent to mathematical fitting to the sum of exponentials, or, alternatively put, to the analysis when the parallel model is applied. Anytime another model is used (e.g. sequential), the fitting procedure is considered as *target analysis*.[10] However, here the term *global fitting* is used in a wider context, including the application of the sequential model. Only the advanced *model testing* is considered as *target analysis*, consistently with numerous studies.[11,12]

(Pascher Instruments). Before the fitting alone, the data were adapted by the program: the background was subtracted, the deconvolution of the IRF was conducted, and the data were corrected for chirp. The only kinetic model available in this software is the sequential model.

References

1. Atkins PW, Friedman R (2005) Molecular quantum mechanics (4th ed.). *Oxford University Press*, Oxford, UK.
2. Takahashi A, Nishizawa M, Inagaki Y, Koishi M, Kinoshita K. New femtosecond streak camera with temporal resolution of 180 fs, In: *Generation, amplification, and measurement of ultrashort laser pulses*; Trebino RP, Walmsley IA, Eds. *Proc SPIE 2116*, Los Angeles, CA, USA, 1994.
3. Lakowicz JR (2006) Principles of fluorescence spectroscopy (3rd ed.). *Springer*, Berlin, Germany.
4. Alfano RR, Shapiro SL (1970) Observation of self-phase modulation and small-scale filaments in crystals and glasses. *Phys Rev Lett* 24: 592–594.
5. Berera R, van Grondelle R, Kennis JTM (2009) Ultrafast transient absorption spectroscopy: Principles and application to photosynthetic systems. *Photosynth Res* 101: 105–118.
6. Nishimura K, Rondonuwu FS, Fujii R, Akahane J, Koyama Y, Kobayashi T (2004) Sequential singlet internal conversion of $1B_u^+ \rightarrow 3A_g^- \rightarrow 1B_u^- \rightarrow 2A_g^-$ ($1A_g^-$ ground) in all-*trans*-spirilloxanthin revealed by two-dimensional sub-5-fs spectroscopy. *Chem Phys Lett* 392: 68–73.
7. Jonas DM (2003) Two-dimensional femtosecond spectroscopy. *Annu Rev Phys Chem* 54: 425–463.
8. Walla PJ (2009) Modern biophysical chemistry. *Wiley–VCH*, Weinheim, Germany.
9. Holzwarth AR. Data analysis of time-resolved measurements, In: *Biophysical techniques in photosynthesis*; Amesz J, Hoff AJ, Eds. *Kluwer academic publishers*, Dordrecht, The Netherlands, 1996.
10. van Stokkum IHM, Larsen DS, van Grondelle R (2004) Global and target analysis of time-resolved spectra. *Biochim Biophys Acta* 1657: 82–104.
11. Gradinaru CC, Kennis JTM, Papagiannakis E, van Stokkum IHM, Cogdell RJ, Fleming GR, Niederman RA, van Grondelle R (2001) An unusual pathway of excitation energy deactivation in carotenoids: Singlet–to–triplet conversion on an ultrafast timescale in a photosynthetic antenna. *Proc Natl Acad Sci USA* 98: 2364–2369.
12. Polívka T, Balashov SP, Chábera P, Imasheva ES, Yartsev A, Sundström V, Lanyi JK (2009) Femtosecond carotenoid to retinal energy transfer in xanthorhodopsin. *Biophys J* 96: 2268–2277.

Research Sections

This part of the thesis is based on six studies to which I contributed (see page VIII). The motivation for dividing it into two sections is that the latter (Research Section B) forms a very coherent ensemble. The former section (Research Section A) then contains separate studies which do not directly contribute to the story presented in Research Section B. Although the style and format of the following chapters may slightly differ from the original publications, its content is maintained.

Research Section A

3. Carotenoid Response to Retinal Excitation and Photoisomerization Dynamics in Xanthorhodopsin

This chapter is based on Paper I.:
Šlouf V, Balashov SP, Lanyi JK, Pullerits T, Polívka T (2011) Carotenoid response to retinal excitation and photoisomerization dynamics in xanthorhodopsin. *Chem Phys Lett* 516: 96–101.

Abstract

We present a comparative study of xanthorhodopsin, a proton pump with the carotenoid salinixanthin serving as an antenna, and the closely related bacteriorhodopsin. Upon excitation of retinal, xanthorhodopsin exhibits a wavy transient absorption pattern in the region between 470 and 540 nm. We interpret this signal as due to electrochromic effect of the transient electric field of excited retinal on salinixanthin. The spectral shift decreases during the retinal dynamics through the ultrafast part of the photocycle. Differences in dynamics of bacteriorhodopsin and xanthorhodopsin are discussed.

4. Role of Carotenoids in Light-Harvesting Processes in an Antenna Protein from the Chromophyte *Xanthonema debile*

This chapter is based on Paper II.:
Durchan M, Tichý J, Litvín R, Šlouf V, Gardian Z, Hříbek P, Vácha F, Polívka T (2012) Role of carotenoids in light-harvesting processes in an antenna protein from the chromophyte *Xanthonema debile*. *J Phys Chem B* 116: 8880−8889.

Abstract

Chromophytes are an important group of microorganisms that contribute significantly to the carbon cycle on Earth. Their photosynthetic capacity depends on efficiency of the light-harvesting system that differs in pigment composition from that of green plants and other groups of algae. Here we employ femtosecond transient absorption spectroscopy to study energy transfer pathways in the main light-harvesting complex of *Xanthonema debile*, denoted XLH, which contains four carotenoids, diadinoxanthin, heteroxanthin, diatoxanthin and vaucheriaxanthin, and Chl-*a*. Overall carotenoid-to-chlorophyll energy transfer efficiency is about 60%, but energy transfer pathways are excitation wavelength dependent. Energy transfer from the carotenoid S_2 state is active after excitation at both 490 nm (maximum of carotenoid absorption) and 510 nm (red edge of carotenoid absorption), but this channel is significantly more efficient after 510 nm excitation. Concerning the energy transfer pathway from the S_1 state, XLH contains two groups of carotenoids: those that have the S_1 route active (~25%) and those having the S_1 pathway silent. For a fraction of carotenoids that transfer energy via the S_1 channel, energy transfer is observed after both

excitation wavelengths, though energy transfer times are different, yielding 3.4 ps (490 nm excitation) and 1.5 ps (510 nm excitation). This corresponds to efficiencies of the S_1 channel of ~85% that is rather unusual for a donor–acceptor pair consisting of a non-carbonyl carotenoid and Chl-*a*. Moreover, major carotenoids in XLH, diadinoxanthin and diatoxanthin, have their S_1 energies in solution lower than the energy of the acceptor state, Q_y state of Chl-*a*. Thus, binding of these carotenoids to XLH must tune their S_1 energy to allow for efficient energy transfer. Besides the light-harvesting function, carotenoids in XLH also have photoprotective role; they quench Chl-*a* triplets via triplet–triplet energy transfer from Chl-*a* to carotenoid.

5. Low-Temperature Time-Resolved Spectroscopic Study of the Major Light-Harvesting Complex of *Amphidinium carterae*

This chapter is based on Paper III.:
Šlouf V, Fuciman M, Johanning S, Hofmann E, Frank HA, Polívka T (2013) Low-temperature time-resolved spectroscopic study of the major light-harvesting complex of *Amphidinium carterae*. Accepted in *Photosynth Res*, doi: 10.1007/s11120-013-9900-8.

Abstract

The major light-harvesting complex of *Amphidinium* (*A.*) *carterae*, chlorophyll-a–chlorophyll-c_2–peridinin protein complex (acpPC), was studied using ultrafast pump-probe spectroscopy at low temperature (60 K). An efficient peridinin–Chl-a energy transfer was observed. The stimulated emission signal monitored in the near-infrared spectral region was stronger when redder part of peridinin pool was excited, indicating that these peridinins have the S_1/ICT state with significant charge-transfer character. This may lead to enhanced energy transfer efficiency from "red" peridinins to Chl-a. Contrary to the water-soluble antenna of *A. carterae*, peridinin–chlorophyll-a protein (PCP), the energy transfer rates in acpPC were slower under low-temperature conditions. This fact underscores the influence of the protein environment on the excited-state dynamics of pigments and/or the specificity of organization of the two pigment–protein complexes.

Research Section B

6. Photoprotection in a Purple Phototrophic Bacterium Mediated by Oxygen-Dependent Alteration of Carotenoid Excited-State Properties

This chapter is based on Paper IV.:
Šlouf V, Chábera P, Olsen JD, Martin EC, Qian P, Hunter CN, Polívka T (2012) Photoprotection in a purple phototrophic bacterium mediated by oxygen-dependent alteration of carotenoid excited-state properties. *Proc Natl Acad Sci USA* 109: 8570–8575.

Abstract

Carotenoids are known to offer protection against the potentially damaging combination of light and oxygen encountered by purple phototrophic bacteria, but the efficiency of such protection depends on the type of carotenoid. *Rhodobacter sphaeroides* synthesizes spheroidene as the main carotenoid under anaerobic conditions, whereas in the presence of oxygen the enzyme spheroidene monooxygenase catalyses the incorporation of a keto group forming spheroidenone. We performed ultrafast transient absorption spectroscopy on membranes containing RC-LH1-PufX complexes and show that when oxygen is present the incorporation of the keto group into spheroidene, forming spheroidenone, reconfigures the energy transfer pathway in the LH1, but not the LH2, antenna. The spheroidene/spheroidenone transition acts as a molecular switch, which is suggested to twist spheroidenone into an s-*trans* configuration, increasing its conjugation length and lowering the energy of the lowest triplet state so it can act as an effective quencher of singlet oxygen. The other consequence of converting carotenoids in RC-LH1-PufX complexes is that S_2/S_1/triplet pathway for spheroidene is replaced with a new pathway for spheroidenone

involving an activated ICT state. This strategy for RC-LH1-PufX-spheroidenone complexes maintains the light-harvesting cross-section of the antenna by opening an active, ultrafast S_1/ICT channel for energy transfer to LH1 Bchls, while optimizing the triplet energy for singlet oxygen quenching. We propose that spheroidene/spheroidenone switching represents a simple and effective photoprotective mechanism, of likely importance for phototrophic bacteria that encounter both light and oxygen.

Introduction

Carotenoids are natural pigments that absorb light in the 450–550 nm spectral region and transfer the energy to (B)Chls, thereby acting as important energy donors in photosynthesis.[1] In addition to extending the spectral range for absorption of solar energy, carotenoids play a structural role in light-harvesting (antenna) complexes.[2,3] Finally, carotenoids play a photoprotective role by dissipating unwanted excited states in antenna complexes.[4,5] It is well documented that carotenoids in purple phototrophic bacteria perform both light harvesting and structural roles, and the availability of carotenoidless mutants showed early on that carotenoids are essential for protection against oxygen radicals.[6,7] The present study demonstrates the mechanistic basis for photoprotection in photosynthetic bacteria, using the purple bacterium *Rhodobacter (R.) sphaeroides* as a model. The photosynthetic complexes of this bacterium form interconnected membrane domains representing ~4,000 BChl molecules;[8–10] the membranes are found within the cell as hundreds of spherical intracytoplasmic membrane vesicles ~50 nm in diameter.[11] Light-harvesting LH2 complexes form the bulk light harvesting antenna, which donates energy to RC-LH1 complexes.[12]

In terms of their light-harvesting function, it is now well-established that carotenoids have two excited states that serve as energy donors: the S_2 state, responsible for the strong absorption in the 400–550 nm region, and the dark S_1 state, which is located below the absorbing state and is forbidden for one-photon transitions from the ground state.[13] In LH2 complexes both the S_2 and S_1 states act as energy donors. The actual energy transfer efficiency, however, depends on the conjugation length N (the number of the conjugated C=C bonds) of the carotenoid. While the S_2-mediated energy transfer is nearly constant (~50%) for carotenoids with $N = 9–11$ and decreases to ~30% only for $N > 12$,[1] the S_1 route reaches 90% efficiency for $N = 9$ and drops to less than 10% for $N > 11$.[14–16] This strong dependence is ascribed to unfavourable spectral overlap between the carotenoid S_1 state and Q_y band of BChl-a.[1] Essentially the same situation was found for either native LH1

complexes[17] or LH1 reconstituted with different carotenoids,[18] or for genetically modified LH2 complexes.[19]

In other types of light-harvesting complexes such as the peridinin-chlorophyll protein from dinoflagellates, carotenoids with a conjugated C=O group facilitate S_1-mediated energy transfer by coupling to an ICT state.[20] This light-harvesting strategy seems common among certain genera of marine algae that utilize carbonyl carotenoids.[21-23]

The existence of different paths of energy transfer from carotenoids in nature, involving either the S_1/S_2 or the S_1/ICT states, raises the possibility that a biosynthetic transition from spheroidene to spheroidenone (see Fig. 6–S1 for structures) in *R. sphaeroides*, known to occur when anaerobically grown cells are aerated, could act as a molecular 'switch' to a photoprotective mode. Spheroidenone is known to be very effective in protecting against singlet oxygen.[24] Furthermore, photostability studies on spheroidenone-containing LH1 and LH2 complexes in the presence of oxygen, and attached to gold surfaces in either the membrane-bound or purified state, showed a remarkable resilience, but only for the LH1 complex.[25,26] In the present study we used an LH2-minus *crtA* mutant that only contains spheroidene to demonstrate that in anaerobic, photosynthetic cells energy transfer in membrane-bound RC-LH1-PufX complexes proceeds via the S_1/S_2 states. When oxygen is present, the CrtA enzyme spheroidene monooxygenase present in the wild-type bacterium catalyses the incorporation of a keto group forming spheroidenone,[27] which transforms energy transfer within the LH1 complex by shutting off ultrafast triplet formation and initiating an S_1/ICT pathway. Furthermore, a specific spheroidenone configuration in LH1 decreases the energy of the triplet state, promoting photoprotective quenching of triplet BChl, or singlet oxygen. This effect is specific for the RC-LH1-PufX complex, and is not observed for the peripheral LH2 complex. We propose that spheroidene/spheroidenone switching in RC-LH1-PufX complexes represents a simple and effective photoprotective mechanism, of likely importance for phototrophic bacteria that encounter both light and oxygen.

Materials and methods

Preparation of intracytoplasmic membranes. The *R. sphaeroides* deletion strain DD13 was complemented with the plasmid p(RKEHWT).[28] The resultant transconjugant DD13[pRKEHWT], contains WT RC-LH1-PufX core complexes but no LH2 complexes. Cultures of this strain were grown in the dark semi-aerobically at 30°C with shaking, so that the carotenoid spheroidenone was incorporated into the core complexes. The LH2-minus *crtA* mutant DBCΩ Δ*crtA* was constructed by in-frame deletion of the *crtA* gene, using an LH2-minus background, DBCΩ,[28] so spheroidene became the dominant carotenoid in the core complexes; this mutant was grown photosynthetically. Intracytoplasmic membrane vesicles were then prepared from both LH2-minus mutants according to published methods.[46] PufX-minus membranes were prepared from a PufX-minus mutant with monomeric core complexes.[29]

Time-resolved spectroscopy. The femtosecond laser setup is based on mode-locked Ti:sapphire oscillator (Tsunami, Spectra Physics) and Nd:YLF pumped Ti:sapphire amplifier (Spitfire Pro XP, Spectra Physics) with central output wavelength of 795 nm and 1 kHz repetition rate (6 mJ per pulse), delivering ~80 fs pulses. The output beam was split into two parts, one for pumping a collinear optical parametric amplifier (TOPAS-C, Light Conversion) to generate the pump beam while the second one was led through a computer-controlled delay line and focused onto a 2-mm sapphire plate to generate a white light continuum. Subsequently, the probe pulses were split into two parts, the former overlapping with the pump pulse in the sample volume and the latter serving as a reference, while not passing through the sample. The probe and the reference beams were then brought to the slit of a spectrograph and dispersed onto a double photodiode array, each with 512 elements. All samples were measured in a quartz shaking cuvette preventing sample degradation caused by long-term exposure to laser light. The intensity of excitation pulses was kept below 4×10^{14} photons pulse^{-1} cm^{-2}. Absorption spectra were measured before and after experiments to check for possible sample degradation, which did not exceed 6% in any case. Mutual polarization between pump and probe beams was set to the magic angle (54.7°). All data from time-resolved measurements were fitted globally (DAFit, Pascher Instruments) to a sum of exponentials using a sequential kinetic scheme with increasing lifetimes.[30]

Results and discussion

Absorption spectra of membrane-bound RC-LH1-PufX complexes, containing either spheroidene or spheroidenone and hereafter referred to as RC-LH1-PufX(sph) and RC-LH1-PufX(spn), respectively, are shown in

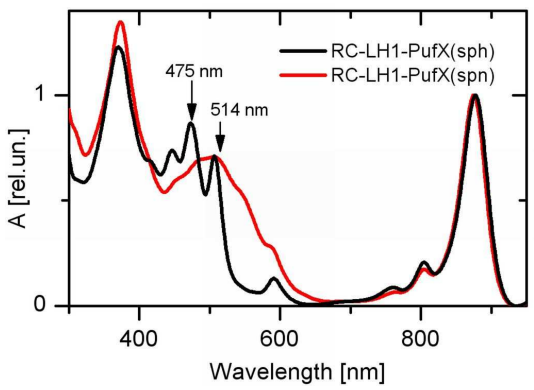

Figure 6-1: Absorption spectra of RC-LH1-PufX complexes containing spheroidene (sph) and spheroidenone (spn). The excitation wavelengths are indicated by vertical arrows.

Figure 6-1. The PufX polypeptide is an integral component of the *R. sphaeroides* RC-LH1 core complex, and is essential for efficient photosynthetic growth.[31] The spectra are dominated by BChl-a Q_y and Soret bands peaking at ~876 and ~372 nm, respectively; the BChl-a Q_x band appears at 590 nm. The RC contributions to the absorption spectra are also very similar in both complexes; the BChl monomers in the RC give rise to ~805-nm bands, while those around ~760 nm are due to RC bacteriopheophytins.[32] Differences between the RC-LH1-PufX complexes are most pronounced in the blue-green region where carotenoids absorb. Spheroidene has three well-resolved vibrational bands in the RC-LH1-PufX(sph) complex. The lowest energy transition due to the 0–0 band is readily identified at 507 nm. The absorption spectrum of spheroidenone in the RC-LH1-PufX(spn) complex is shifted to longer wavelengths; moreover, the resolution of its vibrational bands is significantly diminished, as seen in other LH complexes binding the carbonyl carotenoid spheroidenone[14,15] or okenone.[33] The weakly pronounced 0–0 band of spheroidenone in RC-LH1-PufX(spn) appears at ~545 nm.

Intramolecular charge-transfer state in RC-LH1-PufX complexes

To search for possible identifiers of an ICT state in RC-LH1-PufX complexes, we recorded their transient absorption spectra after excitation of carotenoids at 475 nm (spheroidene) and 514 nm (spheroidenone). Figure 6-2A shows a comparison of transient absorption spectra of both complexes recorded at 500 fs after excitation. The spectrum of the RC-LH1-PufX(sph)

complex is dominated by a band at 553 nm, which is typical of the S_1-S_N band of spheroidene.[14,15] In addition, a shoulder appears on the high-energy side of the main peak, which we attribute to the transition associated with the S* state.[34] However, the transient absorption spectrum of the RC-LH1-PufX(spn) complex is significantly different, and a new spectral band, reminiscent of the ICT-like transition of carbonyl carotenoids in polar solvents,[35,36] is observed around 750 nm. While the broadening of the S_1-S_N transition of spheroidenone is observed in LH2 complexes, the band at 750 nm has never been observed in LH2,[14,15] although a similar, but much weaker, band was detected in the spheroidenone-containing LH4 antenna of *Roseobacter denitrificans*.[37]

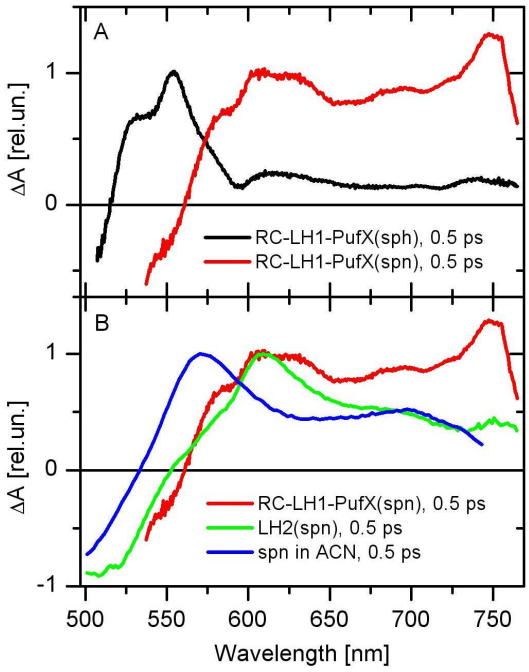

Figure 6-2: Transient absorption spectra recorded after excitation of the S_2 state of carotenoid in (A) RC-LH1-PufX complexes containing spheroidene (sph) and spheroidenone (spn). The transient absorption spectra were recorded 0.5 ps after excitation at 475 nm (sph) and 514 nm (spn). **(B) Comparison of transient absorption spectra of the RC-LH1-PufX(spn) complex, LH2 complex containing spn, and spn in acetonitrile.** Excitation wavelengths were 514 nm (RC-LH1-PufX), 515 nm (LH2), and 500 nm (acetonitrile). Data on LH2 and spheroidenone in solution are taken from Refs. 15 and 36. All spectra are normalized to S_1-S_N maximum.

In Figure 6-2B we compare the transient absorption spectra of spheroidenone in acetonitrile, and in the RC-LH1-PufX(spn) and LH2 complexes. It is clear that spheroidenone in LH2 resembles that in solution, exhibiting only a weak feature around 690 nm attributable to the ICT-S_n transition. On the other hand, in RC-LH1-PufX(spn) the ICT-S_n transition

of spheroidenone is far more intense and shifted to ~750 nm. Thus, binding of spheroidenone to the RC-LH1-PufX complex stabilizes the ICT state that consequently must play a role in excited-state dynamics. Since no such effect is observed in spheroidenone-containing LH2 complexes, there must be significant differences in spheroidenone-protein interactions between RC-LH1-PufX and LH2 complexes of *R. sphaeroides*. Because a high-resolution atomic structure of the RC-LH1-PufX complex is not available, it is not possible to identify the origin of the difference between RC-LH1-PufX and LH2 complexes from structural data. Yet, there are spectroscopic indicators that allow us to hypothesize about possible origins of the observed differences in excited-state properties.

First, it must be noted that the intensity of the ICT-like transition of spheroidenone in the RC-LH1-PufX(spn) complex is significantly stronger than that observed in the most polar solvents (Figure 6-2B). It is known that although it is possible to separate the S_1-like and ICT-like transitions in transient absorption spectra, the S_1 and ICT states of carbonyl carotenoids are strongly coupled in the S_1/ICT state,[35,38] and the intensity of the ICT-like transition is a measure of a degree of charge-transfer character of the S_1/ICT state. It was recently shown that the intensity of the ICT-like transition significantly increases if a single conjugated carbonyl group of a carotenoid is positioned in an s-*trans* configuration with respect to the main conjugated backbone.[39] However, this is not the case for spheroidenone in solution, where the carbonyl group is in an s-*cis* orientation as evidenced by molecular modelling showing that s-*cis* configuration is far more stable (Fig. 6–S2). Consequently, the significantly stronger ICT band in the RC-LH1-PufX(spn) complex could be explained if the binding site in the RC-LH1-PufX(spn) 'twists' the carbonyl group of spheroidenone into the s-*trans* configuration (Fig. 6–S2).

Further support for this hypothesis is provided by a comparison of transient absorption spectra of spheroidenone in the RC-LH1-PufX(spn) complex with those of the carotenoid hydroxyechinenone in the OCP from cyanobacteria, which exhibits very similar behaviour. Whereas no ICT-like transitions are detected for hydroxyechinenone in solution, a red-shifted ICT

band dominates the transient absorption spectrum of hydroxyechinenone bound to OCP.[40] Unlike the RC-LH1-PufX complex, the atomic structure of OCP has been determined to 1.65 Å resolution,[41] allowing identification of the changes leading to 'activation' of the ICT state. The carbonyl group of hydroxyechinenone is in the s-*cis* orientation in solution, minimizing the charge-transfer character of the S_1/ICT state.[39] However, the hydroxyechinenone binding site in OCP forces the terminal 4-keto-*β*-ionylidene ring of hydroxyechinenone to twist, aligning the conjugated carbonyl group into the s-*trans* orientation with respect to the rest of the conjugated bond system.[40] Moreover, the conjugated carbonyl group of hydroxyechinenone in OCP forms hydrogen bonds to nearby tryptophan and tyrosine residues. These structural changes result in the appearance of the ICT band in the transient absorption spectrum; however, it disappears in the closely related red carotenoid protein, where the part of the protein forming the carbonyl binding site in OCP is missing.[42]

Thus, comparison of data recorded for the RC-LH1-PufX(spn) complex and the OCP protein suggests that a conformational change of spheroidenone in RC-LH1-PufX(spn), which does not occur in LH2, causes the enhancement of the charge-transfer character of the S_1/ICT state of spheroidenone, resulting in observation of the ICT-like band at 750 nm. It is likely that hydrogen bonding to the carbonyl group also contributes to this effect, however, hydrogen bonding alone cannot generate an ICT band of such magnitude, as is seen when comparing the intensity of the ICT band of spheroidenone in the hydrogen bonding solvent methanol[35] and in aprotic acetonitrile;[36] the ICT bands in both solvents are weak and of comparable magnitude. Thus, the magnitude of the ICT band of spheroidenone in RC-LH1-PufX(spn) complexes cannot be reproduced in any solvent, suggesting that the introduction of the keto group probably twists the carotenoid molecule, a significant structural change that has to be accommodated by an alteration of the binding site within the LH1 complex.

Based on the arguments presented above we propose that spheroidenone bound to the RC-LH1-PufX(spn) complex of *R. sphaeroides* has the keto group in the s-*trans* orientation, whereas the s-*cis* orientation

most likely occurs in LH2. In addition, hydrogen bonding of LH1 side chains to the carbonyl oxygen may further enhance the charge-transfer character of the S_1/ICT state of spheroidenone in the RC-LH1-PufX(spn) complex.

Carotenoid excited-state dynamics

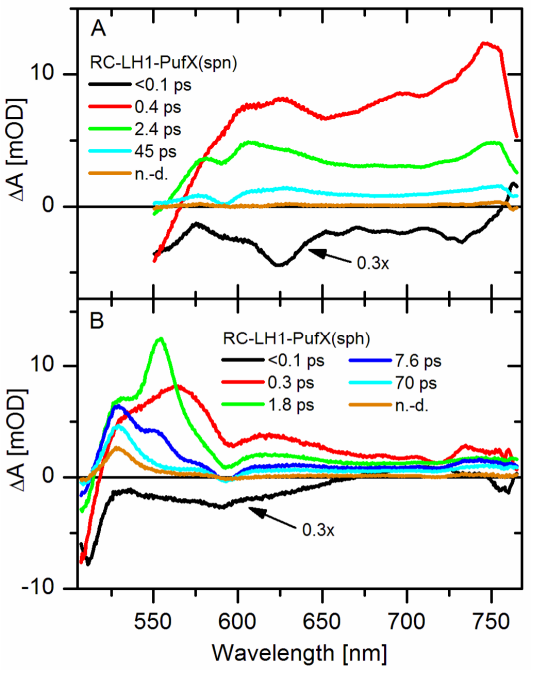

Figure 6-3: EADS resulting from global fitting the data in the visible spectral region measured for (A) RC-LH1-PufX(spn) and (B) RC-LH1-PufX(sph) complexes. The data at wavelengths shorter than 550 nm are omitted for the RC-LH1-PufX(spn) complex due to strong scattering from excitation. n.d. - non-decaying component.

Having established that the 750 nm band in transient absorption spectra of the RC-LH1-PufX(spn) complex arises from the ICT state, we may proceed with an analysis of excited-state dynamics. Results of global fitting of data recorded for both RC-LH1-PufX complexes are shown in Figure 6-3. For the RC-LH1-PufX(spn) complex (Figure 6-3A) the first EADS corresponding to the S_2 state decays in <0.1ps to the second EADS (red) that is clearly due to the S_1/ICT state, because it contains both S_1-like (600 nm) and ICT-like (750 nm) transitions. Interestingly, this second EADS contains only a weak signal attributable to Q_x bleaching (~590 nm), suggesting that the S_2 channel is of minor importance in this complex. This also implies that S_2-S_1/ICT internal conversion occurs in s-*trans* spheroidenone in the RC-LH1-PufX(spn) complex significantly faster than for spheroidene in the RC-LH1-PufX(sph) complex (see below). This observation agrees with a previous study of S_2 decay of hydroxyechinone, where activation of the ICT state significantly

shortens the S_2 lifetime in the OCP in comparison with the lifetime in solution.[40] The S_1/ICT state decays in 0.4 ps during which process the appearance of a dip is clearly visible, superimposed on the broad S_1-S_N transition. This feature is due to the Q_x bleaching and identifies the 0.4 ps process as energy transfer from the S_1/ICT state. The next EADS (green) decays in 2.4 ps. The EADS generated by the 2.4 ps process (cyan) does not contain any spheroidenone bleaching and is thus solely due to BChl-a; the 45 ps time constant of the decay of this EADS is associated with the overall trapping time of excited states in these photosynthetic membranes. It is important to note that the monomer/dimer status of the spheroidenone complexes has no influence on the carotenoid excited state dynamics. Both the activation of the ICT state and excited-state dynamics of spheroidenone in the PufX-minus and PufX-containing RC-LH1(spn) complexes are essentially identical (Fig. 6–S3).

Global analysis of data measured for the RC-LH1-PufX(sph) complex (Figure 6-3B) reveals that the S_2 state decays on the sub-100 fs timescale (black EADS). When going to the next EADS (red), the clear dip around 590 nm indicates that the S_2-mediated energy transfer is far more important here in comparison with the RC-LH1-PufX(spn) complex. This EADS decays in 0.3 ps, which is nearly the same time constant as for RC-LH1-PufX(spn), but the spectral properties are qualitatively different as it exhibits the characteristics of a hot S_1 state.[15,43] The pathway from the hot S_1 state of carotenoids has been observed in other LH complexes.[34,44,45] Whether or not this energy transfer channel is active in RC-LH1-PufX(sph) needs to be elucidated by complementary measurements of BChl-a dynamics in the NIR spectral region (see below). The EADS of the hot S_1 state relaxes to form the EADS associated with the S_1 state (green) which decays in 1.8 ps. The shape of the next EADS (blue) is reminiscent of the S* state.[34] The last dynamic process (cyan to orange EADS) occurs with a 70 ps time constant and again reflects the overall trapping time for these membranes. At present, we cannot explain the slower trapping time for RC-LH1-PufX(sph) than for RC-LH1-PufX(spn) membranes, and a systematic study of trapping times in the presence of LH2 complexes will be required to examine this point further.

The final, non-decaying EADS of the RC-LH1-PufX(sph) contains a clear band at 530 nm that arises from the triplet state of spheroidene.

Carotenoid to BChl-a energy transfer

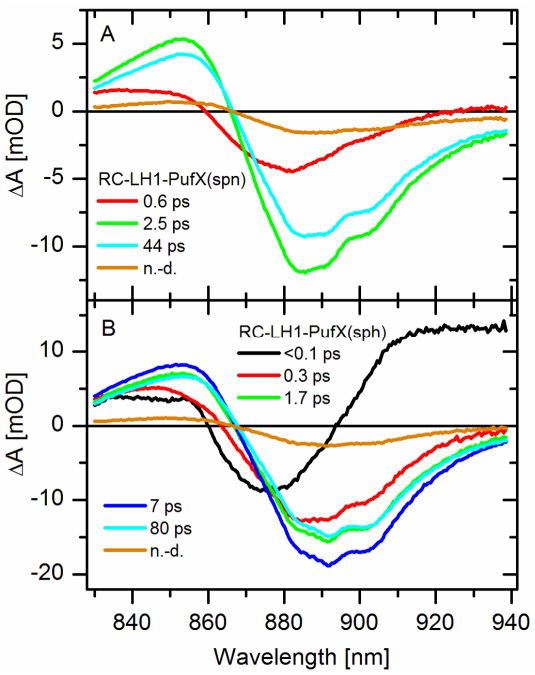

Figure 6-4: EADS resulting from global fitting the data in the NIR spectral region measured for (A) RC-LH1-PufX(spn) and (B) RC-LH1-PufX(sph) complexes. n.d. - non-decaying component.

In order to confirm that the 0.4 ps (spheroidenone) and 0.3 and 1.8 ps (spheroidene) components observed in the visible spectral region are associated with energy transfer, we carried out experiments probing the NIR region, monitoring the signal of the BChl-a Q_y band. The global fitting results are depicted in Figure 6-4; for membranes containing the RC-LH1-PufX(spn) complex (Figure 6-4A) the first EADS (red) contains some BChl-a signal, but its contribution is smaller in comparison with the RC-LH1-PufX(sph) sample (Figure 6-4B). This observation confirms the hypothesis that the S_2 state of spheroidenone is a minor donor of excitation energy for BChl-a in RC-LH1-PufX(spn) complexes. The magnitude of the BChl-a bleaching in the NIR region increases greatly with a 0.6 ps component that matches the 0.4 ps component associated with the S_1/ICT state observed in the visible region. Thus, energy transfer from spheroidenone to BChl-a in the RC-LH1-PufX(spn) complex proceeds predominantly via the S_1/ICT route. The second EADS (green) decays with a 2.5 ps component; during this process there is only a slight decrease of the BChl-a signal, indicating that no energy

transfer occurs with this time constant. Virtually the same component of 2.4 ps was observed in the visible region (Figure 6-3A) and its presence in the NIR region indicates that it is associated with BChl-a dynamics. Indeed, the 2.4 ps EADS in the visible region has a shape similar to the 45 ps EADS, except in its intensity, and is clearly due to BChl-a (Figure 6-3A). The next EADS (cyan) has a lifetime of 44 ps and evidently corresponds to the trapping time in RC-LH1-PufX(spn) complex.

Figure 6-4B shows the EADS obtained from global fits of the data measured in the NIR region for the RC-LH1-PufX(sph) complex. Unlike the RC-LH1-PufX(spn) complex, the first EADS (black) already contains a significant BChl-a bleaching component, which increases further during the <100 fs step. These observations indicate that a substantial part of the energy is transferred from the S_2 state of spheroidene. A further increase (red to green EADS) is characterized by a 0.3 ps component that matches the decay of the hot S_1 state observed in the visible region (Figure 6-3B), supporting the notion of energy transfer via the hot S_1 state of spheroidene. The green EADS has a 1.7 ps lifetime and the process associated with this component increases the BChl-a signal further. The match between this time constant and that observed in the visible region allows an assignment as energy transfer from the relaxed S_1 state of spheroidene. During the next process, associated with the 7 ps time constant, the cyan EADS is formed. Because it is accompanied by the decrease of the BChl-a signal, this EADS is most probably associated with relaxation of BChl-a excited states. Although it would be tempting to couple the ~7 ps time constants in the visible and NIR regions, the dominating processes are most probably unrelated. Whilst the NIR decrease of the signal is unequivocally associated with BChl-a relaxation, the 7.6 ps EADS in the visible region exhibits characteristic carotenoid features. The cyan EADS decays with an 80 ps time constant, again due to trapping events in RC-LH1-PufX(sph) complex.

Thus, three energy transfer pathways, via the S_2, hot S_1 and relaxed S_1 states, are active in the RC-LH1-PufX(sph) complex, whereas only two pathways, mediated by the S_1/ICT state and to a lesser extent by S_2, exist in RC-LH1-PufX(spn) complex (see Fig. 6–S4 for a scheme of energy transfer

pathways). Multiple pathways involving both S_2 and S_1 routes are common in LH2 and LH1 complexes of purple bacteria binding carotenoids with $N < 11$.[1,15,18] When carotenoids with a longer conjugated bond system, such as lycopene[16,18,19] or spirilloxanthin,[18,34] are bound to LH2 or LH1 complexes the S_1 route becomes inactive, but the S_2 pathway is functional in all purple bacterial antenna studied so far. It is worth noting that the S_2 route is significantly diminished in light-harvesting complexes of dinoflagellates or diatoms binding the carbonyl carotenoids peridinin or fucoxanthin; then, the pathway through the S_1/ICT state becomes the major pathway,[20-22] reminiscent of the situation studied here in RC-LH1-PufX(spn) complexes.

The RC-LH1-PufX(spn) complex represents a unique light-harvesting system among purple bacteria. The biosynthetic incorporation of a single keto oxygen into the structure of spheroidene changes the energy transfer pathways, and the S_1/ICT route becomes dominant. Because the ICT state is not active in LH2 complexes binding the same carotenoid, spheroidenone, an LH1-specific interaction must exist between the keto group of spheroidenone and amino acid residues such as tryptophan and tyrosine, as found for interactions of these residues with LH1 BChls.[46,47] There is evidence that the Trp residue of the highly conserved Lys-Ile-Trp (KIW) motif, found in the N-terminal domain of the LH1α polypeptide, plays a role in binding spheroidenone in the LH1 complex of *R. capsulatus*;[48,49] however, the same KIW motif is found in LH2, and no ICT state is found in this complex. It is possible that the neighbouring αTyr–27 residue provides the hydrogen bond to the C2 keto group of spheroidenone that stabilizes the s-*trans* configuration as the corresponding residue in LH2 is a Gly.

Carotenoid triplet state formation in RC-LH1-PufX complexes

The transient absorption data in Figure 6-2A and the EADS in Figure 6-3 show that also the blue parts of these spectra differ significantly in the two RC-LH1-PufX complexes. While spheroidenone bleaching dominates below 560 nm, the transient absorption spectrum of the RC-LH1-PufX(sph)

complex contains a positive signal below 540 nm that does not decay within the time window of the experiment. This non-decaying signal forms a narrow peak centred at 530 nm and is generated within the first picosecond after excitation; the same signal was observed in LH1 complexes of *Rhodospirillum rubrum* reconstituted with spheroidene and it was identified as a T_1-T_n transition due to a spheroidene triplet state.[18]

However, the observed picosecond dynamics of the 530 nm band are not consistent with known lifetimes of the triplet state. Thus, Papagiannakis et al. (Ref. 34) interpreted the early signal as arising from the S* state that is the precursor of the triplet state in native LH complexes of *R. sphaeroides*. In fact, the time constants extracted here from global fitting of the RC-LH1-PufX(sph) data are remarkably similar to those obtained for LH2 complex from the same organism.[34] Consequently, we assign the 7.6 ps component to decay of the S* state, formed from the S_2 state of spheroidene. Since the process associated with the 7.6 ps component is accompanied also by a loss of ground state bleaching (Figure 6-3B), it implies that the S* state decays into both triplet and ground states. Comparing the amplitudes of the components obtained here (Figure 6-3B) and in LH2,[34] the branching ratio is shifted more towards the triplet state in RC-LH1-PufX(sph) complex. The underlying dynamics are, however, essentially identical in RC-LH1-PufX(sph) and LH2(sph) complexes.

Whereas in the RC-LH1-PufX(sph) complex the resulting triplet yield is higher than in corresponding LH2 complexes, the change of spheroidene to spheroidenone, which involves only the addition of a keto group to the carotenoid conjugated system, switches off the pathway toward the triplet state completely. Although the scattering prevents the inclusion of <550 nm data in the global fitting (Figure 6-3A), comparison of transient absorption spectra at 100 ps recorded for RC-LH1-PufX(sph) and RC-LH1-PufX(spn) complexes (Fig. 6–S5), clearly shows that no triplet signal is observed in the RC-LH1-PufX(spn) complex. Consequently, incorporation of spheroidenone in RC-LH1-PufX(spn) not only alters energy transfer pathways but also prevents ultrafast triplet formation.

A possible biological role for spheroidene/spheroidenone conversion in photosynthetic bacteria

The conversion of spheroidene to spheroidenone, mediated by spheroidene monooxygenase, alters the conformation of the carotenoid, which twists in the s-*trans* configuration that is likely stabilized by a hydrogen-bonding interaction within the LH1 binding site. The effect of this change is to increase the conjugation length of the carotenoid, lowering the energy of the lowest triplet state[50] so it can act as an effective quencher of singlet oxygen and/or BChl-a triplet states. The other consequence of the conversion of spheroidene to spheroidenone is a modification of the energy transfer properties of RC-LH1-PufX complexes, which switch from an S_2/S_1/triplet mechanism to one involving mainly the S_1/ICT state. The s-*trans* configuration of spheroidenone leads to activation of the ICT state, which maintains an active S_1-channel for energy transfer to LH1 Bchls while allowing the triplet energy drop to effectively quench singlet oxygen. This functional flexibility contrasts with that of lycopene, which has effective conjugation comparable to spheroidenone in s-*trans* configuration, and is found in some other light-harvesting complexes.[51] This carotenoid evidently has an ideal triplet energy for scavenging singlet oxygen and, indeed, lycopene is the most effective carotenoid for singlet oxygen scavenging;[52] however, the S_1 energy of lycopene is too low to transfer energy to BChl-a.[1,16]

The basis for biological role of this process probably originates in the differing levels of light and oxygen encountered by purple phototrophic bacteria. As they move from a low-light, anaerobic environment to one nearer the surface where both the light and oxygen levels increase, there is a need to protect the photosynthetic apparatus. Similar requirements are found in the aerobic anoxygenic phototrophs that represent almost 10% of microbes in the oceans.[53] The proposed quenching mechanism offers effective protection against singlet oxygen without sacrificing the light-harvesting cross-section of the antenna, in line with work on other systems involving the ICT state.[20] Quenching of BChl-a triplet states that may lead to singlet

oxygen formation, or quenching the singlet oxygen itself, are of vital importance in conditions when light and oxygen is present. This is underlined by the recent study of Magis et al. (Ref. 26), which compared the photostability of surface-immobilized LH1 and LH2 complexes with spheroidenone as the major carotenoid. LH1 complexes withstood 180 min of irradiation at 650 $W.cm^{-2}$, whereas LH2 complexes were destroyed in less than 2 minutes. Thus, the ability of spheroidenone to optimize triplet energy in RC-LH1-PufX(spn) complexes and simultaneously maintain energy transfer channel between spheroidenone and BChl-a is a vital environmental response mechanism for this bacterium and likely for the many other phototrophic bacteria that also contain spheroidenone. In conclusion, we suggest that spheroidene/spheroidenone conversion in RC-LH1-PufX complexes represents a simple and effective photoprotective mechanism, to add to other photoprotective mechanisms found in nature such as the OCP of cyanobacteria and the xanthophyll cycle of plants.

References

1. Polívka T, Frank HA (2010) Molecular factors controlling photosynthetic light harvesting by carotenoids. *Acc Chem Res* 43: 1125–1134.
2. Lang HP, Hunter CN (1994) The relationship between carotenoid biosynthesis and the assembly of the light-harvesting LH2 complex in *Rhodobacter sphaeroides. Biochem J* 298: 197–205.
3. Plumley FG, Schmidt GW (1987) Reconstitution of chlorophyll a/b light-harvesting complexes–xanthophyll-dependent assembly and energy transfer. *Proc Natl Acad Sci USA* 84: 146–150.
4. Demmig-Adams B, Adams WW (1996) The role of xanthophyll cycle carotenoids in the protection of photosynthesis. *Trends Plant Sci* 1: 21–26.
5. Wilson A, Punginelli C, Gall A, Bonetti C, Alexandre M, Routaboul JM, Kerfeld CA, van Grondelle R, Robert B, Kennis JTM, Kirilovsky D (2008) A photoactive carotenoid protein acting as light intensity sensor. *Proc Natl Acad Sci USA* 105: 12075–12080.
6. Sistrom WR, Griffiths M, Stanier RY (1956) The biology of a photosynthetic bacterium which lacks coloured carotenoids. *J Cell Comp Physiol* 48: 473–516.
7. Clayton RK, Smith C (1960) *Rhodopseudomonas sphaeroides*: high catalase and blue-green double mutants. *Biochem Biophys Res Commun* 3: 143–145.
8. Hunter CN, Kramer HJM, van Grondelle R (1985) Linear dichroism and fluorescence emission of antenna complexes during photosynthetic unit assembly in *Rhodopseudomonas sphaeroides*. *Biochim Biophys Acta* 807: 44–51.
9. Frese RN, Siebert CA, Niederman RA, Hunter CN, Otto C, van Grondelle R (2004) The long-range organization of a native photosynthetic membrane. *Proc Natl Acad Sci USA* 101: 17994–17999.
10. Şener MK, Olsen JD, Hunter CN, Schulten K (2007) Atomic-level structural and functional model of a bacterial photosynthetic membrane vesicle. *Proc Natl Acad Sci USA* 104: 15723–15728.
11. Tucker JD, Siebert CA, Escalante M, Adams PG, Olsen JD, Otto C, Stokes DL, Hunter CN (2010) Membrane invagination in *Rhodobacter sphaeroides* is initiated at curved regions of the cytoplasmic membrane, then forms both budded and fully detached spherical vesicles. *Mol Microbiol* 76: 833–847.
12. Sundström V, Pullerits T, van Grondelle R (1999) Photosynthetic light-harvesting: Reconciling dynamics and structure of purple bacterial LH2 reveals function of photosynthetic unit. *J Phys Chem B* 103: 2327–2346.

13. Polívka T, Sundström V (2004) Ultrafast dynamics of carotenoid excited states: From solution to natural and artificial systems. *Chem Rev* 104: 2021–2071.
14. Polívka T, Pullerits T, Frank HA, Cogdell RJ, Sundström V (2004) Ultrafast formation of a carotenoid radical in LH2 antenna complexes of purple bacteria. *J Phys Chem B* 108: 15398–15407.
15. Cong H, Niedzwiedzki DM, Gibson GN, LaFountain AM, Kelsh RM, Gardiner AT, Cogdell RJ, Frank HA (2008) Ultrafast time-resolved carotenoid to bacteriochlorophyll energy transfer in LH2 complexes from photosynthetic bacteria. *J Phys Chem B* 112: 10689–10703.
16. Zhang JP, Fujii R, Qian P, Inaba T, Mizoguchi T, Koyama Y, Onaka K, Watanabe Y, Nagae H (2000) Mechanism of the carotenoid-to-bacteriochlorophyll energy transfer via the S_1 state in the LH2 complexes from purple bacteria. *J Phys Chem B* 104: 3683–3691.
17. Rademaker H, Hoff AJ, van Grondelle R, Duysens LNM (1980) Carotenoid triplet yields in normal and deuterated *Rhodospirillum rubrum*. *Biochim Biophys Acta* 592: 240–257.
18. Akahane J, Rondonuwu FS, Fiedor L, Watanabe Y, Koyama Y (2004) Dependence of singlet-energy transfer on the conjugation length of carotenoids reconstituted into the LH1 complex from *Rhodospirillum rubrum* G9. *Chem Phys Lett* 393: 184–191.
19. Billsten HH, Herek JL, Garcia-Asua G, Hashoj L, Polívka T, Hunter CN, Sundström V (2002) Dynamics of energy transfer from lycopene to bacteriochlorophyll in genetically-modified LH2 complexes of *Rhodobacter sphaeroides*. *Biochemistry* 41: 4127–4136.
20. Zigmantas D, Hiller RG, Sundström V, Polívka T (2002) Carotenoid to chlorophyll energy transfer in the peridinin-chlorophyll-*a*-protein complex involves an intramolecular charge transfer state. *Proc Natl Acad Sci USA* 99: 16760–16765.
21. Polívka T, Hiller RG, Frank HA (2007) Spectroscopy of the peridinin-chlorophyll-a protein: Insight into light-harvesting strategy of marine algae. *Arch Biochem Biophys* 458: 111–120.
22. Papagiannakis E, van Stokkum IHM, Fey H, Büchel C, van Grondelle R (2005) Spectroscopic characterization of the excitation energy transfer in the fucoxanthin–chlorophyll protein of diatoms. *Photosynth Res* 86: 241–250.
23. Polívka T, van Stokkum IHM, Zigmantas D, van Grondelle R, Sundström V, Hiller RG (2006) Energy transfer in the major intrinsic light-harvesting complex from *Amphidinium carterae*. *Biochemistry* 45: 8516–8526.

24. Glaeser J, Klug G (2005) Photo-oxidative stress in *Rhodobacter sphaeroides*: Protective role of carotenoids and expression of selected genes. *Microbiology* 151: 1927–1938.
25. Magis GJ, den Hollander MJ, Onderwaater WG, Olsen JD, Hunter CN, Aartsma TJ, Frese RN (2010) Light harvesting, energy transfer and electron cycling of a native photosynthetic membrane adsorbed onto a gold-surface. *BBA-Biomembranes* 1798: 637–645.
26. Magis GJ, Olsen JD, Reynolds NP, Leggett GJ, Hunter CN, Aartsma TJ, Frese RN (2011) Use of engineered unique cysteine residues to facilitate oriented coupling of proteins directly to a gold substrate. *Photochem Photobiol* 87: 1050–1057.
27. Yeliseev AA, Eraso JM, Kaplan S (1996) Differential carotenoid composition of the B875 and B800-850 photosynthetic antenna complexes in *Rhodobacter sphaeroides* 2.4.1: Involvement of spheroidene and spheroidenone in adaptation to changes in light intensity and oxygen availability. *J Bacteriol* 178: 5877–5883.
28. Jones MR, Fowler GJS, Gibson LCD, Grief GG, Olsen JD, Crielaard W, Hunter CN (1992) Mutants of *Rhodobacter sphaeroides* lacking one or more pigment protein complexes and complementation with reaction centre, LH1, and LH2 genes. *Mol Microbiol* 6: 1173–1184.
29. Ratcliffe EC, Tunnicliffe RB, Ng IW, Adams PG, Qian P, Holden-Dye K, Jones MR, Williamson MP, Hunter CN (2011) Experimental evidence that the membrane-spanning helix of PufX adopts a bent conformation that facilitates dimerisation of the *Rhodobacter sphaeroides* RC-LH1 complex through N–terminal interactions. *Biochim Biophys Acta* 1807: 95–107.
30. van Stokkum IHM, Larsen DS, van Grondelle R (2004) Global and target analysis of time-resolved spectra. *Biochim Biophys Acta* 1657: 82–104.
31. Farchaus JW, Barz WP, Grunberg H, Oesterhelt D (1992) Studies on the expression of the pufX polypeptide and its requirement for photoheterotrophic growth in *Rhodobacter sphaeroides*. *EMBO J* 11: 2779–2788.
32. Pan J, Lin S, Allen JP, Williams JC, Frank HA, Woodbury NW (2011) Carotenoid excited-state properties in photosynthetic purple bacterial reaction centers: Effects of the protein environment. *J Phys Chem B* 115: 7058–7068.
33. Andersson PO, Cogdell RJ, Gillbro T (1996) Femtosecond dynamics of carotenoid-to-bacteriochlorophyll a energy transfer in the light-harvesting antenna complexes from the purple bacterium *Chromatium purpuratum*. *Chem Phys* 210: 195–217.

34. Papagiannakis E, Kennis JTM, van Stokkum IHM, Cogdell RJ, van Grondelle R (2002) An alternative carotenoid-to-bacteriochlorophyll energy transfer pathway in photosynthetic light harvesting. *Proc Natl Acad Sci USA* 99: 6017–6022.
35. Frank HA, Bautista JA, Josue J, Pendon Z, Hiller RG, Sharples FP, Gosztola D, Wasielewski MR (2000) Effect of the solvent environment on the spectroscopic properties and dynamics of the lowest excited states of carotenoids. *J Phys Chem B* 104: 4569–4577.
36. Zigmantas D, Hiller RG, Sharples FP, Frank HA, Sundström V, Polívka T (2004) Effect of a conjugated carbonyl group on the photophysical properties of carotenoids. *Phys Chem Chem Phys* 6: 3009–3016.
37. Niedzwiedzki DM, Fuciman M, Frank HA, Blankenship RE (2011) Energy transfer in an LH4-like light harvesting complex from the aerobic purple photosynthetic bacterium *Roseobacter denitrificans*. *Biochim Biophys Acta* 1807: 518-528.
38. Zigmantas D, Hiller RG, Yartsev A, Sundström V, Polívka T (2003) Dynamics of excited states of the carotenoid peridinin in polar solvents: Dependence on excitation wavelength, viscosity, and temperature. *J Phys Chem B* 107: 5339–5348.
39. Enriquez MM, Fuciman M, LaFountain AM, Wagner NL, Birge RR, Frank HA (2010) The intramolecular charge transfer state in carbonyl-containing polyenes and carotenoids. *J Phys Chem B* 114: 12416–12426.
40. Polívka T, Kerfeld CA, Pascher T, Sundström V (2005) Spectroscopic properties of the carotenoid 3'-hydroxyechinenone in the orange carotenoid protein from the cyanobacterium *Arthrospira maxima*. *Biochemistry* 44: 3994–4003.
41. Wilson A, Kinney JN, Zwart PH, Punginelli C, D'Haene S, Perreau F, Klein M, Kirilovsky D, Kerfeld CA (2010) Structural determinants underlying photoprotection in the photoactive orange carotenoid protein of cyanobacteria. *J Biol Chem* 285: 18364–18375.
42. Chábera P, Durchan M, Shih PM, Kerfeld CA, Polívka T (2011) Excited-state properties of the 16 kDa red carotenoid protein from *Arthrospira maxima*. *Biochim Biophys Acta* 1807: 30–35.
43. de Weerd FL, Dekker JP, van Grondelle R (2003) Dynamics of beta-carotene-to-chlorophyll singlet energy transfer in the core of photosystem II. *J Phys Chem B* 107: 6214–6220.
44. Walla PJ, Linden PA, Ohta K, Fleming GR (2002) Excited-state kinetics of the carotenoid S_1 state in LHC II and two-photon excitation spectra of lutein and beta-carotene in solution: Efficient car S_1-Chl electronic energy transfer via hot S_1 states? *J Phys Chem A* 106: 1909–1916.

45. Durchan M, Herbstová M, Fuciman M, Gardian Z, Vácha F, Polívka T (2010) Carotenoids in energy transfer and quenching processes in Pcb and Pcb–PS I complexes from *Prochlorothrix hollandica*. *J Phys Chem B* 114: 9275–9282.
46. Olsen JD, Sockalingum GD, Robert B, Hunter CN (1994) Modification of a hydrogen bond to a bacteriochlorophyll-*a* molecule in the light-harvesting 1 antenna of *Rhodobacter sphaeroides*. *Proc Natl Acad Sci USA* 91: 7124–7128.
47. Sturgis J, Olsen CN, Robert B, Hunter CN (1997) The functions of conserved tryptophan residues of the core light-harvesting complex of *Rhodobacter sphaeroides*. *Biochemistry* 36: 2772–2778.
48. Babst M, Albrecht H, Wegmann I, Brunisholz R, Zuber H (1991) Single amino acid substitutions in the B870 alpha and beta light-harvesting polypeptides of *Rhodobacter capsulatus*. Structural and spectral effects. *Eur J Biochem* 202: 277–284.
49. Richter P, Brand M, Drews G (1992) Characterization of LHI^- and LHI^+ *Rhodobacter capsulatus pufA* mutants. *J Bacteriol* 174: 3030–3041.
50. Kleinschmidt M, Marian CM, Waletzke M, Grimme S (2009) Parallel multireference configuration interaction calculations on mini-beta-carotenes and beta-carotene. *J Chem Phys* 130: 044708.
51. Koepke J, Hu XC, Muenke C, Schulten K, Michel H (1996) The crystal structure of the light-harvesting complex II (B800-850) from *Rhodospirillum molischianum*. *Structure* 4: 581-597.
52. Di Mascio P, Kaiser S, Sies H (1989) Lycopene as the most efficient biological carotenoid singlet oxygen quencher. *Arch Biochem Biophys* 274: 532–538.
53. Yurkov V, Csotonyi JT. New light on aerobic anoxygenic phototrophs, In: *The purple phototrophic bacteria*; Hunter CN, Daldal F, Thurnauer MC, Beatty JT, Eds. *Springer*, Dordrecht, The Netherlands, 2009.

Supporting information

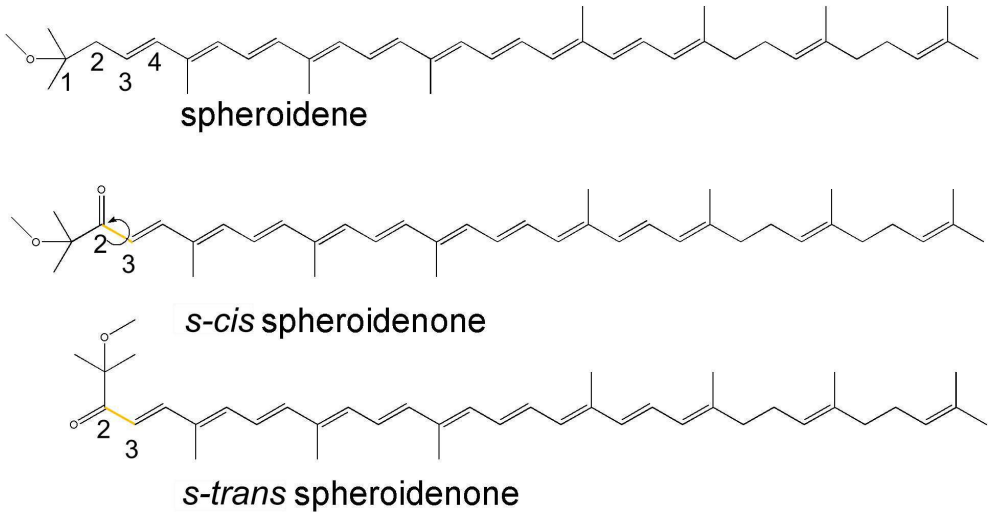

Figure 6–S1: Chemical structures of spheroidene and two configurations of spheroidenone. Numbers 1-4 indicate first four carbon atoms; rotation around the C2-C3 bond (yellow) produces the *s-cis* and *s-trans* configurations.

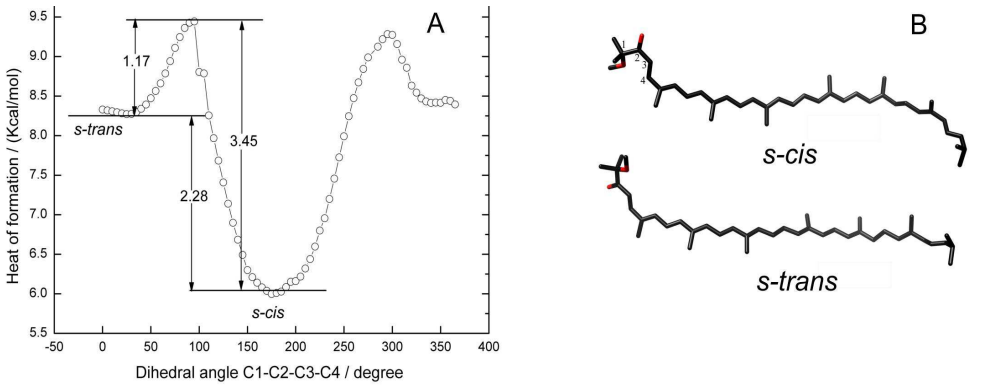

Figure 6–S2: (A) Calculated dependence of the heat of formation on the rotation of the dihedral C1-C2-C3-C4 system. (B) Optimized geometry of the s-*cis* and s-*trans* configurations of spheroidenone, corresponding to the minima in (A). Oxygen atoms are marked in red.

A semi-empirical QM method AM1 incorporated in MOPAC2009 (http://OpenMOPAC.net) was used for energy minimization. The dihedral angle for C1-C2-C3-C4 was rotated with a step size of 5 degrees, keeping the rest of the parameters for other atoms in the molecule, such as bond distance, bond angle and dihedral angle, open for optimization during the calculation for each step. The most stable configuration was found for each rotational step, and the total heat of formation of the configuration was calculated, then plotted against the rotated dihedral angle. The minimum heat of formation (5.99 Kcal.mol^{-1}) is at 175 degrees rotation, near the *s-cis* configuration, and the maximum is at 95 degrees (9.44 Kcal.mol^{-1}). The *s-trans* configuration is found at a local minimum at 25 degrees rotation, with a heat of formation of 8.27 Kcal.mol^{-1}. The total energy barrier for moving from s-*cis* to s-*trans* is 3.45 Kcal.mol^{-1}.

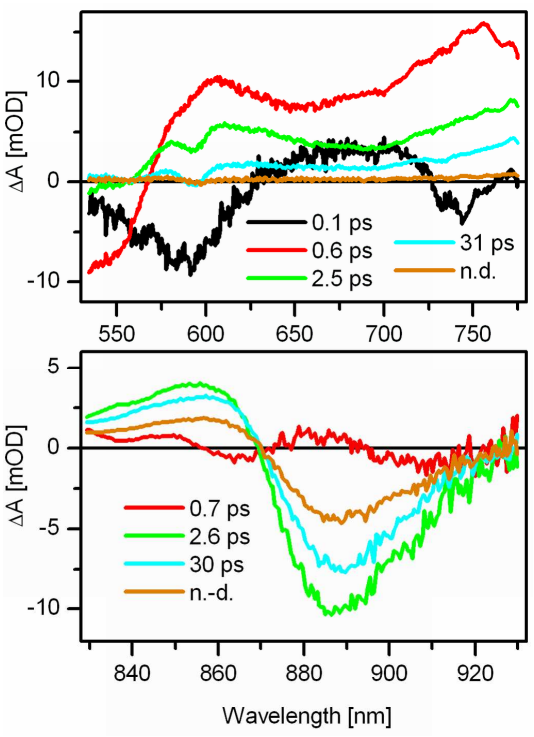

Figure 6–S3: EADS extracted from global fitting the data measured on LH1-RC complexes containing spheroidenone.

It is obvious that lacking the PufX complex does not affect the activation of the ICT state and overall spheroidenone-to-BChl-a energy transfer as the time constants obtained from the complex lacking PufX matches those shown in Fig. 6–3A and 6–4A. However, there is a slight difference in the time constant associated with the trapping time that yields 30 ps in the RC-LH1(spn) complex and 40 ps in the RC-LH1-PufX(spn) complex. As the RC-LH1(spn) complex cannot form dimers, it confirms our hypothesis that variations in trapping time are due to different degree of dimerization of the core complexes. n.d. - non-decaying component.

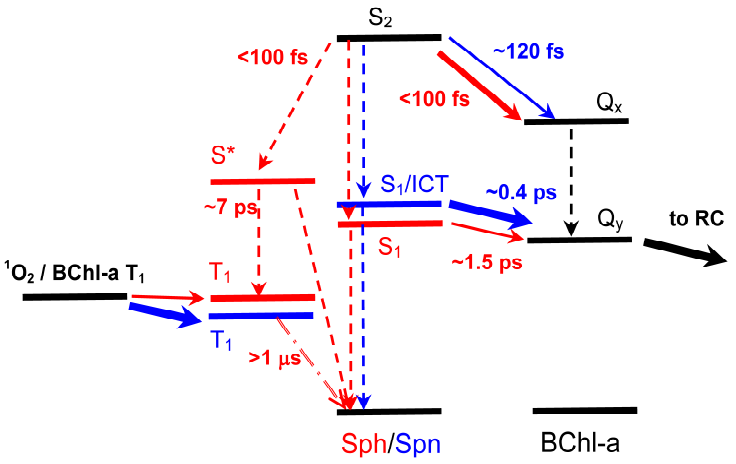

Figure 6–S4: Energy transfer pathways in RC-LH1-PufX(sph) and RC-LH1-PufX(spn) complexes.

Excited-state processes involving carotenoid spheroidene are shown in red while blue arrows denote energy transfer and relaxation channels involving the carotenoid spheroidenone. The dashed arrows represent internal conversion and intersystem crossing pathways and solid arrows depict energy transfer channels. Thickness of the arrows representing energy transfer is proportional to the efficiency of the particular energy transfer channel. Rates of excited-state processes whose time constants could be inferred from experiment are also shown. In RC-LH1-PufX(sph) complex the major energy transfer pathway is via the S_2 state and a side-relaxation channel populating spheroidene triplet via the S* state is active. On the other hand, in RC-LH1-PufX(spn) the activation of the S_1/ICT state, which also slightly increases the energy of the S_1/ICT state,[1] facilitates energy transfer via this coupled state, which becomes the major pathway, and the side-channel leading to the triplet state is switched off completely. However, the longer effective conjugation induced by the proposed linearization of the conjugated chain of spheroidenone in RC-LH1-PufX(spn) decreases the triplet energy of spheroidenone,[2] resulting in better quenching of singlet oxygen and/or BChl-a triplet than in RC-LH1-PufX(sph).

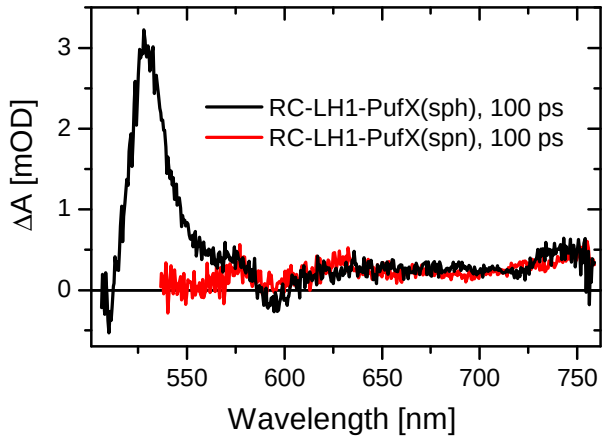

Figure 6–S5: Comparison of transient absorption spectra of RC-LH1-PufX(sph) and RC-LH1-PufX(spn) at 100 ps.

References

1. Zigmantas D, Hiller RG, Sharples FP, Frank HA, Sundström V, Polívka T (2004) Effect of a conjugated carbonyl group on the photophysical properties of carotenoids. *Phys Chem Chem Phys* 6: 3009–3016.
2. Kleinschmidt M, Marian CM, Waletzke M, Grimme S (2009) Parallel multireference configuration interaction calculations on mini-*β*-carotenes and *β*-carotene. *J Chem Phys* 130: 044708.

7. Carotenoid Charge Transfer States and Their Role in Energy Transfer Processes in LH1−RC Complexes from Aerobic Anoxygenic Phototrophs

This chapter is based on Paper V.:
Šlouf V, Fuciman M, Dulebo A, Kaftan D, Koblížek M, Frank HA (2012) Carotenoid charge transfer states and their role in energy transfer processes in LH1–RC complexes from aerobic anoxygenic phototrophs. *J Phys Chem B* 117: 10987−10999.

Abstract

Light-harvesting complexes ensure necessary flow of excitation energy into photosynthetic reaction centres. In the present work, transient absorption measurements were performed on LH1-RC complexes isolated from two aerobic anoxygenic phototrophs (AAPs), *Roseobacter* sp. COL2P containing the carotenoid spheroidenone, and *Erythrobacter* sp. NAP1 which contains the carotenoids zeaxanthin and bacteriorubixanthinal. We show that the spectroscopic data from the LH1-RC complex of *Roseobacter* sp. COL2P are very similar to those previously reported for *Rhodobacter sphaeroides*, including the transient absorption spectrum originating from the ICT state of spheroidenone. Although the ICT state is also populated in LH1-RC complexes of *Erythrobacter* sp. NAP1, its appearance is probably related to the polarity of the bacteriorubixanthinal environment rather than to the specific configuration of the carotenoid, which we hypothesize is responsible for populating the ICT state of spheroidenone in LH1-RC of *Roseobacter* sp. COL2P. The population of the ICT state enables efficient S_1/ICT-to-BChl energy transfer which would otherwise be largely inhibited for spheroidenone and bacteriorubixanthinal due to their low energy S_1 states. In

addition, the triplet states of these carotenoids appear well-tuned for efficient quenching of singlet oxygen or BChl-a triplets, which is of vital importance for oxygen-dependent organisms such as AAPs.

8. Activation of the Intramolecular Charge-Transfer State in LH1 Complexes of Various Purple Bacteria

This chapter is based on Paper VI.:
Šlouf V, Chábera P, Cogdell RJ, Cranston L, Dulebo A, Hunter CN, Kaftan D, Koblížek M, Martin EC, Olsen JD, Polívka T. Activation of the intramolecular charge-transfer state in LH1 complexes of various purple bacteria. *Manuscript in preparation.*

Abstract

We have recently observed a specific spectroscopic feature associated with a keto carotenoid, spheroidenone, in LH1 complexes of *Rhodobacter sphaeroides.* It is a strong transient absorption peaking around 750 nm, which we attribute to the ICT state of spheroidenone. We hypothesize that the crucial factor for the ICT state activation is the interaction of the carotenoid keto group with the protein environment. Our aim is to find the activator of the ICT state at the level of protein primary structure. To obtain such information, we studied LH1 complexes of other organisms with both active and inactive ICT states.

9. Summary and Future Prospects

In this summary, I will highlight the most important findings and try to justify the relevance of the title of this thesis with respect to particular studies presented in both Research Sections. That proteins influence the photophysics of carotenoids (and of pigments in general) is not surprising. For instance, due to electrostatic interactions, carotenoid spectra are red-shifted in the proteins compared to solution. However, besides these "traditional" examples (demonstrated e.g. in Section 3), the results of this thesis also present rather unique "manipulations" of carotenoids by proteins (in Section 4 and Research Section B).

In Section 3, it was demonstrated that the main source of the carotenoid red-shift in the protein can be explained by local electrostatic interactions. Furthermore, it was realized that retinal excited states exhibit slower decay in XR than in BR. One of the hypotheses is that it is again the protein that forces retinal into different configurations in the two complexes resulting in distinct excited-state dynamics. The other hypothesis is that the differences are caused by an interaction between retinal and the neighbouring carotenoid, salinixanthin. Our experiments in the near future will hopefully provide an answer to the question of which of the two effects is decisive.

Section 4 brings forward a unique finding that the carotenoid diadinoxanthin, usually connected with photoprotection, is active in energy transfer to Chl-a in the XLH antenna. Surprisingly, its S_1 energy must be significantly higher in XLH than in solution, highlighting the role of the protein environment in tuning the spectroscopic properties so that the carotenoid can serve a particular function in one protein (light harvesting), but a distinctly different function in another (photoprotection). This result also sheds new light on the possible role of diadinoxanthin and diatoxanthin in algal NPQ. The proposed gear-shift mechanism was based on the assumption that diatoxanthin, but not diadinoxanthin, may serve as a sink for excitation energy from Chl-a due to its S_1 state position below that of Q_y.[1]

This mechanism was challenged by locating the S_1 states of both carotenoids in solution below that of Q_y.[2] However, the gear-shift mechanism could be revived by our finding that the protein can push the S_1 state of diadinoxanthin above that of Q_y. Using the same line of reasoning, the diatoxanthin S_1 state could remain below that of Q_y, enabling the gear-shift mechanism.

In Section 5, it was shown that the temperature dependence of the energy transfer rate in the acpPC complex is reversed with respect to PCP. This points either to the different overall organization of the two complexes, or to a distinct local protein environment around the chromophores in the respective complexes. (The former feature is also ultimately governed by the protein because it serves as a scaffold.) Furthermore, there even exist multiple spectral variants of peridinins, which is undoubtedly a product of local pigment-protein interactions because the photophysical properties of carbonyl carotenoids are known to be sensitive to polarity of the environment.[3]

The Research Section B forms an integrated unit, which deals with the activation of the ICT state of spheroidenone in LH1 complexes of some purple bacteria.

In Section 6, it was proven that it really is the ICT state, which is responsible for the strong spheroidenone ESA around 750 nm in the LH1 of *R. sphaeroides*. This band was only recorded in LH1, and could not be reproduced in solvent of any polarity, underscoring the role of the protein in ICT state activation. Moreover, the activation is conditioned by a special spheroidenone configuration, s-*trans*. In this configuration, spheroidenone excited-state energies are lower than those of the s-*cis* configuration, which is the most stable in solution. Consequently, s-*trans* spheroidenone can serve as a quencher of singlet oxygen due to the match of carotenoid T_1 state with the lowest excited state of singlet oxygen. The enzymatic exchange of spheroidene by spheroidenone can thus be viewed as a photoprotective mechanism, which is "responsive" as NPQ (is turned on when the external conditions require it), but acts on $^1O_2^*$ (and, possibly $^3Chl^*$), typically quenched by "non-responsive" mechanisms. The novel photoprotective

mechanism thus represents a “mix” of the established photoprotective mechanisms.

The study presented in Section 7 shows that the ICT state is also activated in the LH1 complex of *Roseobacter* sp. COL2P in the same way as in *R. sphaeroides*. The situation was, however, different in the LH1 from *Erythrobacter* sp. NAP1. Although the carbonyl carotenoid bacteriorubixanthinal also exhibited a strong ESA related to the ICT state in LH1, the ICT state is also activated when the carotenoid is dissolved in the polar solvent methanol. Therefore, the ICT activation in this LH1 is most probably achieved solely by the protein environment, which must be highly polar mainly around the carbonyl group of bacteriorubixanthinal.

Finally, Section 8 aims at drawing more general conclusions on the concepts and observations presented in Sections 6 and 7. Firstly, it is realized that the ICT state is not generally activated upon the binding of a carbonyl carotenoid to LH1. Further, a tyrosine residue close to the LH1-α polypeptide N-terminus was identified as the likely site responsible for the ICT state activation. In addition, it is concluded that the ICT state activity of carbonyl carotenoids (so far proven only for spheroidenone) is related to the photoprotective mechanism described earlier (Section 6) for *R. sphaeroides*. In the near future, we plan to test the hypothesis of the ICT state activation by the tyrosine. This will be achieved by constructing mutants, in which the tyrosine will be replaced by another residuum such as phenylalanine that is unable to form hydrogen bonds with the neighbouring carbonyl group of the carotenoid. If our hypothesis is correct, the s-*trans* configuration of spheroidenone should not be stabilized in these mutants, leading to a decreased ICT-related transient signal.

To conclude this thesis, I believe that the presented studies justify what is stated in the title: that the protein controls carotenoid photophysics to a hopefully larger extent than the reader might have anticipated upon simply reading the title.

References

1. Frank HA, Cua A, Chynwat V, Young A, Gosztola D, Wasielewski MR (1996) The lifetimes and energies of the first excited singlet states of diadinoxanthin and diatoxanthin: The role of these molecules in excess energy dissipation in algae. *Biochim Biophys Acta* 1277: 243−252.
2. Enriquez MM, LaFountain AM, Budarz J, Fuciman M, Gibson GN, Frank HA (2010) Direct determination of the excited state energies of the xanthophylls diadinoxanthin and diatoxanthin from *Phaeodactylum tricornutum*. *Chem Phys Lett* 493: 353–357.
3. Schulte T, Niedzwiedzki DM, Birge RR, Hiller RG, Polívka T, Hofmann E, Frank HA (2009) Identification of a single peridinin sensing Chl-a excitation in reconstituted PCP by crystallography and spectroscopy. *Proc Natl Acad Sci USA* 106: 20764–20769.

sloufv00@prf.jcu.cz

Proof reading by Chris Steer (Sections 1, 2, and 9)

Protein Control over Carotenoid Spectroscopy and Functions
Ph.D. Thesis Series, 2013, No. 12

Printed in the Czech Republic by Vlastimil Johanus
Edition of 40 copies

University of South Bohemia in České Budějovice
Faculty of Science
Branišovská 31
CZ-37005 České Budějovice
Czech Republic
Phone: +420 387 772 244
www.prf.jcu.cz, e-mail: sekret@prf.jcu.cz